DOI 10.1007/s10778-016-0749-3
International Applied Mechanics, Vol. 52, No. 3, May, 2016

THREE-DIMENSIONAL PROBLEMS OF THERMOVISCOPLASTICITY: FOCUS ON UKRAINIAN RESEARCH (REVIEW)

Yu. N. Shevchenko and V. G. Savchenko

Methods and results of studying the three-dimensional viscoplastic stress–strain state of engineering structures under thermomechanical loading are presented. The following classes of thermoviscoelastic problems are considered: axisymmetric problems, nonaxisymmetric problems for bodies of revolution, three-dimensional problems for arbitrarily shaped bodies, three-dimensional problems for isotropic and anisotropic bodies of revolution

Keywords: thermoviscoelasticity, deformation process, axisymmetric and nonaxisymmetric problems, isotropic and orthotropic materials, damage, stress mode

Introduction. Elements of various machines, which are three-dimensional bodies of simple or complex shape, can simultaneously be subject to nonuniform heating and surface and body forces. At some point of these bodies, the stresses may exceed the yield point of the material. If the loading process is nonisothermal, not only elastic and instantaneous plastic strains, but also creep strains can occur; i.e., the deformation of each element of the body can strongly depend on the rate of loading. High temperatures change the mechanical properties of the material (reduce the elastic modulus, yield point, and strength), except for some temperatures at which structural alloys are embrittled.

During heating, high temperature gradients can occur in the body, taking some of its parts adjoining the heated zones to a plastic state. In these zones, compressive plastic strains and associated stresses usually arise. As the body is heated, the temperatures gradients decrease and unloading occurs in the plastic zones, which can in some cases change the plastic strains, i.e., secondary plastic strains occur. During unloading, the elastic zones of the body tend to return to the initial state of the material, while the plastic strains resist this process, resulting in stretching of the plastic zones. Such varying loading of an element of the body can lead to accumulation of plastic strains and to its failure. Establishing the condition in which irreversible strains can be accumulated is an important task of solid mechanics.

Nonuniform heating in combination with external mechanical loading can cause complex deformation of an element of the body along paths that are substantially different from straight paths or event paths of small curvature. To establish the optimal conditions for the operation and manufacturing of structural members, it is necessary to determine the elastoplastic stress–strain state of the body taking into account the loading history of some of its elements and the above-mentioned factors accompanying the nonisothermal loading. To this end, foreign and domestic scientists have intensively developed fracture mechanics, which deals with the final stage of fracture, i.e., development of cracks in brittle materials.

The initial stage of fracture, i.e., damage of materials during deformation, is given much less attention. However, a crack nucleates and grows in a material prepared for fracture during a period when a variety of irreversible physical and mechanical processes occur in it at micro- or macroscales. In this process, the initial structure of the material changes, pores nucleate, grow, and coalesce, and microdefects form. Defects weaken the cross-section, reducing the effective area over which stresses are distributed, thus contributing to further fracture. Therefore, fracture under combined loading can be considered to occur in several stages. At the first stage, damages that are much smaller than some typical size of the structure are accumulated.

S. P. Timoshenko Institute of Mechanics, National Academy of Sciences of Ukraine, 3 Nesterova St., Kyiv, Ukraine 03057, e-mail: plast@inmech.kiev.ua. Translated from Prikladnaya Mekhanika, Vol. 52, No. 3, pp. 3–70, May–June, 2016. Original article submitted January 18, 2016.

This process dominates until microcracks form, which lead to the formation of a main crack, followed by the fracture of the material. Therefore, the development of methods for determining the elastoplastic stress–strain state and damage of solids under nonisothermal loading that adequately describe their deformation features mentioned above is an important task of solid mechanics.

Various isolated studies on three-dimensional elastoplastic stress–strain state of solids under nonisothermal loading began to be published in the late 1950–60s, reporting solutions to some three-dimensional problems of the stress–strain state of solids of mainly canonical shape under nonuniform heating and external force. These studies used the model of perfectly plastic body [160], the theory of small elastoplastic deformations regardless of the loading history [2–4, 22–24, 48–50, 122], the theory of flow with isotropic hardening [84], and, later, the theory of flow with anisotropic hardening. The creep strains were determined using various aging theories. However, the validity of the constitutive equations used in these studies was not analyzed.

The thermoviscoplastic state of solids began to be regularly studied in the 1970–80s using experimentally validated constitutive equations, taking into account the loading history, and analyzing the applicability of these equations to specific processes of nonisothermal loading [36, 87, 88, 91, 92, 95, 99, etc.]. In fact, these monographs provided the basis for the new thermoviscoplasticity division of solid mechanics, which studies the occurrence and development of displacements, strains, and stresses in solids nonisothermally loaded beyond the elastic limit in some regions of the material.

The main task of thermoviscoplasticity is to develop methods for determining the stresses, strains, and displacements in solids subject to the combined action of external nonuniform heating and surface and body forces that causes irreversible deformation of some elements of the body.

Generally, the solutions of boundary-value problems of thermoviscoplasticity are strongly dependent on the applicability of constitutive equations based on one thermoviscoplasticity theory or another. It is well to bear in mind that modern solid mechanics uses many models of the behavior of solids at various stages of deformation. Hence, there are many constitutive equations describing various deformation processes in solids.

Despite the great variety of constitutive equations, the deformation processes they describe are, in fact, classed as simple or nearly simple deformation or combined deformation along paths of small curvature. The applicability of constitutive equations to the description of the deformation processes in a structural member is not even questioned. The S. P. Timoshenko Institute of Mechanics of the National Academy of Sciences of Ukraine was the first to formulate and resolve this issue using the shape of deformation paths.

The experiments [96] revealed that the applicability of constitutive equations with clear formulation of reference tests can be ascertained from the shape of the deformation path of an element of the structural member subject to the loading process of interest. The shape of the deformation path is determined by the lag path of the vector properties of the material, i.e., its memory. The lag path of the vector properties of a material is the arc length of its deformation path after it kinks at a right angle at which the stress vector stabilizes relative to the deformation path. The lag path is usually 10 to 15 yield strains.

Deformation paths are classed as straight and slightly curved (paths of small curvature). The minimum radius of curvature of such paths is much greater than the lag path of the vector properties of the material.

There are also nearly straight paths. These are deformation paths that deviate from the straight line coming through the origin of coordinates in the strain space and the point at which the deformation path goes beyond the yield point by less than the lag path length. Deformation paths with minimum radius of curvature commensurable with the lag path are called path of medium curvature. If the radius of curvature of a deformation path is shorter than the lag path, then it is a path of large curvature or an arbitrary plane path. There are also paths of small curvature and small torsion in which not only the minimum radius of curvature, but also the minimum radius of torsion is greater than the lag path. Two-link and multilink broken-line deformation paths are also possible.

The results reported in [96] show that when an element of a body deforms along a straight or nearly straight path, the theory of small elastoplastic deformations taking the loading history into account and generalized to nonisothermal loading [90, 95, 96] is in good agreement with experimental data. In this case, the stress and strain vectors (deviators) in an isotropic body are almost coaxial. The theory of elastoplastic deformation along paths of small curvature [87, 95] accurately describes the nonisothermal deformation of an element of a body along a path of small curvature. In this case, the stress vector in an isotropic body is tangential to the path of irreversible deformation (close to the path of total small deformation).

In the two theories of thermoviscoplasticity mentioned above, the relationship between the stress and strain intensities is established using instantaneous thermomechanical surfaces and associated creep curves at different values of stresses and

temperature. An instantaneous thermomechanical surface is the locus of tensile stress–strain curves at fixed temperatures and a loading rate at which the material does not exhibit rheological properties. The same rate is used to load specimens to different levels of stress at which creep curves are plotted at the corresponding temperatures.

To study the deformation of an element of a body along more complex paths, several versions of experimentally validated constitutive equations were derived and reference tests for particularization of the scalar functionals appearing in these equations were set up. These constitutive equations were constructed using the postulate of isotropy [21] generalized to the case of nonisothermal loading [87]. These constitutive equations are detailed in [81–83, 92, 96]. Since the deformation paths of separate elements of a solid are usually unknown during loading, the shape of these paths is determined by finding solutions of boundary-value problems along them by the method of successive approximations. In the first approximation, the deformation paths are found by solving a boundary-value problem using the theory of small elastoplastic deformations and taking into account the loading history. To this end, the loading process is divided into stages. If it appears that the deformation paths of elements of the body are straight or nearly straight, the problem is considered solved. If, however, there are nonstraight or nearly straight paths, then the boundary-value problem is solved again using more complex constitutive equations, such as those following from the theory describing the deformation of an element of a body along a path of small curvature if such paths are among those obtained at the previous stage of solution. If the deformation paths are more complex, the boundary-value problem is solved using constitutive equations whose scalar functions are concretized taking into account the geometry of the deformation path obtained at the first stage of solution [92, 96]. An algorithm and results of thermoviscoplastic analysis of shells of revolution that undergo axisymmetric deformation along various plane paths are detailed in [83] and omitted here.

Note that all the above thermoviscoplastic equations are based on the assumption that the relationship between the stress and strain intensities is independent of the stress mode, i.e., these equations are the same for tension, compression, and torsion. Actually, the majority of structural steels are moderately sensitive to the stress mode. The tensile (compressive) or torsional stress–strain curves at small strains of these materials differ by less than 10%. However, the difference of the tensile (compressive) and torsional stress–strain curves for D16T aluminum alloy reaches 40% [19], i.e., its mechanical characteristics depend on the third deviatoric stress invariant (stress mode). The materials sensitive to the stress mode include various grades of cast iron whose tensile, torsional, and compressive stress–strain curves differ substantially.

To characterize the stress mode, use is made of an angle indicating how the shear stress is oriented in the octahedral plane with respect to the projection (onto this plane) of the principal axis along which one of the principal stresses acts [29, 158]. This angle is in a simple relationship with the Lode parameter [119], but, unlike it, is expressed in terms of the second and third deviatoric stress invariants rather than the principal stresses. The stress state of structural members made of such materials is analyzed using constitutive equations that disregard the stress mode and allowing for the difference between the elastic moduli of an orthotropic material by manipulating the compliance matrix [1, 102, 130, 135]. The stress mode was allowed for in plasticity problems for the first time in [97, 155–157] where constitutive equatins for simple deformation [97] and deformation along paths of small curvature [157] were derived. These equations relate the components of the engineering stress and strain tensors, assuming that the strains have elastic and inelastic components. The equations include two nonlinear functions found experimentally. One of these functions relates the first invariants of the stress and strain tensors, while the other function relates the second invariants of the respective deviatoric tensors. These functions are individualized in two series of reference tests on tubular specimens under proportional loading at several constant values of the stress mode angle and several temperatures.

Experiments showed that if the strains are lower than 5–6%, then the first stress and strain invariants are in linear relationship. The constitutive equations describing deformation along paths of small curvature are based on the assumption that the directional tensors of stresses and inelastic-strain increments coincide, while the constitutive equations describing deformation along straight paths are based on the assumption that the directional stress and strain tensors coincide. The constitutive equations from [157], which allow for the stress mode, were experimentally validated in [156, 157] and are widely used to solve boundary-value problems.

If the first invariants of the stress and strain tensors are in linear relationship and the material properties are independent of the stress mode and the relationship between the second invariants of the stress and strain deviators, then the constitutive equations [97, 157] go over into the conventional equations [92, 96] describing deformation along paths of small curvature and along straight paths based on the Prandtl–Reuss [123, 124] and Hencky [112] theories, respectively.

Various approaches are used to describe the damage of a material during deformation. When continuum mechanics is used to describe damage accumulation in isotropic materials during viscoplastic deformation, a scalar damage parameter is

introduced [53, 95], which follows from the kinematic equation [98] relating the rate of variation in damage and some equivalent stress. This approach describes the damage process as loosening of a microvolume.

Another approach [115, 116] to the description of the damage of a homogeneous material is to model dispersed single microdamages by quasispherical micropores either empty or filled with particles of damaged material and to use a theory of porous materials. Both approaches assume that all arbitrarily area elements are subject to the same damage.

However, experiments reveal that the distribution of damages in a deformed element under combined loading is anisotropic, which may strongly affect the behavior of the material. Therefore, as Ilyushin pointed out in [20], one damage measure may appear insufficient to characterize the moment of fracture if for no other reason than because the failure mechanisms due to the tangental and normal stresses are different. He proposed to introduce a symmetric damage tensor dependent on the loading history.

Kachanov [28] proposed to characterize the damage at a given point of a material by a parameter ψ_n, where $\vec{n}$ is the normal to the area element of interest. Hazhinskii [85] distinguishes intragranular and intergranular damage. He associated intragranular damage with the loosening of the material and used a scalar function ω to describe it. To describe intergranular damage on an area with normal $\vec{n}$, he used a parameter ω_n similar to ψ_n used in [28]. A possible way to study microdamage in a homogeneous material is the model proposed in [37], in which the damage parameter is the vector $\overline{\omega}$ whose components are related to the space of principal stresses. Then the damage of a material on an area with normal n is characterized by the projection of this vector onto the normal.

In addition to the constitutive equations describing the thermoviscoplastic deformation of structural members made of isotropic materials, in [86, 143, 147], tensor-linear constitutive equations were derived and reference tests for studying the elastoplastic deformation of orthotropic bodies were set up. In the orthotropic materials being considered, the principal axes of thermomechanical anisotropy are assumed to coincide with the axes of a cylindrical or Cartesian coordinate system.

In what follows, we will discuss the results on three-dimensional thermoviscoplastity [140, 142] obtained at the Thermoplasticity Department of the S. P. Timoshenko Institute of Mechanics under the supervision of the authors of the present review. Let us formulate general constitutive equations that can be used to study various processes of nonisothermal loading of various isotropic and orthotropic structural members with and without regard to damage, stress mode, and loading history.

We will address axisymmetric three-dimensional thermoviscoplastic problems for bodies of canonical shape and solids of revolution with arbitrary meridional section; nonaxisymmetric three-dimensional thermoviscoplastic problems for solids of revolution; three-dimensional thermoviscoplastic problems for bodies of arbitrary shape, including circumferentially nonclosed solids of revolution; three-dimensional thermoviscoplastic problems for compound structural members in the form of solids of revolution made of isotropic and orthotropic materials with the principal axes of anisotropy not coinciding with the axes of the coordinate system in which the boundary-value problem is solved.

1. Thermoviscoplastic Problem Formulation. Let us formulate the general thermoviscoplastic problem. This problem statement can then be adapted to the geometry of the object of interest, its material, type of thermomechanical loading, etc.

Consider a compound body made of isotropic and orthotropic inelastic materials. To describe it, we will use an orthogonal coordinate system q_i ($i = 1, 2, 3$). The body is subject to volume $\vec{K}(K_1, K_2, K_3)$ and surface $\vec{t}_n(t_{n1}, t_{n2}, t_{n3})$ forces and nonuniform heating that cause small strains in its elements. Assume that the material characteristics depend on temperature. The body is loaded and heated so that its elements undergo simple (or nearly simple) deformation or deformation along paths of small curvature, accompanied by inelastic deformation and unloading.

The compound body is a discretely inhomogeneous solid of revolution, and each of its components is a solid of revolution too. The body and all its components have a common axis of revolution aligned with the coordinate axis q_1. The components of the body are made of dissimilar materials and were joined without tension at temperature T_0 so that they are in perfect mechanical and thermal contact. The stress–strain state of such solids is analyzed by determining the temperature T (nonstationary heat conduction problem) and the displacements u_i, strains ε_{ij}, and stresses σ_{ij} $(i, j = 1, 2, 3)$ at fixed time points (thermoviscoplastic problems). The strain tensor is represented as the sums of the tensors of elastic and plastic strains and creep strains. Inelastic volume changes during deformation are also assumed.

The analysis carried out when deriving the constitutive equations that allow for the stress mode shows that this assumption is valid for strains higher than 4–5%. The variation in the elastic strains with stresses follows the generalized Hooke's law.

To account for the deformation history, the whole process of loading and heating is divided into rather small time intervals (steps) so that their endpoints are as close as possible to the onsets of unloading of elements of the body. The history is traced by solving the problem at each step.

The relations between the components of the stress tensor σ_{ij} and the components of the strain tensor ε_{ij} (constitutive equations) for isotropic and anisotropic materials have the same form, irrespective of the stage of deformation. Let us represent these relations in the form of the generalized Hooke's law for anisotropic materials when the orthogonal curvilinear coordinate axes q_i do not coincide with the principal axes q_i' of thermal and mechanical anisotropy of the orthotropic material:

$$\sigma_{ij} = A_{ijmn}\varepsilon_{mn} - \sigma_{ij}^{*} \quad (m, n = 1, 2, 3) \tag{1.1}$$

provided that

$$A_{ijmn} = A_{jimn} = A_{ijnm} = A_{mnij}, \tag{1.2}$$

where A_{ijmn}, … and additional terms σ_{ij}^{*} depend on the type of anisotropy of the material, the theories of plasticity and creep used, and the method of linearization of the constitutive equations. To linearize the constitutive equations, use is made of methods of successive linear approximations: in each approximation, the original nonlinear problem is reduced to a linear problem of elasticity including additional terms introduced to describe thermal deformation, inelasticity, damage, the dependence of the stress–strain curves on the stress mode and temperature, etc. They are determined from the solution of the problem found at the previous approximation. The summation is over repeated indices in monomial expressions within the limits indicated in parentheses and no summation is over indices in angular brackets.

To particularize the relationship among the stress and strain intensities, temperature, and time, it is proposed to use instantaneous thermomechanical surface, creep curves, and stress rupture curves. These curves are plotted using experimental data for different temperatures. The temperature distribution and stress–strain state in the body are found numerically by solving variational equations.

2. Constitutive Equations of Thermoviscoplasticity for Isotropic and Orthotropic Materials. Let us discuss in detail the constitutive equations of thermoviscoplasticity for isotropic and orthotropic materials. We will consider elastic orthotropic materials, elastic materials with different tensile and compressive moduli of elasticity, inelastic materials undergoing simple deformation, inelastic materials deforming along paths of small curvature, and damaged elastic materials. For isotropic materials, we will present constitutive equations describing simple deformation, constitutive equations describing deformation along paths of small curvature, constitutive equations allowing for the stress mode, and constitutive equations allowing for creep damage.

Since we will mainly consider compound solids of revolution, all the equations will be written in a cylindrical coordinate system. In the case of orthotropy, we will consider only cylindrically or rectilinearly orthotropic materials, one of the axes of anisotropy coinciding with the axis of revolution of the body.

2.1. Orthotropic Materials. Modern mechanical engineering, aircraft construction, shipbuilding, rocketry, etc. cannot be imagined without composite materials. The combination of a light, fragile, compliant matrix and very strong and rigid reinforcing fibers or particles results in light, yet strong and rigid materials, which are widely used to fabricate a great variety of articles: from crucial elements of aircraft wings, firings of reentry vehicles, and control rods of nuclear reactors to golf-clubs, hockey sticks, jumping poles, and fishing rods. A peculiar feature of composites is that their properties in different directions can be predefined, i.e., they initially possess pronounced mechanical and thermal anisotropy. Along with anisotropy, composites often have an original property: their tensile and compressive moduli of elasticity or tensile and compressive stiffnesses are different [107, 109, 110].

For example, the compressive moduli are 20 to 25% less than the tensile moduli in epoxy-resin composites reinforced with unidirectional glass fibers and 15 to 20% larger than the tensile moduli in epoxy-resin composites reinforced with unidirectional boron fibers. The tensile moduli may exceed the compressive moduli by 40% and more in epoxy-resin composites reinforced with unidirectional carbon fibers. The tensile moduli of other fibrous composites, such as carbon composites reinforced with carbon fibers, are 2 to 5 times as high as the compressive moduli.

Thus, it is impossible to be certain of whether the compressive moduli of fibrous composites are higher or lower than their tensile moduli. The situation is similar for particulate materials. There is yet no physically plausible explanation of this

phenomenon. The further development of composite micromechanics will possibly explain it. Until then, the stress analysis of composite members has to neglect their heterogeneous structure and to use a phenomenological description of the material. In other words, the behavior of a composite member with different tensile and compressive moduli is described using anisotropic elasticity theory [33].

2.1.1. Perfectly Elastic State of an Orthotropic Body. If the material of the body is perfectly elastic and the position of the coordinate system q_i relative to the principal axes of mechanical and thermal anisotropy q'_i is determined by direction cosines l_{ij}, then the coefficients A_{ijmn} in (1.1) are defined by

$$A_{ijmn} = A'_{kp\alpha\beta} l_{ki} l_{pj} l_{km} l_{\beta n}. \tag{2.1}$$

The additional terms σ^*_{ij} in (1.1) are given by

$$\sigma^*_{ij} = \sigma^T_{ij} = \beta_{ij} (T - T_0), \tag{2.2}$$

where T_0 is the initial temperature T of an element of the body in stress–strain-free state, $\beta_{ij} = \beta'_{ij} l_{mi} l_{nj}$ (m, n = 1, 2, 3). The nonzero thermal parameters β'_{mn} are defined by

$$\beta'_{11} = A'_{11}\alpha_1 + A'_{12}\alpha_2 + A'_{13}\alpha_3 \quad (1, 2, 3), \tag{2.3}$$

where α_i are the coefficients of linear thermal expansion along the principal axes of anisotropy q'_i; the symbol (1, 2, 3) means that the missing expressions for β'_{ij} can be obtained by circular permutation of the indices.

For an elastic orthotropic material with the principal axes of mechanical and thermal anisotropy aligned with the axes of an orthogonal coordinate system X_1, X_2, X_3, the components of the strain and stress tensors can be expressed in terms of the engineering constants as follows [33]:

$$\begin{Bmatrix} \varepsilon_{11} - \varepsilon^T_{11} \\ \varepsilon_{22} - \varepsilon^T_{22} \\ \cdots \\ \varepsilon_{23} \end{Bmatrix} = \begin{bmatrix} \frac{1}{E_1} & -\frac{\nu_{21}}{E_2} & -\frac{\nu_{31}}{E_3} & 0 & 0 & 0 \\ -\frac{\nu_{12}}{E_1} & \frac{1}{E_2} & -\frac{\nu_{32}}{E_3} & 0 & 0 & 0 \\ \vdots & \vdots & \vdots & \vdots & \vdots & \\ 0 & 0 & 0 & 0 & 0 & \frac{1}{2G_{23}} \end{bmatrix} \begin{Bmatrix} \sigma_{11} \\ \sigma_{22} \\ \vdots \\ \sigma_{23} \end{Bmatrix}, \tag{2.4}$$

where E_i are the elastic moduli along the principal axes of anisotropy coinciding with the coordinate axes; G_{ij} are the shear moduli in the corresponding coordinate planes; ν_{ij} is Poisson's ratio characterizing the compression of an element along the X_j-axis caused by its tension along the X_i-axis; $\varepsilon^T_{ii} = \alpha^T_{ii}(T - T_0)$, α^T_{ii} are the coefficients of linear thermal expansion along the principal axes of anisotropy. From the existence condition for a positive definite strain energy function, it follows that $\nu_{ij} / E_i = \nu_{ji} / E_j$ and the compliance matrix in (2.4) is symmetric.

In the orthotropic materials being considered, the principal axes of thermal and mechanical anisotropy can coincide with the axes of a cylindrical or Cartesian coordinate system whose one axis is the body's axis of revolution.

Thus, X_i denote either the Cartesian coordinates z, x, y or the cylindrical coordinates z, r, φ. Resolving the system of equations (2.4) for the stresses, we obtain their expressions in terms of the strains in the principal axes of anisotropy, i.e., in the coordinate system z, r, φ in the case of cylindrical orthotropy and in the Cartesian coordinate system z, x, y in the case of rectilinear orthotropy. Transforming, using well-known formulas, from the Cartesian coordinates to the cylindrical coordinates, we obtain the following stress–strain relationship:

$$\sigma_{ij} = A_{ijkl} (\varepsilon_{kl} - \varepsilon^T_{kl}), \tag{2.5}$$

where the expressions for A_{ijkl} $(i, j, k, l = z, r, \varphi)$ depend on the type of material.

In the cylindrically orthotropic case, they are

$$A_{zzzz} = \Delta_{11} / \Delta, \quad A_{zzrr} = A_{rrzz} = \Delta_{12} / \Delta, \quad A_{zz\varphi\varphi} = A_{\varphi\varphi zz} = \Delta_{13} / \Delta,$$

$$A_{rrrr}=\Delta_{22}/\Delta,\quad A_{rr\varphi\varphi}=A_{\varphi\varphi rr}=\Delta_{23}/\Delta,\quad A_{\varphi\varphi\varphi\varphi}=\Delta_{33}/\Delta,$$

$$A_{zrzr}=G_{zr},\quad A_{z\varphi z\varphi}=G_{z\varphi},\quad A_{r\varphi r\varphi}=G_{r\varphi},$$

$$A_{zzzr}=A_{zzz\varphi}=A_{zzr\varphi}=A_{rrzr}=A_{rrz\varphi}=A_{rrr\varphi}=A_{\varphi\varphi zr}=A_{\varphi\varphi z\varphi}=A_{\varphi\varphi r\varphi}$$

$$=A_{zrzz}=A_{zrrr}=A_{zr\varphi\varphi}=A_{zrz\varphi}=A_{zrr\varphi}=A_{z\varphi zz}=A_{z\varphi rr}A_{z\varphi\varphi\varphi}=A_{z\varphi zr}$$

$$=A_{z\varphi r\varphi}=A_{r\varphi zz}=A_{r\varphi rr}=A_{r\varphi\varphi\varphi}=A_{r\varphi zr}=A_{r\varphi z\varphi}=0, \tag{2.6}$$

where

$$\Delta_{11}=(1/E_{\varphi}-\nu_{r\varphi}^2/E_r)/E_r,\quad \Delta_{12}=(\nu_{z\varphi}\nu_{r\varphi}/E_r+\nu_{zr}/E_{\varphi})/E_z,$$

$$\Delta_{13}=(\nu_{zr}\nu_{r\varphi}+\nu_{z\varphi})/E_zE_r,\quad \Delta_{22}=(1/E_{\varphi}-\nu_{z\varphi}^2/E_z)/E_z,$$

$$\Delta_{23}=(\nu_{zr}\nu_{z\varphi}/E_z+\nu_{r\varphi}/E_r)/E_z,\quad \Delta_{33}=(1/E_r-\nu_{zr}^2/E_z)/E_z,$$

$$\Delta=(\Delta_{11}-\nu_{zr}\Delta_{12}-\nu_{z\varphi}\Delta_{13})/E_z, \tag{2.7}$$

$$\varepsilon_{zz}^T=\alpha_{zz}^T(T-T_0),\quad \varepsilon_{rr}^T=\alpha_{rr}^T(T-T_0),\quad \varepsilon_{\varphi\varphi}^T=\alpha_{\varphi\varphi}^T(T-T_0),$$

$$\varepsilon_{zr}^T=\varepsilon_{z\varphi}^T=\varepsilon_{r\varphi}^T=0. \tag{2.8}$$

In the rectilinearly orthotropic case, the coefficients A_{ijkl} and the thermal strains ε_{kl}^T are expressed as

$$A_{zzzz}=\Delta_{11}^*,\quad A_{zzr\varphi}=(\Delta_{13}^*-\Delta_{12}^*)\sin 2\varphi/2,$$

$$\left.\begin{matrix}A_{zzrr}\\A_{zz\varphi\varphi}\end{matrix}\right\}=[\Delta_{12}^*+\Delta_{13}^*\pm(\Delta_{12}^*-\Delta_{13}^*)\cos 2\varphi]/2,$$

$$\left.\begin{matrix}A_{rrrr}\\A_{\varphi\varphi\varphi\varphi}\end{matrix}\right\}=[(3\Delta_{22}^*+3\Delta_{33}^*+2\Delta_{23}^*+4G_{xy})\pm 4(\Delta_{22}^*-\Delta_{33}^*)\cos 2\varphi$$

$$+(\Delta_{22}^*+\Delta_{33}^*-2\Delta_{23}^*-4G_{xy})\cos 4\varphi]/8,$$

$$A_{rr\varphi\varphi}=[(\Delta_{22}^*+\Delta_{33}^*+6\Delta_{23}^*-4G_{xy})-(\Delta_{22}^*+\Delta_{33}^*-2\Delta_{23}^*-4G_{xy})\cos 4\varphi]/8, \tag{2.9}$$

$$\left.\begin{matrix}A_{rrr\varphi}\\A_{\varphi\varphi r\varphi}\end{matrix}\right\}=[2(\Delta_{33}^*-\Delta_{22}^*)\sin 2\varphi\pm(\Delta_{22}^*+\Delta_{33}^*-2\Delta_{23}^*-4G_{xy})\sin 4\varphi]/8,$$

$$\left.\begin{matrix}A_{zrzr}\\A_{z\varphi z\varphi}\end{matrix}\right\}=[(G_{zx}+G_{zy})\pm(G_{zx}-G_{zy})\cos 2\varphi]/2,$$

$$A_{r\varphi r\varphi}=[(\Delta_{22}^*+\Delta_{33}^*-2\Delta_{23}^*+4G_{xy})-(\Delta_{22}^*+\Delta_{33}^*-2\Delta_{23}^*-4G_{xy})\cos 4\varphi]/8,$$

$$A_{zzzr}=A_{zzz\varphi}=\cdots=A_{zrzz}=A_{zrrr}=A_{zr\varphi\varphi}=A_{zrr\varphi}=\cdots=A_{r\varphi z\varphi}=0,$$

$$\Delta_{ij}^*=\Delta_{ij}/\Delta,\quad \Delta_{11}=(1/E_y-\nu_{xy}^2/E_x)/E_x,\quad \Delta_{12}=(\nu_{zy}^2\nu_{xy}/E_x+\nu_{zx}/E_y)/E_z,$$

$$\Delta_{13}=(\nu_{zx}\nu_{xy}+\nu_{zy})/(E_zE_x),\quad \Delta_{22}=(1/E_y-\nu_{zy}^2/E_z)/E_z, \tag{2.10}$$

$$\Delta_{23} = (\nu_{zx}\nu_{zy}/E_z + \nu_{xy}/E_x)/E_z, \qquad \Delta_{33} = (1/E_x - \nu_{zx}^2/E_z)/E_z,$$

$$\Delta = (\Delta_{11} - \nu_{zx}\Delta_{12} - \nu_{zy}\Delta_{13})/E_z, \qquad \varepsilon_{ij}^T = \alpha_{ij}^T(T - T_0) \qquad (i,j = z,r,\varphi), \tag{2.11}$$

$$\left.\begin{matrix}\alpha_{rr}^T \\ \alpha_{\varphi\varphi}^T\end{matrix}\right\} = (\alpha_{xx}^T + \alpha_{yy}^T)/2 \pm (\alpha_{xx}^T - \alpha_{yy}^T)\cos 2\varphi/2,$$

$$\alpha_{r\varphi}^T = (\alpha_{yy}^T - \alpha_{xx}^T)\sin 2\varphi/2, \qquad \alpha_{zr}^T = \alpha_{z\varphi}^T = 0.$$

Let us represent the stress–strain relation (1.1) in the form of Hooke's law for homogeneous isotropic materials. To this end, we represent the coefficients A_{ijkl} as $A_{ijkl} = A_{ijkl}^0(1 - \omega_{ijkl})$, where A_{ijkl}^0 are their average values independent of the circumferential coordinate, and $A_{ijkl}^0\omega_{ijkl}$ are functions characterizing the circumferential variation in and the temperature dependence of A_{ijkl}. Then the stresses and the strains can be related as

$$\begin{Bmatrix}\sigma_{zz}\\ \sigma_{rr}\\ \sigma_{\varphi\varphi}\\ \sigma_{zr}\\ \sigma_{z\varphi}\\ \sigma_{r\varphi}\end{Bmatrix} = \begin{bmatrix} A_{zzzz}^0 & A_{zzrr}^0 & A_{zz\varphi\varphi}^0 & 0 & 0 & 0\\ A_{zzrr}^0 & A_{rrrr}^0 & A_{rr\varphi\varphi}^0 & 0 & 0 & 0\\ A_{zz\varphi\varphi}^0 & A_{rr\varphi\varphi}^0 & A_{\varphi\varphi\varphi\varphi}^0 & 0 & 0 & 0\\ 0 & 0 & 0 & A_{zrzr}^0 & 0 & 0\\ 0 & 0 & 0 & 0 & A_{z\varphi z\varphi}^0 & 0\\ 0 & 0 & 0 & 0 & 0 & A_{r\varphi r\varphi}^0 \end{bmatrix} * \begin{Bmatrix}\varepsilon_{zz}\\ \varepsilon_{rr}\\ \varepsilon_{\varphi\varphi}\\ \varepsilon_{zr}\\ \varepsilon_{z\varphi}\\ \varepsilon_{r\varphi}\end{Bmatrix} - \begin{Bmatrix}\sigma_{zz}^*\\ \sigma_{rr}^*\\ \sigma_{\varphi\varphi}^*\\ \sigma_{zr}^*\\ \sigma_{z\varphi}^*\\ \sigma_{r\varphi}^*\end{Bmatrix}, \tag{2.12}$$

where

$$\sigma_{zz}^* = A_{zzzz}\varepsilon_{zz}^T + A_{zzrr}\varepsilon_{rr}^T + A_{zz\varphi\varphi}^T\varepsilon_{\varphi\varphi}^T + A_{zzzz}^0\omega_{zzzz}\varepsilon_{zz} + A_{zzrr}^0\omega_{zzrr}\varepsilon_{rr} + A_{zz\varphi\varphi}^0\omega_{zz\varphi\varphi}\varepsilon_{\varphi\varphi},$$

$$\cdots\cdots \tag{2.13}$$

$$\sigma_{r\varphi}^* = 2A_{r\varphi r\varphi}^0\omega_{r\varphi r\varphi}\varepsilon_{r\varphi}$$

for cylindrically orthotropic materials and

$$\sigma_{zz}^* = A_{zztz}^0\omega_{zzzz}\varepsilon_{zz} + A_{zzrr}^0\omega_{zzrr}\varepsilon_{rr} + A_{zz\varphi\varphi}^0\omega_{zz\varphi\varphi}\varepsilon_{\varphi\varphi}$$

$$-2A_{zzr\varphi}(\varepsilon_{r\varphi} - \varepsilon_{r\varphi}^T) + A_{zzzz}\varepsilon_{zz}^T + A_{zzrr}\varepsilon_{rr}^T + A_{zz\varphi\varphi}\varepsilon_{\varphi\varphi}^T,$$

$$\cdots\cdots \tag{2.14}$$

$$\sigma_{r\varphi}^* = 2A_{r\varphi r\varphi}^0\omega_{r\varphi r\varphi}\varepsilon_{r\varphi} + 2A_{r\varphi r\varphi}\varepsilon_{r\varphi}^T - A_{zzr\varphi}(\varepsilon_{zz} - \varepsilon_{zz}^T)$$

$$-A_{rrr\varphi\varphi}(\varepsilon_{rr} - \varepsilon_{rr}^T) - A_{\varphi\varphi r\varphi}(\varepsilon_{\varphi\varphi} - \varepsilon_{\varphi\varphi}^T)$$

for rectilinearly orthotropic materials.

Then the boundary-value problem can be solved by the method of successive approximations. In the first approximation, $\omega_{ijmn} = 0$ is set and the boundary-value problem is solved for constant coefficients A_{ijmn}^0 and additional terms σ_{ij}^*. Then, the values of ε_{ij} and the functions ω_{ijmn} are used, to refine the additional terms σ_{ij}^* in (2.13) or (2.14), and the boundary-value problem is solved again. The process of successive approximations is terminated once the difference between the values of σ_{ij}^* has become less than a predefined error. Note that ω_{ijmn} do not change in this process.

2.1.2. Elastic State of Orthotropic Bodies Made of Materials with Different Tensile and Compressive Moduli of Elasticity. As mentioned earlier, the compliance matrix in (2.5) for an anisotropic material with equal tensile and compressive moduli is symmetric. For a bimodulus material, the relations between Poisson's ratios and Young's moduli do not hold and the compliance matrix is asymmetric. The compliance matrix can be made symmetric by defining certain relations between the tensile and compressive moduli that would allow satisfying the well-known transformations of anisotropic elasticity theory. Such an approach was proposed by Ambartsumyan and his followers [1]. However, these relations would restrict the use of real engineering materials.

The compliance matrix can be symmetrized by one of the following methods [60].

1. Identification of the sign of the mean stress, i.e., the first invariant of the stress tensor in the neighborhood of the point of interest. Depending on the sign, either tensile or compressive material characteristics are used.

2. Use of the stress mode angle [81, 82, 87] expressed in terms of the third and second deviatoric stress invariants.

3. Another approach proposed in [109] is to sum the coefficients of the tensile and compressive compliance matrices in proportion to the corresponding compressive and tensile stresses. This can be done by introducing weighting coefficients to allow for the influence of the sign of the normal stresses in two perpendicular directions on the corresponding coefficients of the compliance matrix. Depending on the sign of the stresses, the coefficients of the compliance matrix in (2.4) are the following:

$$\text{if} \quad \sigma_{11} < 0, \quad \text{then} \quad \frac{1}{E_1} = \frac{1}{E_1^-}; \quad \text{if} \quad \sigma_{11} > 0, \quad \text{then} \quad \frac{1}{E_1} = \frac{1}{E_1^+},$$

$$\ldots\ldots\ldots\ldots\ldots\ldots\ldots\ldots\ldots\ldots$$

$$\text{if} \quad \begin{matrix}\sigma_{11} > 0,\\ \sigma_{22} > 0\end{matrix} \quad \text{then} \quad \frac{\nu_{12}}{E_1} = \frac{\nu_{21}}{E_2} = \frac{\nu_{12}^+}{E_1^+}; \quad \text{if} \quad \begin{matrix}\sigma_{11} < 0,\\ \sigma_{22} < 0\end{matrix} \quad \text{then} \quad \frac{\nu_{12}}{E_1} = \frac{\nu_{21}}{E_2} = \frac{\nu_{12}^-}{E_1^-};$$

$$\ldots\ldots\ldots\ldots\ldots\ldots\ldots\ldots\ldots\ldots$$

$$\text{if} \quad \begin{matrix}\sigma_{11} > 0,\\ \sigma_{22} < 0\end{matrix} \quad \text{then} \quad \frac{\nu_{12}}{E_1} = \frac{\nu_{21}}{E_2} = \frac{|\sigma_{11}|}{|\sigma_{11}|+|\sigma_{22}|}\frac{\nu_{12}^+}{E_1^+} + \frac{|\sigma_{22}|}{|\sigma_{11}|+|\sigma_{22}|}\frac{\nu_{21}^-}{E_2^-}; \tag{2.15}$$

$$\text{if} \quad \begin{matrix}\sigma_{11} < 0,\\ \sigma_{22} > 0\end{matrix} \quad \text{then} \quad \frac{\nu_{12}}{E_1} = \frac{\nu_{21}}{E_2} = \frac{|\sigma_{11}|}{|\sigma_{11}|+|\sigma_{22}|}\frac{\nu_{12}^-}{E_1^-} + \frac{|\sigma_{22}|}{|\sigma_{11}|+|\sigma_{22}|}\frac{\nu_{21}^+}{E_2^+};$$

$$\ldots\ldots\ldots\ldots\ldots\ldots\ldots\ldots\ldots\ldots$$

$$\text{if} \quad \sigma_{12} > 0, \quad \text{then} \quad \frac{1}{G_{12}} = \frac{1}{G_{12}^+} = \frac{1}{E_{12}^{45+}} - \left(\frac{1}{E_1^+} + \frac{1}{E_2^+} - \frac{\nu_{12}^+}{E_1^+}\right);$$

$$\text{if} \quad \sigma_{12} < 0, \quad \text{then} \quad \frac{1}{G_{12}} = \frac{1}{G_{12}^-} = \frac{1}{E_{12}^{45-}} - \left(\frac{1}{E_1^-} + \frac{1}{E_2^-} - \frac{\nu_{12}^-}{E_1^-}\right).$$

Though there is yet no theory behind such approaches, they allow us to simmetrize the compliance matrix and to use anisotropic elasticity theory to solve the problem posed. Such approaches were used to develop a method for analyzing the stress–strain state of layered cylindrically or rectilinearly orthotropic solids of revolution under nonaxisymmetric thermomechanical loading [56–59, 60, 65, 135, etc.].

It should be noted that the shear moduli in tension or compression cannot be measured. They are determined from experimental values of other material characteristics. For example, because of the nonuniform cross-sectional distribution of mechanical characteristics of a rectilinearly orthotropic material, the σ_{ij}-vs.-ε_{ij} curve for $i \neq j$ can experimentally be obtained only by averaging the shear stresses and shear strains over the circumference. In this case, the real (measured) shear moduli are the average values of the shear moduli in tension and compression. Therefore, the tensile or compressive moduli are determined

by the following formula from tension or compression tests on specimens cut out along the plane *ij* at an angle of 45° to one of the axes:

$$\frac{1}{G_{ij}} = \frac{4}{E_{ij}^{45}} - \left(\frac{1}{E_i} + \frac{1}{E_j} - \frac{2\nu_{ij}}{E_i} \right),$$

where E_{ij}^{45} is the shear modulus in tension or compression of a specimen cut out along the plane *ij* at an angle of 45°.

Resolving the system of equations with symmetric compliance matrix for stresses, we obtain an expression for the stresses in terms of the principal strains. Transforming, using well-known formulas, from the Cartesian coordinates to the cylindrical coordinates, we obtain a stress–strain relationship in the form (2.5).

Since the material properties depend on the stress state, the determination of the stress–strain state is a problem with unknown mechanical characteristics. However, we can get rid of this uncertainty by using the following iterative procedure. First, the displacements and stresses are determined in the cylindrical coordinate system with characteristics (for example, average Poisson's ratios and tensile and compressive moduli) originally specified in the Cartesian coordinate system. Then the new material characteristics are determined considering the sign of the stresses calculated at the previous step. The process is terminated once the required accuracy has been achieved. Since the problem is solved in the cylindrical coordinate system, well-known formulas can be used to transform to the Cartesian coordinate system.

2.1.3. Inelastic State of Orthotropic Bodies Undergoing Simple Deformation [36, 147]. If an orthotropic body undergoes irreversible deformation, we will use the constitutive equations (1.1), (2.5) or (2.12) if the elastic parameters A_{ijmn} are defined by (2.1), (2.6)–(2.11) in terms of the engineering elastic constants [33], the parameters A_{ijmn}^0 are averages of A_{ijmn} over some temperature range, and the additional terms σ_{ij}^* are defined by

$$\sigma_{ij}^* = \sigma_{ij}^T + \sigma_{ij}^n \tag{2.16}$$

in the former case and

$$\sigma_{ij}^* = \sigma_{ij}^\varepsilon + \sigma_{ij}^n \tag{2.17}$$

in the latter case, where

$$\sigma_{ij}^T = \beta_{ij}(T - T_0), \quad \sigma_{ij}^* = \sigma_{ij}^\varepsilon = A_{ijmn}^0 \omega_{ijmn} \varepsilon_{mn} + \beta_{ij}(T - T_0), \quad \sigma_{ij}^n = \sigma_{ij}'^n l_{im} l_{in} \quad (m, n = 1, 2. 3), \tag{2.18}$$

$$\sigma_{11}'^n = A_{11}' \varepsilon_{11}'^n + A_{12}' \varepsilon_{12}'^n + A_{13}' \varepsilon_{13}'^n, \quad \sigma_{12}'^n = 2G_{12}' \varepsilon_{12}'^n \quad (1, 2, 3). \tag{2.19}$$

It is assumed that the total strain ε_{ij}' in the coordinate system q_i' is the sum of elastic ($\varepsilon_{ij}'^{\,e}$) and irreversible ($\varepsilon_{ij}'^{\,n}$) strains:

$$\varepsilon_{ij}' = \varepsilon_{ij}'^{\,e} + \varepsilon_{ij}'^{\,n}. \tag{2.20}$$

The elastic strains $\varepsilon_{ij}'^{\,e}$ are determined by Hooke's law for orthotropic materials [33], while the irreversible strains $\varepsilon_{ij}'^{\,n}$ are represented as the sum of instantaneous plastic strains $\varepsilon_{ij}'^{\,p}$ and creep strains $\varepsilon_{ij}'^{\,c}$:

$$\varepsilon_{ij}'^{\,n} = \varepsilon_{ij}'^{\,p} + \varepsilon_{ij}'^{\,c}. \tag{2.21}$$

The principal plastic strains are expressed as

$$\varepsilon_{11}'^{\,p} = \psi_{11}' \sigma_{11}' + \psi_{12}' \sigma_{22}' + \psi_{13}' \sigma_{33}', \quad \varepsilon_{12}'^{\,p} = g_{12}' \sigma_{12}' \quad (1, 2, 3). \tag{2.22}$$

To determine the creep strains, we will divide the loading process into steps. Then at the end of the *m*th step of loading and heating, the creep strains are defined by

$$(\varepsilon'^{\,c}_{ij})_m = \sum_{k=1}^{m} \Delta_k \varepsilon'^{\,c}_{ij}. \tag{2.23}$$

The increments of principal creep strains are given by

$$\Delta_k \varepsilon'^{\,c}_{11} = C'_{11}\sigma'_{11} + C'_{12}\sigma'_{22} + C'_{13}\sigma'_{33}, \quad \Delta_k \varepsilon'^{\,c}_{12} = D'_{12}\sigma'_{12} \quad (1, 2, 3). \tag{2.24}$$

The stresses σ'_{ij} in the principal axes of anisotropy q' are related to the stresses σ_{ij} in the coordinate system q_i by

$$\sigma'_{ij} = \sigma_{mn} l_{im} l_{jn}. \tag{2.25}$$

The functions ψ'_{ij}, g'_{ij}, C'_{ij}, and D'_{ij} are determined experimentally from instantaneous thermomechanical surfaces and associated creep curves, which characterize the material properties along the principal axes of anisotropy and shear between them.

The functions ψ'_{ij} are determined from instantaneous tensile stress–strain curves of plane specimens stretched along the principal axes of anisotropy at different temperatures and measurement of the longitudinal and transverse strains:

$$\psi'_{11} = \frac{|\varepsilon'^{\,p}_{11}|}{\sigma'^{\,D}_{11}}, \quad \psi'_{21} = -\frac{|\varepsilon'^{\,p}_{22}|}{\sigma'^{\,D}_{11}}, \quad \psi'_{31} = -\frac{|\varepsilon'^{\,p}_{33}|}{\sigma'^{\,D}_{11}} \quad (1, 2, 3). \tag{2.26}$$

The functions C'_{ij} are determined from the associated creep curves:

$$C'_{11} = \frac{|\Delta\varepsilon'^{\,c}_{11}|}{\sigma'^{\,D}_{11}}, \quad C'_{21} = -\frac{|\Delta\varepsilon'^{\,c}_{22}|}{\sigma'^{\,D}_{11}}, \quad C'_{31} = -\frac{|\Delta\varepsilon'^{\,c}_{33}|}{\sigma'^{\,D}_{11}} \quad (1, 2, 3). \tag{2.27}$$

The functions g'_{ij} are determined by instantaneous diagrams obtained from pure-shear tests between the principal axes of anisotropy:

$$g'_{12} = g'_{21} = \frac{|\varepsilon'^{\,p}_{12}|}{\sigma'^{\,D}_{12}} \quad (1, 2, 3). \tag{2.28}$$

The functions D'_{ij} are determined by the associated creep curves:

$$D'_{12} = D'_{21} = \frac{\Delta\varepsilon'^{\,p}_{12}}{\sigma'^{\,D}_{12}} \quad (1, 2, 3), \tag{2.29}$$

where $\sigma'^{\,D}_{ij}$ are determined using formulas of instantaneous deformation.

The tests [30, 113, etc.] demonstrate that the functions ψ'_{ij} and C'_{ij} usually form asymmetric matrices, i.e., $\psi'_{ij} \neq \psi'_{ji}$, $C'_{ij} \neq C'_{ji}$ ($i \neq j$). If the material is inelastic and incompressible, then

$$\varepsilon'^{\,p}_{11} + \varepsilon'^{\,p}_{22} + \varepsilon'^{\,p}_{33} = 0, \quad \varepsilon'^{\,c}_{11} + \varepsilon'^{\,c}_{22} + \varepsilon'^{\,c}_{33} = 0 \tag{2.30}$$

and

$$\psi'_{21} = \psi'_{31} = -0.5\psi'_{11}, \quad C'_{21} = C'_{31} = -0.5C'_{11}. \tag{2.31}$$

If the matrices of the functions ψ'_{ij} and C'_{ij} are symmetric, i.e., $\psi'_{ij} = \psi'_{ji}$, $C'_{ij} = C'_{ji}$, and the material is inelastically incompressibloe (2.30), then these functions with unequal indices are expressed in terms of the corresponding functions with equal indices as follows:

$$\varepsilon'^{\,p}_{11} + \varepsilon'^{\,p}_{22} + \varepsilon'^{\,p}_{33} = 0, \quad \varepsilon'^{\,c}_{11} + \varepsilon'^{\,c}_{22} + \varepsilon'^{\,c}_{33} = 0 \quad (1, 2, 3), \tag{2.32}$$

$$C'_{12} = C'_{21} = -0{,}5(C'_{11} + C'_{22} - C'_{33}) \quad (1, 2, 3).$$

To determine the functions ψ'_{ij} and C'_{ij} in these cases, we need to have instantaneous tensile stress–strain curves and associated creep curves only for the three principal axes of anisotropy and to measure only the longitudinal strains.

Note that the functions g'_{ij} and D'_{ij} characterizing shear between the principal axes of anisotropy can be determined not from pure-shear tests (2.28), (2.29), but from uniaxial-tension tests on specimens cut out along axes equally inclined to two principal axes of anisotropy and orthogonal to the third principal axis. It is necessary to use coordinate rotation formulas for the functions $\psi'_{ij}, g'_{ij}, C'_{ij}$, and D'_{ij}, similar to formulas (2.1) for the elastic constants. These formulas hold due to the invariance of the sum of products $\sigma'_{ij}\varepsilon'^{\,\mathrm{p}}_{ij}, \sigma'_{ij}\Delta\varepsilon'^{\,\mathrm{c}}_{ij}$ and formulas (2.22), (2.24). For example, stretching a specimen along the q_i-axis (by stress S_1) inclined to the principal axes q'_1 and q'_2 at an angle of $\pi/4$ and orthogonal to the q'_3-axis and measuring the longitudinal strain ε_{11}, we can determine the functions

$$\psi_{11} = \frac{/\,\varepsilon^{\mathrm{p}}_{11}\,/}{S_1} \quad (1, 2, 3), \qquad C_{11} = \frac{\Delta\varepsilon^{\mathrm{c}}_{11}}{S_1} \quad (1, 2, 3). \tag{2.33}$$

The functions ψ_{11} are determined from the instantaneous thermomechanical surface, and C_{11} from the associated creep curve. Then using formulas similar to (2.1) for the functions ψ_{ij}, g_{ij} ($\psi_{ij} \neq \psi_{ji}$) and C_{ij}, D_{ij} ($C_{ij} \neq C_{ji}$), we obtain

$$2g'_{12} = 2g'_{21'} = 4\psi_{11} - (\psi'_{11} + \psi'_{22} + \psi'_{12} + \psi'_{21}) \quad (1, 2, 3), \tag{2.34}$$

$$2D'_{12} = 2D'_{21'} = 4C'_{11} - (C'_{11} + C'_{22} + C'_{12} + C'_{21}) \quad (1, 2, 3). \tag{2.35}$$

With (2.30) and (2.31), Eqs. (1.34) and (2.35) become

$$g'_{12} = g'_{21'} = 2\psi_{11} - \frac{1}{4}(\psi'_{11} + \psi'_{22}) \quad (1, 2, 3), \tag{2.36}$$

$$D'_{12} = D'_{21'} = 2C_{11} - \frac{1}{4}(C'_{11} + C'_{22}) \quad (1, 2, 3). \tag{2.37}$$

If relations (2.30) and (2.32) hold and the functions ψ'_{ij} and C'_{ij} are symmetric ($\psi'_{ij} = \psi'_{ji}$ and $C'_{ij} = C'_{ji}$), then Eqs. (2.34) and (2.35) become

$$2g'_{12} = 2g'_{21'} = 4\psi_{11} - \psi'_{33} \quad (1, 2, 3), \tag{2.38}$$

$$2D'_{12} = 2D'_{21'} = 4C_{11} - C'_{33} \quad (1, 2, 3). \tag{2.39}$$

Hence, formulas (2.34)–(2.39) allow determining the functions g'_{ij} and D'_{ij} from the functions ψ_{ij}, ψ'_{ij} and C_{ij}, C'_{ij}, respectively.

The functions $\psi'_{ij}, g'_{ij}, C'_{ij}$, and D'_{ij} are determined when solving the boundary-value problem by the method of successive approximations. The process of loading and heating is divided into steps. Assume that the plastic strains $\varepsilon'^{\,\mathrm{p}}_{ij}$ and creep strains $\varepsilon'^{\,\mathrm{c}}_{ij}$ obtained in the last approximation of the previous step (they are zero at the first step) are known at the beginning of the *k*th step of loading and heating.

Then in the first approximation of the *k*th step, we solve the elastic boundary-value problem with additional stresses in (1.1), (2.5) or (2.12), which are defined by (2.16) or (2.17), respectively, for the load and the temperature field of the end of this step. The values of $\sigma'^{\,\mathrm{n}}_{ij}$ are defined by (2.18) and (2.19) in which the values of $\varepsilon'^{\,\mathrm{n}}_{ij}$ (2.21) are referred to the beginning of the current step. As a result, we obtain the components of the stress tensor σ_{ij} and strain tensor ε_{ij} in the coordinate system q_i. Then, using coordinate rotation formulas similar to (2.25) for the components of the stress and strain tensors, we determine the components of the stress (σ'_{ij}) and strain (ε'_{ij}) tensors in the principal axes of anisotropy. Using these strains and the creep strains $\varepsilon'^{\,\mathrm{c}}_{ij}$ at the beginning of the step, we determine the purely mechanical instantaneous strains:

$$\bar{\varepsilon}'^{\,*}_{11} = \varepsilon'_{11} - \varepsilon'^{\,\mathrm{c}}_{11} - \alpha_1(T - T_0), \qquad \bar{\varepsilon}'^{\,*}_{12} = \varepsilon'_{12} - \varepsilon'^{\,\mathrm{c}}_{12} \quad (1, 2, 3), \tag{2.40}$$

where α_i is the coefficient of linear thermal expansion along the principal axes of anisotropy q'_i of an orthotropic material; T is the temperature of an element of the body at the end of the kth step. The instantaneous mechanical strains (2.40) and the instantaneous thermomechanical surfaces $\sigma'^{\,\mathrm{D}}_{ij} = f_{ij}(\bar{\varepsilon}'^{\,*}_{ij}, T)$ are then used to determine the stresses $\sigma'^{\,\mathrm{D}}_{ij}$, the elastic strains $\sigma'^{\,\mathrm{D}}_{11} / E_1$, $\sigma'^{\,\mathrm{D}}_{12} / 2G_{12}$ (1, 2, 3), and the instantaneous plastic strains for the temperature of an element of the body:

$$\varepsilon'^{\,\mathrm{p}}_{11} = \bar{\varepsilon}'^{\,*}_{11} - \frac{\sigma'^{\,\mathrm{D}}_{11}}{E_1}, \qquad \varepsilon'^{\,\mathrm{p}}_{12} = \varepsilon'^{\,*}_{12} - \frac{\sigma'^{\,\mathrm{D}}_{12}}{2G_{12}} \qquad (1, 2, 3). \tag{2.41}$$

Then formulas (2.26), (2.28), (2.31), and (2.32) are used to determine the functions ψ'_{ij} and g'_{ij} at the kth step of loading in the first approximation. After that, the found values of $\sigma'^{\,\mathrm{D}}_{ij}$ and temperature are used to choose the creep curve obtained by interpolation of experimental diagrams. The increments of the creep strains $\Delta_k \varepsilon'^{\,\mathrm{c}}_{ij}$ over the step is determined from this curve. Then formulas (2.27), (2.29), (2.31), and (2.32) are used to determine the functions C'_{ij} and D'_{ij} in the first approximation. If the functions g'_{ij} and D'_{ij} are defined by (2.34)–(2.39), then in addition to the values of ψ'_{ij} and C'_{ij} calculated above, it is necessary to determine the functions ψ_{ij} and C_{ij} (2.33). To this end, we use the transformation formulas for the purely mechanical instantaneous strains (2.40) in the principal axes of anisotropy q'_i to calculate the strains $\bar{\varepsilon}^*_{11}, \bar{\varepsilon}^*_{22}, \bar{\varepsilon}^*_{33}$ along axes equally inclined to two principal axes and orthogonal to the third principal axis. These strains and the instantaneous thermomechanical surfaces $S_i = \Phi_i(\bar{\varepsilon}^*_{ii}, T)$ for the temperature T of an element of the body are then used to find the stresses S_i, the elastic strains S_1 / E_{12} (1, 2, 3) along these axes, and the instantaneous plastic strains:

$$\varepsilon^{\mathrm{p}}_{11} = \bar{\varepsilon}^*_{11} - \frac{S_1}{E_{12}} \qquad (1, 2, 3), \tag{2.42}$$

where E_{12} is the elastic modulus along axes equally inclined to the principal axes q'_1 and q'_2 and orthogonal to the third principal axis.

The values of ψ_{ij} are determined by formulas (2.33) and the corresponding values of g'_{ij} are found in the first approximation by formulas (2.34), (2.36), or (2.38). Then the values of S_1 and corresponding creep curves along these axes for the temperature T and the time of the step of loading are used to determine the increments of the creep strains $\Delta_k \varepsilon^{\mathrm{c}}_{11}$ over the step and, hence, and the functions c_{11} (1, 2, 3) (2.33). After that, the functions D'_{ij} are calculated in the first approximation by one of formulas (2.35) and (2.37) or (2.39).

When the functions $\psi'_{ij}, g'_{ij}, C'_{ij}$, and D'_{ij} are found in one way or another in the first approximation at the kth step of loading for each an element of the body, it is possible to find $\varepsilon'^{\,\mathrm{p}}_{ij}$ (2.22), $\Delta_k \varepsilon'^{\,\mathrm{c}}_{ij}$ (2.24), and cumulative creep strains $\varepsilon'^{\,\mathrm{c}}_{ij}$ at the end of the kth step (2.23) and, hence, the total irreversible strains $\varepsilon'^{\,\mathrm{n}}_{ij}$ (2.21). To this end, we use the stresses σ'_{ij} found in the first approximation and the values of the parameters $\sigma'^{\,\mathrm{n}}_{ij}$ (2.19) and σ^{n}_{ij} (2.18) and the additional stresses σ^*_{ij} (2.16) or (2.17) found in the second approximation. Then the boundary-value problem of elasticity is solved again for the new values of the additional stresses σ^*_{ij}. As a result, we obtain the stresses σ_{ij} and strains ε_{ij} in the second approximation of the kth step of loading and heating. Next the first-order algorithm is used. The process of approximations is terminated when the stresses σ'_{ij} obtained by solving the boundary-value problem differ from the respective stresses $\sigma'^{\,\mathrm{D}}_{ij}$ calculated from instantaneous tensile or shear stress–strain curves by a predefined amount. After that, it is necessary to check whether the process is loading

$$\sigma'_{ij} \Delta_k \varepsilon'^{\,\mathrm{p}}_{ij} > 0 \tag{2.43}$$

or unloading

$$\sigma'_{ij} \Delta_k \varepsilon'^{\,\mathrm{p}}_{ij} \le 0. \tag{2.44}$$

If it appears that the loading condition (2.43) fails in some element of the body, then this step of loading is calculated again assuming that the plastic strains $\varepsilon'^{\,\mathrm{p}}_{ij}$ in this element do not change and equal those at the beginning of the step. The increments of the creep strains are determined from the creep curves.

The above relations of the deformation theory of orthotropic thermoviscoplasticity, similarly to the isotropic case, can be used to study the deformation of elements of a body along straight or nearly straight paths, and the constitutive equations for an isotropic body transform into the equations of the theory of small elastoplastic deformations that allow for the loading history [91, 95].

2.1.4. Inelastic State of Orthotropic Bodies Deforming along Paths of Small Curvature [36, 143]. When an orthotropic body undergoes irreversible deformation along paths of small curvature, the process of loading and heating is divided into steps, as in the previous case. Then the irreversible strains $\varepsilon'^{\,\mathrm{n}}_{ij}$ in (2.19) at the end of the mth stage of loading are defined by

$$(\varepsilon'^{\,\mathrm{n}}_{ij})_m = \sum_{k=1}^{m} \Delta_k \varepsilon'^{\,\mathrm{n}}_{ij}, \tag{2.45}$$

where the increments of irreversible strains are expressed as follows [143]:

$$\Delta_k \varepsilon'^{\,\mathrm{n}}_{11} = \left\langle \frac{a'^{\,\mathrm{n}}_{1111}\sigma'_{11} + a'^{\,\mathrm{n}}_{1122}\sigma'_{22} + a'_{1133}\sigma'_{33}}{S} \right\rangle \Delta_k \Gamma^{\mathrm{n}},$$

$$\Delta_k \varepsilon'^{\,\mathrm{n}}_{12} = \left\langle \frac{a'^{\,\mathrm{n}}_{1212}}{S} \right\rangle \Delta_k \Gamma^{\mathrm{n}} \quad (1, 2, 3), \tag{2.46}$$

where the angular brackets denote averaging over the mth step of loading. The coefficients $a'^{\,\mathrm{n}}_{ijmn}$ form a symmetric compliance matrix and are determined from tension tests on specimens cut out from an orthotropic material in different directions at different fixed temperatures. These coefficients can depend on temperature and, due to the invariance of $\sigma'_{ij}\Delta_k \varepsilon'^{\,\mathrm{n}}_{ij}$, transform by formulas similar to (2.1) upon rotation of the coordinate system. The quantity S is called the reduced shear stress intensity for an orthotropic body undergoing irreversible deformation, $\Delta_k \Gamma^{\mathrm{n}}$ is the increment of the irreversible shear strain intensity, which are determined from tests described above. If the material is inelastically incompressible and the matrix of coefficients is symmetric, $a'^{\,\mathrm{n}}_{ijmn}$ become:

$$a'^{\,\mathrm{n}}_{1122} = -\frac{1}{2}(a'^{\,\mathrm{n}}_{1111} + a'^{\,\mathrm{n}}_{2222} - a'^{\,\mathrm{n}}_{3333}) \quad (1, 2, 3), \tag{2.47}$$

i.e., only three of the nine coefficients in the first three equations in (2.46) are independent. The equations coincide with those in [113]. The irreversible-strain increments $\Delta_k \varepsilon'^{\,\mathrm{n}}_{ij}$ are represented as the sum of the plastic-strain increments $\Delta_k \varepsilon'^{\,\mathrm{p}}_{ij}$ and the creep-strain increments $\Delta_k \varepsilon'^{\,\mathrm{c}}_{ij}$. Each of the terms is defined by formulas coinciding with (2.46), but having different coefficients $a'^{\,\mathrm{n}}_{ijmn}$ and parameters $\Delta_k \Gamma^{\mathrm{n}}$ and S. These coefficients and parameters are denoted by $a'^{\,\mathrm{p}}_{ijmn}$, $\Delta_k \Gamma^{\mathrm{p}}$, and S^{p} in the former case and by $a'^{\,\mathrm{c}}_{ijmn}$, $\Delta_k \Gamma^{\mathrm{c}}$, and S^{c} in the latter case. To determine the coefficients $a'^{\,\mathrm{p}}_{ijmn}$, we assume that S^{p} is a function of the parameter $\xi = \sum_k \Delta_k \Gamma^{\mathrm{p}}$ and temperature. This function can be found from tension tests on specimens cut out along one of the principal axes of anisotropy at different fixed temperatures, i.e., from an instantaneous thermomechanical surface. For $\xi = 0$, the value of S^{p} is equal to the limiting elastic value Φ_0 for specimens stretched along one of the principal axes of anisotropy. The parameter Φ_0 can be equal to the average limiting value of S^{p} in tension of specimens along three principal axes of anisotropy. This assumption means that the instantaneous thermomechanical surfaces for all axes of an orthotropic body are similar.

The following expressions for the coefficients can be obtained from tension tests in three principal directions and pure-shear tests between these directions for $S = \Phi_0$:

$$a'^{\,\mathrm{p}}_{1111} = 2\left(\frac{\Phi_0}{\sigma_{1T}}\right)^2 \quad (1, 2, 3),$$

$$a'^{\,\mathrm{p}}_{1212} = \frac{1}{2}\left(\frac{\Phi_0}{\tau^T_{12}}\right)^2 \quad (1, 2, 3), \tag{2.48}$$

where σ_{iT}, τ^T_{ij}, and T are the yield stresses of an orthotropic body along the three principal axes of anisotropy and the three shear yield stress between these directions, respectively. These yield stresses are functions of temperature T. The last three coefficients (2.48) can also be determined not from pure-shear tests, but from tension tests along axes equally inclined to two principal axes of anisotropy and orthogonal to the third one. The yield stresses of an orthotropic material in these directions (between the axes i and j) are denoted by σ^T_{ij} $(i \neq j)$. If the coordinate system q'_i is rotated by an angle of 45° about the principal axes of anisotropy, we can use the coordinate rotation formulas for the coefficients x_1, x_2, x_3 to obtain the following expressions for the last three coefficients in (2.48):

$$a'^{\,\mathrm{p}}_{1212} = \frac{\Phi_0^2}{2}\left[\left(\frac{2}{\sigma^T_{12}}\right)^2 - \left(\frac{1}{\sigma_{3T}}\right)^2\right] \quad (1, 2, 3). \tag{2.49}$$

When the parameter Φ_0 is determined by the instantaneous thermomechanical surface in the first principal direction of anisotropy

$$\sigma'_{11} = f(\bar{\varepsilon}'^{\,*}_{11}, T), \tag{2.50}$$

$\Phi_0 = \sigma_{ij} / \sqrt{3}$ and the coefficients $a'^{\,\mathrm{p}}_{ijmn}$ are defined by

$$a'^{\,\mathrm{p}}_{1111} = \frac{2}{3}, \quad a'^{\,\mathrm{p}}_{2222} = \frac{2}{3}\left(\frac{\sigma_{1T}}{\sigma_{2T}}\right)^2, \quad a'^{\,\mathrm{p}}_{3333} = \frac{2}{3}\left(\frac{\sigma_{1T}}{\sigma_{3T}}\right)^2,$$

$$a'^{\,\mathrm{p}}_{1212} = \frac{1}{6}\left(\frac{\sigma_{1T}}{\tau^T_{12}}\right)^2, \quad a'^{\,\mathrm{p}}_{2323} = \frac{1}{6}\left(\frac{\sigma_{1T}}{\tau^T_{23}}\right)^2, \quad a'^{\,\mathrm{p}}_{3131} = \frac{1}{6}\left(\frac{\sigma_{1T}}{\tau^T_{31}}\right)^2. \tag{2.51}$$

Expressions (2.49) also take the corresponding form.

The reduced shear-stress intensity $S^{\,\mathrm{p}}$ and the strains $\varepsilon'^{\,\mathrm{p}}_{11}$ are defined by

$$S^{\,\mathrm{p}} = \sigma'_{11} / \sqrt{3}, \quad \varepsilon'^{\,\mathrm{p}}_{11} = \frac{2\sqrt{3}}{3}\xi. \tag{2.52}$$

Then the total instantaneous mechanical strain is given by

$$\varepsilon'^{\,*}_{11} = \frac{S^{\,\mathrm{p}}\sqrt{3}}{E_1} + \frac{2\sqrt{3}}{3}\xi, \tag{2.53}$$

where E_1 is the elastic modulus along the first principal axis of anisotropy.

The coefficients in (2.46) can be found in a similar way to determine the creep strain increments $\Delta_k \varepsilon'^{\,\mathrm{c}}_{ij}$. It is this case where the limiting elastic state of an element of the body is defined by the creep strengths rather than the yield stresses [96]. Usually, the creep strengths are a little lower than the yield stresses. The coefficients $a'^{\,\mathrm{c}}_{ijmn}$ are determined by formulas (2.48) and (2.49) or (2.51) where the yield stresses should be replaced by the creep strengths along the respective axes of anisotropy.

The shear-stress intensities and the increments $\Delta_k \Gamma^{\mathrm{p}} = \Delta_k \xi^{\mathrm{p}}$, $\Delta_k \Gamma^{\mathrm{c}} = \Delta_k \xi^{\mathrm{c}}$ are determined by the method of successive approximations during the solution of the boundary-value problem.

Let the strains $(\varepsilon'^{\mathrm{p}}_{ij})_{m-1}$, $(\varepsilon'^{\mathrm{c}}_{ij})_{m-1}$ and the parameters $\xi^{\mathrm{p}}_{m-1} = \sum_{k=1}^{m-1} \Delta_k \Gamma^{\mathrm{p}}$, $\xi^{\mathrm{c}}_{m-1} = \sum_{k=1}^{m-1} \Delta_k \Gamma^{\mathrm{c}}$ be known at the beginning of the mth step of loading and heating.

Let us find their values at the end of the mth step. Using the known values of $(\varepsilon'^{\mathrm{n}}_{ij})_{m-1} = (\varepsilon'^{\mathrm{p}}_{ij})_{m-1} + (\varepsilon'^{\mathrm{c}}_{ij})_{m-1}$ and formulas (2.19), (2.18) and (2.16) or (2.17), we determine the additional terms in the corresponding constitutive equations (1.1) or (2.12) and we solve the boundary-value problem in the coordinate system q_i. As a result, we obtain the stresses σ_{ij} and strains ε_{ij}. Using the coordinate rotation formulas, we obtain σ'_{ij} and ε'_{ij} in the coordinate system q'_i. After that, we determine $S^{\mathrm{p}}_{\mathrm{F}}$ and $\bar{\varepsilon}'^{*}_{ij}$ (2.53) on the assumption that $\xi = \xi^{\mathrm{p}}_{m-1}$ and $S = S^{\mathrm{p}}_{\mathrm{F}}$. Using these values and the instantaneous thermomechanical surface (2.50) for the temperature of an element of the body, we determine $\sigma'_{11} = S^{\mathrm{p}}_{\mathrm{D}} \sqrt{3}$. Then

$$\Delta_m \xi^{\mathrm{p}} = \Delta_m \Gamma^{\mathrm{p}} = \frac{S^{\mathrm{p}}_{\mathrm{F}} - S^{\mathrm{p}}_{\mathrm{D}}}{E_1} \sqrt{3} \tag{2.54}$$

and formulas (2.46) can be used to determine the increments of plastic strains $\Delta_m \varepsilon'^{\mathrm{p}}_{ij}$ in the first approximation. Then we calculate $\xi^{\mathrm{p}}_m = \xi^{\mathrm{p}}_{m-1} + \Delta_m \xi^{\mathrm{p}}$ and $(\varepsilon'^{\mathrm{p}}_{ij})_m = (\varepsilon'^{\mathrm{p}}_{ij})_{m-1} + \Delta_m \varepsilon'^{\mathrm{p}}_{ij}$ at the end of the mth step of loading in the first approximation. Then, using the creep curve coupled to the instantaneous thermomechanical surface (2.50) with respect to the loading rate and corresponding to the stress $\sigma'_{11} = S^{\mathrm{p}}_{\mathrm{D}} \sqrt{3}$ and temperature of the element of the body at the end of the step, we determine the creep strain increment over the step and the parameters $\Delta_m \varepsilon'^{\mathrm{c}}_{11} = \frac{2\sqrt{3}}{3} \Delta_m \xi^{\mathrm{c}} = \frac{2\sqrt{3}}{3} \Delta_m \Gamma^{\mathrm{c}}$ and $\xi^{\mathrm{c}}_m = \xi^{\mathrm{c}}_{m-1} + \Delta_m \xi^{\mathrm{c}}$ at the end of the step. After that, it is possible to calculate the creep strain increments $\Delta_m \varepsilon'^{\mathrm{c}}_{ij}$ and the total creep strains $(\varepsilon'^{\mathrm{c}}_{ij})_m = (\varepsilon'^{\mathrm{c}}_{ij})_{m-1} + \Delta_m \varepsilon'^{\mathrm{c}}_{ij}$ at the end of the mth step of loading in the first approximation.

The first-order values of $(\varepsilon'^{\mathrm{p}}_{ij})_m$, $(\varepsilon'^{\mathrm{c}}_{ij})_m$ and parameters ξ^{p}_m, ξ^{c}_m can then be used to calculate the second approximation. Beginning from the second approximation, we determine the corrections to the increments $\Delta_m \Gamma^{\mathrm{p}}$ (2.54) obtained in the first approximation. The process of successive approximations is terminated once the difference between $S^{\mathrm{p}}_{\mathrm{F}}$ and $S^{\mathrm{p}}_{\mathrm{D}}$ has become less than some predefined error.

After convergence of the process of successive approximations, we test conditions (2.43) and (2.44). If the process is loading, then it is possible to go to the next step of loading and heating. If the loading condition fails in some element of the body, the step is run again for the instantaneous plastic strains equal to their values at the beginning of the step and $\Delta_m \varepsilon'^{\mathrm{p}}_{ij}$ equal to zero. The creep strain increments are still determined from creep curves. If $\sigma_{1\mathrm{c}} > S^{\mathrm{c}}_{\mathrm{F}} \sqrt{3}$, then $\Delta_m \varepsilon'^{\mathrm{c}}_{ij} = 0$, and for $\sigma_{1\mathrm{c}} < S^{\mathrm{c}}_{\mathrm{F}} \sqrt{3}$, the increment $\Delta_m \varepsilon'^{\mathrm{c}}_{ij} \neq 0$ is determined from creep curves as described above. The parameter ξ^{c} is calculated only when cyclic deformation of a solid is considered [96].

The above theory of irreversible deformation of an orthotropic body along paths of small curvature can be used to analyze the stress–strain state of solids whose elements deform not only along paths of small curvature, but also along straight and nearly straight paths. Similarly to the isotropic case, a path of small curvature is a curve whose minimum radius of curvature is much greater than 10 to 15 maximum yield strains.

If the body is isotropic $\sigma_{iT} = \sigma^T_{ij} = \tau^T_{ij} = \sigma_T$, $\Phi_0 = \sigma_T \sqrt{3}$, $a'^{\mathrm{n}}_{1111} = a'^{\mathrm{n}}_{2222} = a'^{\mathrm{n}}_{3333} = 2/3$, $a'^{\mathrm{n}}_{1212} = a'^{\mathrm{n}}_{2323} = a'^{\mathrm{n}}_{3131} = 1/2$, $a'^{\mathrm{n}}_{1122} = a'^{\mathrm{n}}_{2233} = a'^{\mathrm{n}}_{3311} = -1/3$, and relations (2.46) go over into the equations of thermoviscoplasticity describing the deformation of elements of the isotropic body along paths of small curvature.

2.2. Isotropic Materials. Let us establish the relationship between the stress and strain tensors for isotropic bodies undergoing small elastoplastic deformation along straight paths and paths of small curvature.

2.2.1. Thermoviscoplastic State of Isotropic Bodies Undergoing Simple Deformation. If we use the equations of the theory of small elastoplastic deformations for an isotropic body allowing for the loading history [87, 95, 144] and linearized by the method of elastic solutions, the coefficients A_{ijmn} in the constitutive equations (1.1) are expressed as

$$A_{ijmn} = G_0(\delta_{im}\delta_{jn} + \delta_{in}\delta_{jm}) + \frac{1}{3}(K_0 - 2G_0)\delta_{ij}\delta_{mn}, \tag{2.55}$$

and the additional terms are

$$\sigma_{ij}^* = 2G_0\omega e_{ij} + 2G^* e_{ij}^{1n} + \left[K_0\omega_1\varepsilon_0 + K^*(\varepsilon_0^{1n} + \varepsilon_T)\right]\delta_{ij}, \tag{2.56}$$

where G_0 and K_0 are the shear and bulk moduli of the material at temperature T_0; δ_{ij} is the Kronecker delta; $\varepsilon_0 = \varepsilon_{ii}/3$ is the first invariant of the strain tensor; $\varepsilon_T = \alpha_T(T - T_0)$ is the thermal strain; α_T is the coefficient of linear thermal expansion; $e_{ij} = \varepsilon_{ij} - \varepsilon_0\delta_{ij}$ are the components of the deviatoric strain tensor. The plastic functions

$$\omega = 1 - \frac{G^*}{G_0} \quad \text{and} \quad \omega_1 = 1 - \frac{K^*}{K_0}, \tag{2.57}$$

$$2G^* = \frac{S}{\Gamma}, \qquad K^* = \frac{\sigma_0}{\varepsilon_0 - \varepsilon_T}, \tag{2.58}$$

$\sigma_0 = 1/3\,\sigma_{ii}$ is the mean normal stress; $S = \left(\frac{1}{2}s_{ij}s_{ij}\right)^{1/2}$ is the shear-stress intensity, $s_{ij} = \sigma_{ij} - \sigma_0\delta_{ij}$ are the components of the deviatoric stress tensor; $\Gamma = \left(\frac{1}{2}e_{ij}e_{ij}\right)^{1/2}$ is the shear-strain intensity; e_{ij}^{1n} and ε_0^{1n} are the irreversible deviatoric strains and the mean strain at the time of unloading of an element of the body. If the process is loading, they are equal to zero. If the process is unloading, then

$$e_{ij}^{1n} = e_{ij}^* - \frac{s_{ij}}{2G^1}, \qquad \varepsilon_0^{1n} = \varepsilon_0^1 - \varepsilon_T^1 - \frac{\sigma_0^1}{K^*}, \tag{2.59}$$

where the superscript "1" refers to the moment of unloading. Assume that S and σ_0 in (2.57), (2.58) are determined from tests and used to plot the instantaneous thermomechanical surface

$$S = F^*(\Gamma^*, T), \qquad \sigma_0 = \Phi^*(\bar{\varepsilon}_0^*, T) \tag{2.60}$$

and the associated creep curves at different fixed temperatures and stresses. The tests are simple loading of tubular specimens, measuring the longitudinal (ε_{11}) and circumferential (ε_{22}) strains. Here $\Gamma = \Gamma^* + \Gamma^c$, $\varepsilon_0 = \bar{\varepsilon}_0^* + \varepsilon^c + \varepsilon_T$, Γ^c and ε_0^c are determined from the creep curves (Γ^c versus t). In these tests,

$$S = \frac{\sigma}{\sqrt{3}}, \qquad \Gamma^* = \frac{\varepsilon_{11}^* - \varepsilon_{22}^*}{\sqrt{3}}, \qquad \Gamma^c = \frac{\varepsilon_{11}^c - \varepsilon_{22}^c}{\sqrt{3}},$$

$$\sigma_0 = \frac{\sigma}{\sqrt{3}}, \qquad \bar{\varepsilon}_0^* = \frac{\varepsilon_{11}^* + \varepsilon_{22}^*}{3} - \varepsilon_T, \qquad \varepsilon_0^c = \frac{\varepsilon_{11}^c + 2\varepsilon_{22}^c}{3}, \tag{2.61}$$

σ is the normal tensile stress; $\varepsilon_{ij}^* = \varepsilon_{ij} - \varepsilon_{ij}^c$ are instantaneous strains; $\bar{\varepsilon}_{ij}^* - \varepsilon_T\delta_{ij}$ are purely mechanical instantaneous strains.

The plastic functions (2.57) based on tests are determined by the method of successive approximations during the solution of the boundary-value problem. These functions are set equal to zero in the first approximation of the first step of loading and heating. At the subsequent steps, they are set equal to their values obtained in the last approximation of the previous

step. In each approximation, the plastic functions are taken from the previous approximation. Similarly, Γ^{c} and $\varepsilon_0^{\mathrm{c}}$ are set equal to zero at the beginning of the first step of loading and heating. At the beginning of the subsequent steps, they are set equal to their values obtained in the last approximation of the previous step. By solving the perfectly elastic boundary-value problem with additional stresses (2.56) in the first approximation of the *m*th step of loading and heating, we determine the shear-strain intensity Γ_m and the first invariant of the strain tensor ε_0^m in the first approximation at the end of this step for the load and temperature at the end of the step. Then $\Gamma_m^* = \Gamma_m - \Gamma_{m-1}^{\mathrm{c}}$ and $(\bar{\varepsilon}_0^*)_m = \varepsilon_0^m - \varepsilon_T^m - (\varepsilon_0^{\mathrm{c}})_{m-1}$ are determined and used to find S_{D}^m and $(\sigma_0^m)_{\mathrm{D}}$ using Eqs. (2.60) for the temperature of each element of the body at the end of the step. These values and the temperature are then used to plot, by interpolation, the creep curve. These curves are used to determine $\Delta_m \Gamma^{\mathrm{c}}$ and $\Delta_m \varepsilon_0^{\mathrm{c}}$ over the step, the shear-strain intensity $\Gamma_m^{\mathrm{c}} = \Gamma_{m-1}^{\mathrm{c}} + \Delta_m \Gamma^{\mathrm{c}}$, and the first invariant $(\varepsilon_0^{\mathrm{c}})_m = (\varepsilon_0^{\mathrm{c}})_{m-1} + \Delta_m \varepsilon_0^{\mathrm{c}}$ in the first approximation at the end of the *m*th step of loading and heating. After that, we calculate the total shear-strain intensity $\Gamma_m = \Gamma_m^* + \Gamma_m^{\mathrm{c}}$ and the first invariant of the strain tensor $\varepsilon_0^m = (\varepsilon_0^*)_m + (\varepsilon_0^{\mathrm{c}})_m$, where $\varepsilon_0^* = \bar{\varepsilon}_0^* + \varepsilon_T$. Next, we calculate the secant moduli G^* and K^* (2.58) and the plastic functions ω and ω_1 (2.57) at the end of the *m*th step of loading in the second approximation and so on. The process of successive approximations is terminated once the shear-stress intensity $S = \left(\frac{1}{2} s_{ij} s_{ij}\right)^{1/2}$ in each element of the body has differed by less than a predefined error from its value found from the instantaneous surface (2.60). After that, it is necessary to check whether the process is loading:

$$s_{ij} \Delta e_{ij}^{\mathrm{n}} > 0. \tag{2.62}$$

If this condition fails in some element of the body, then this step is calculated again taking into account (2.59) for the irreversible strains at the end of the previous step. It is assumed that creep strains do not develop during unloading.

When the equations of the theory of small elastoplastic deformations are linearized by the method of variable parameters, the coefficients A_{ijmn} in the constitutive equations (1.1) become

$$A_{ijmn} = G^* (\delta_{im}\delta_{jn} + \delta_{in}\delta_{jm}) + \frac{1}{3}(K^* - 2G^*)\delta_{ij}\delta_{mn}, \tag{2.63}$$

and the additional stresses in these equations are expressed as

$$\sigma_{ij}^* = 2G^* e_{ij}^{1\mathrm{n}} + K^* (\varepsilon_0^{1\mathrm{n}} + \varepsilon_T)\delta_{ij}. \tag{2.64}$$

The algorithm of determining G^*, K^*, and σ_{ij}^* remains the same as in the previous case of linearizing the constitutive equations (1.1) by the method of elastic solutions.

To improve the convergence of the method of successive approximations, we propose a somewhat different method to determine the secant moduli and plastic functions. This method differs from the conventional one in the way of determining S_{D}^m and $(\sigma_0^m)_{\mathrm{D}}$, and $\Gamma_m^* = (\Gamma_{\mathrm{D}}^*)_m$, $(\varepsilon_0^*)_m = (\varepsilon_0^*)_{\mathrm{D}}^m$ from the experimental surfaces (2.60). We will illustrate the method by calculating S_{D}^m and $\Gamma_m^* = (\Gamma_{\mathrm{D}}^*)_m$. We use the curve $S = F^*(\Gamma^*, T_m)$ to find values of S_{D}^m and $\Gamma_m^* = (\Gamma_{\mathrm{D}}^*)_m$ such that $S_{\mathrm{F}} \cdot \Gamma_{\mathrm{F}}^* = S_{\mathrm{D}} \cdot \Gamma_{\mathrm{D}}^*$ in each approximation, where S_{F} and Γ_{F}^* are the shear-stress intensity and instantaneous shear-strain intensity obtained by solving the boundary-value problem of thermoviscoplasticity. This is schematized in Fig. 1. This condition means the equality of the areas of the triangles *A*0*B* and *C*0*D*. The curve $\sigma_0 = \Phi^*(\bar{\varepsilon}_0^*, T)$ can similarly be used to determine $(\sigma_0^m)_{\mathrm{D}}$ and $(\varepsilon_0^*)_m = (\varepsilon_0^*)_{\mathrm{D}}^m$. The values of S_{D}^m, $(\sigma_0^m)_{\mathrm{D}}$, $\Gamma_m^* = (\Gamma_{\mathrm{D}}^*)_m$, $(\varepsilon_0^*)_m = (\varepsilon_0^*)_{\mathrm{D}}^m$ found this way are used as described earlier. In [99], it was shown by way of examples that these changes in the standard algorithm of successive approximations reduce the number of approximations by more than one-third when either the method of elastic solutions is used or the equations of thermoviscoplasticity are linearized by the method of variable elastic parameters.

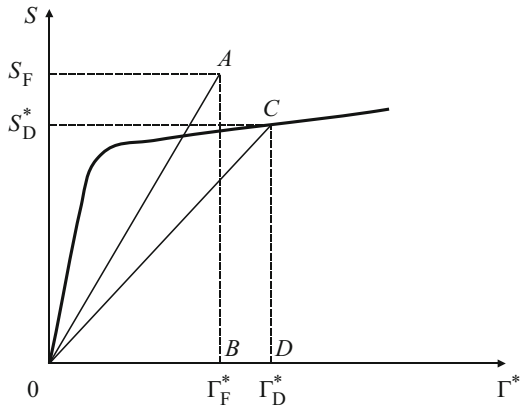

Fig. 1

2.2.2. Thermoviscoplastic State of Isotropic Bodies Undergoing Deformation along Paths of Small Curvature. If the body is isotropic and the equations of thermoviscoplastic deformation along paths of small curvature [87, 95, 144], linearized by the method of additional stresses, the coefficients A_{ijmn} in the constitutive equations (1.1) become:

$$A_{ijmn} = G(\delta_{im}\delta_{jn} + \delta_{in}\delta_{jm}) + \frac{1}{3}(K - 2G)\delta_{ij}\delta_{mn}, \tag{2.65}$$

and the additional stresses σ_{ij}^* in these equations are given by

$$\sigma_{ij}^* = 2Ge_{ij}^{\mathrm{n}} + K(\varepsilon_0^{\mathrm{n}} + \varepsilon_T)\delta_{ij}, \tag{2.66}$$

where G and K are the shear and bulk moduli. They are functions of temperature. If these elastic moduli are represented as

$$G = G_0(1-\omega), \quad K = (1-\omega_1), \tag{2.67}$$

then the coefficients A_{ijmn} are defined by (2.55), while the additional stresses σ_{ij}^* by

$$\sigma_{ij}^* = 2G_0\omega\varepsilon_{ij} + 2Ge_{ij}^{\mathrm{n}} + \left[(K_0\omega_1 + 2G_0\omega)\varepsilon_0 + K(\varepsilon_0^{\mathrm{n}} + \varepsilon_T)\right]\delta_{ij}, \tag{2.68}$$

where G_0 and K_0 are the shear and bulk moduli of the material at the initial temperature T_0; ω and ω_1 are given by

$$\omega = 1 - G/G_0, \quad \omega_1 = 1 - K/K_0. \tag{2.69}$$

The irreversible strains e_{ij}^{n} and $\varepsilon_0^{\mathrm{n}}$ at the end of the mth step of loading are expressed as

$$(e_{ij}^{\mathrm{n}})_m = \sum_{k=1}^{m} \Delta_k e_{ij}^{\mathrm{n}} = \sum_{k=1}^{m} \left\langle \frac{s_{ij}}{S} \right\rangle_k \Delta_k \Gamma^{\mathrm{n}}, \quad (\varepsilon_0^{\mathrm{n}})_m = \sum_{k=1}^{m} \Delta_k \varepsilon_0^{\mathrm{n}}. \tag{2.70}$$

The increments $\Delta_k \Gamma^{\mathrm{n}}$ and $\Delta_k \varepsilon_0^{\mathrm{n}}$ over the kth step of loading are determined from reference tests and Eqs. (2.60) by the method of successive approximations during the solution of the boundary-value problem. We find

$$\Delta_k \Gamma^{\mathrm{n}} = \Delta_k \Gamma^{\mathrm{p}} + \Delta_k \Gamma^{\mathrm{c}}, \quad \Delta_k \varepsilon_0^{\mathrm{n}} = \Delta_k \varepsilon_0^{\mathrm{p}} + \Delta_k \varepsilon_0^{\mathrm{c}} \tag{2.71}$$

and assume that the instantaneous plastic strains are known at the beginning of the mth step of loading:

$$\Gamma_{m-1}^{\mathrm{p}} = \sum_{k=1}^{m-1} \Delta_k \Gamma^{\mathrm{p}}, \quad (\varepsilon_0^{\mathrm{p}})_{m-1} = \sum_{k=1}^{m-1} \Delta_k \varepsilon_0^{\mathrm{p}}, \tag{2.72}$$

i.e., obtained at the end of the (m – 1)th step. Then $\Delta_m \varepsilon_{ij}^{\mathrm{n}}$ and $\Delta_m \varepsilon_0^{\mathrm{n}}$ are assumed equal to zero in the first approximation of the mth step of loading and heating. Next we solve the boundary-value problem using expressions (2.65) or (2.55) for the coefficients A_{ijmn} in Eqs. (1.1) and expressions (2.66) or (2.68) for the additional stresses σ_{ij}^* and assuming that the irreversible strains $\varepsilon_{ij}^{\mathrm{n}}$ and $\varepsilon_0^{\mathrm{n}}$ at the end of the previous step are known. Then we determine the shear-stress intensity $S_{\mathrm{F}} = \left(\frac{1}{2} s_{ij} s_{ij}\right)^{1/2}$, mean stress $\sigma_0^{\mathrm{F}} = \sigma_{ij}\delta_{ij}/3$, and

$$\Gamma^* = \frac{S_{\mathrm{F}}}{2G} + \Gamma_{m-1}^{\mathrm{p}}, \qquad \bar{\varepsilon}_0^* = \frac{\sigma_0^{\mathrm{F}}}{K} - \varepsilon_T + (\varepsilon_0^{\mathrm{p}})_{m-1}, \tag{2.73}$$

using Eqs. (2.60) and the temperature of the element of the body to find S_{D} and σ_0^{D}. In the second approximation, we have

$$\Delta_m \Gamma^{\mathrm{p}} = \frac{S_{\mathrm{F}} - S_{\mathrm{D}}}{2G}, \qquad \Delta_m \varepsilon_0^{\mathrm{p}} = \frac{\sigma_0^{\mathrm{F}} - \sigma_0^{\mathrm{D}}}{K}. \tag{2.74}$$

Using the creep curves and the values of S_{D}, σ_0^{D}, and T at the end of the step, we determine $\Delta_m \Gamma^{\mathrm{c}}$, $\Delta_m \varepsilon_0^{\mathrm{c}}$ and $\Delta_m \Gamma^{\mathrm{n}}$, $\Delta_m \varepsilon_0^{\mathrm{n}}$ (2.71) over the step Δt and $e_{ij}^{\mathrm{n}}, \varepsilon_0^{\mathrm{n}}$ (1.55) and $\Gamma_m^{\mathrm{p}}, (\varepsilon_0^{\mathrm{p}})_m$ (2.72) at the end of the mth stage of loading in the second approximation.

The increments of irreversible strains in the subsequent approximations are found in a similar way. The values of (2.74) found in the second and subsequent approximations are corrections of $\Delta_m \Gamma^{\mathrm{p}}$ and $\Delta_m \varepsilon_0^{\mathrm{p}}$, and the total increments are equal to the sum of all approximations. The criterion for the termination of the process of successive approximations is the same as in the previous case. The values of (2.59) are positive in the case of loading and negative in the case of unloading. In the latter case, $\Delta_m \Gamma^{\mathrm{p}} = \Delta_m \varepsilon_0^{\mathrm{p}} = 0$, and $\Delta_m \Gamma^{\mathrm{c}}$ and $\Delta_m \varepsilon_0^{\mathrm{c}}$ are still determined from creep curves. Whether the process in each element of the body is loading or unloading is checked after the convergence of successive approximations at the end of each step of loading. If it appears that loading changes into unloading in some element of the body at some step, then this step is calculated again for the irreversible strains at the end of the previous step and for $\Delta_m \Gamma^{\mathrm{p}}$ and $\Delta_m \varepsilon_0^{\mathrm{p}}$ equal to zero.

Constitutive equations in the form (1.1) are convenient to use to solve three-dimensional thermoviscoplastic problems for compound bodies made of isotropic and anisotropic materials. For isotropic bodies, Eqs. (1.1) with (2.55), (2.63) or (2.65) take the following form [95]:

$$\sigma_{ij} = 2G'\varepsilon_{ij} + 3\lambda'\varepsilon_0\delta_{ij} - \sigma_{ij}^* \qquad \left[\lambda' = \frac{1}{3}(K' - 2G')\right]. \tag{2.75}$$

In the equations of the theory of small elastoplastic deformations, $G' = G_0, K' = K_0, \sigma_{ij}^*$ are defined by (2.56) if the linearization is performed using the method of elastic solutions and $G' = G^*, K' = K^*, \sigma_{ij}^*$ are defined by (2.64) if the method of variable elastic parameters is used. If we use the equations of the theory of thermoviscoplastic deformation along paths of small curvature linearized by the method of additional stresses, G' and K' are the shear (G) and bulk (K) moduli or their values G_0 and K_0 at the initial temperature T_0, σ_{ij}^* being defined by (2.66) in the former case and by (2.68) in the latter case.

If the body is inelastically incompressible, all the quantities in the previous equations that characterize irreversible change of volume should be set equal to zero. The second equation in (2.60) should be replaced by

$$\sigma_0 = K(\varepsilon_0 - \varepsilon_T), \tag{2.76}$$

where K is the temperature-dependent bulk modulus, $K^* = K$ (2.67); ε_0 with indices n and c are equal to zero. In (2.61), $\varepsilon_{22}^* = -\nu^* \varepsilon_{11}^*$ and Poisson's ratio ν^* is defined by the equality $\nu^* = \frac{1}{2} - \frac{1-2\nu}{2E}\frac{\sigma}{\varepsilon^*}$ [95] following from the condition of elastic

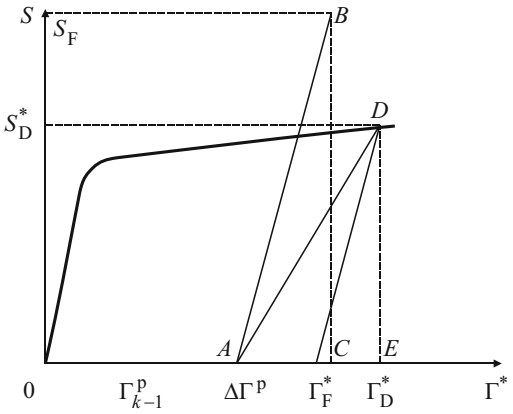

Fig. 2

change of volume, where ν is Poisson's ratio, E is the elastic modulus, σ and ε^* are the normal stress and instantaneous mechanical strain occurring in a specimen stretched at various fixed temperatures. Algorithms for the calculation of irreversible strains remain the same, except that there is no need to calculate the quantities characterizing the irreversible change of volume.

As with the theory of small elastoplastic deformations, when the theory of thermoviscoplasticity describing deformation along paths of small curvature is used, it is proposed to employ a somewhat different method to determine S_D, σ_0^D, $\Delta_k\Gamma^p$, and $\Delta_k\varepsilon_0^p$. The difference is in the way of determining the coordinates of a point on the thermomechanical surfaces $S = F^*(\Gamma^*, T)$ and $\sigma_0 = \Phi^*(\bar{\varepsilon}_0^*, T)$ to continue the process of successive approximations when solving a thermoviscoplastic problem.

For example, S_D in this case and the increment of irreversible strain $\Delta_k\Gamma^p$ is calculated as follows (Fig. 2). After solving the problem in the kth approximation, the known stress state is used to find S_F and Γ^* (2.73), and diagram (2.60) at given temperature of an element of the body is used to determine S_D^k and $\Gamma_k^* = (\Gamma_D^*)_k$ for which the condition $S_F \cdot (\Gamma_F^* - \Gamma_{m-1}^p) = S_D \cdot (\Gamma_D^* - \Gamma_{m-1}^p)$ is satisfied in each approximation. This condition is the equality of the areas of the triangles *ABC* and *ADE*. Then the increment $\Delta_m\Gamma^p$ for the subsequent approximation is defined by $\Delta_m\Gamma^p = \Gamma_D^* - \Gamma_{m-1}^p - \dfrac{S_D}{2G}$ rather than by (2.73). The values of σ_0^D and $\Delta_k\varepsilon_0^p$ are calculated in a similar way. The values thus found are then used as described earlier. This approach applied to the solution of specific problems substantially reduced the necessary number of approximations: by almost 50% when studying the isothermal axisymmetric loading of shells of revolution [100] and by more than 25% when solving the nonaxisymmetric three-dimensional problem of thermoplasticity for a three-layer solid of revolution subject to heating [137].

2.2.3. Thermoviscoplastic Deformation of Isotropic Bodies with the Third Deviatoric Stress Invariant Taken into Account. In all the above algorithms for solving boundary-value problems, the constitutive equations (stress–strain relationship) describing the elastoplastic deformation of elements of an isotropic solid are derived assuming that the relationship between the first and second stress and strain invariants is independent of the stress mode and determined from uniaxial-tension or torsion tests on cylindrical specimens, conducted to plot the instantaneous thermomechanical surfaces (2.60). Actually, as the experiments [31, 41] show, there are isotropic materials for which the relationship between the stress and strain intensities differs in tension, compression, and torsion, i.e., depends on the stress mode.

The concept of stress mode angle is introduced when determining the principal stresses by solving the following cubic equation using Cardano's formula:

$$s^3 - I_2(D_\sigma)s - I_3(D_\sigma) = 0 \tag{2.77}$$

for the components of the principal stress deviator: the second invariant ($I_2(D_\sigma) = s_{ij}s_{ij}/2$) and the third invariant ($I_3 = s_{zz}s_{rr}s_{\varphi\varphi} + 2s_{zr}s_{r\varphi}s_{z\varphi} - s_{zz}s_{r\varphi}^2 - s_{rr}s_{z\varphi}^2 - s_{\varphi\varphi}s_{zr}^2$) of the deviatoric stress tensor, $s_{ij} = \sigma_{ij} - \sigma_0\delta_{ij}$ are the components of the deviatoric stress tensor. It is assumed that $s_1 \geq s_2 \geq s_3$. Then Eq. (2.77) has the following roots:

$$s_1 = \frac{2S}{\sqrt{3}}\cos\vartheta, \qquad s_2 = \frac{2S}{\sqrt{3}}\cos\left(\vartheta + \frac{2\pi}{3}\right), \qquad s_3 = \frac{2S}{\sqrt{3}}\cos\left(\vartheta + \frac{4\pi}{3}\right), \tag{2.78}$$

where ϑ is related to the components of the deviatoric stress tensor by $3\vartheta = \arccos(3\sqrt{3}\,I_3/2S^3)$. It varies as $0 \leq \vartheta \leq \pi/3$ ($\vartheta = 0$ corresponds to uniaxial tension, $\vartheta = \pi/6$ to torsion, and $\vartheta = \pi/3$ to uniaxial compression of a cylindrical specimen) and shows the orientation of the octahedral shear stress in the octahedral plane relative to the projection of the principal axis along which the maximum stress acts onto this plane. The angle ϑ was used in [19, 34, 52, 129, etc.] to specify the stress mode.

Sometimes, the components of the deviatoric stress tensor are expressed in terms of trigonometric functions in a different way, resulting in an expression for the stress mode angle different from (2.78). For example, the parameter ω_σ is used in [29, 76, 87] as the stress mode angle and the roots of the cubic equation (2.77) are the following:

$$s_1 = \frac{2S}{\sqrt{3}}\cos(\omega_\sigma - \pi/3), \qquad s_2 = \frac{2S}{\sqrt{3}}\cos(\omega_\sigma + \pi/3), \qquad s_3 = -\frac{2S}{\sqrt{3}}\cos\omega_\sigma. \tag{2.79}$$

The angle ω_σ is related to the components of the deviatoric stress tensor by $3\omega_\sigma = \arccos(-3\sqrt{3}\,I_3/2S^3)$ and varies, as the angle ϑ, within the limits $0 \leq \omega_\sigma \leq \pi/3$: $\omega_\sigma = 0$ corresponds to uniaxial compression, $\omega_\sigma = \pi/6$ to torsion, and $\omega_\sigma = \pi/3$ to uniaxial tension of a cylindrical specimen. This angle indicates how the octahedral shear stress is oriented in the octahedral plane with respect to the negative projection (onto this plane) of the principal axis along which the minimum stress acts.

Other authors, such as Novozhilov, use an angle indicating the orientation of the octahedral shear stress relative to the bisector between the projections of the axes of maximum and negative minimum principal deviatoric stresses onto the octahedral plane. The interpretation of various parameters used to describe the stress mode is discussed in detail in [158]. More complex expressions that account for all the three invariants of the stress tensor are presented in [161].

The papers [97, 156, 157] were the first to incorporate the stress mode into the constitutive equations for isotropic materials deforming along straight paths or paths of small curvature. These equations relate engineering stresses and finite relative elongations and contain two nonlinear functions:

$$\sigma_0 = \Phi^*(\bar{\varepsilon}_0^*, T, \vartheta), \qquad S = F^*(\Gamma^*, T, \vartheta). \tag{2.80}$$

One of these functions relates the first invariants of the stress and strain tensors, while the other function relates the second invariants of the respective deviatoric tensors. These functions are individualized in two series of reference tests on tubular specimens under loading at several constant values of the stress mode angle and several temperatures. The first series of tests involves instantaneous deformation of specimens (i.e., the loading rate is such that no rheological properties of the material are manifested). The second series includes creep tests at the same loading rate as in the tests of the first series. As experiments show, when strains are small (5–6%), the first stress and strain invariants can be assumed to be in a linear relationship, i.e., the volume of an element of the body changes elastically.

As in the previous cases, to describe the inelastic deformation of elements of the body along various paths, the relationships between the stresses σ_{ij} and the strains ε_{ij} linearized in one way or another are represented in the form of Hooke's law with additional terms σ_{ij}^* describing thermal deformation, inelasticity of the material, dependence of material characteristics on the stress mode and temperature, and linearization methods:

$$\sigma_{ij} = 2G^*\varepsilon_{ij} + (K - 2G^*)\varepsilon_0\delta_{ij} - \sigma_{ij}^* \qquad (i, j = z, r, \varphi). \tag{2.81}$$

The expressions for σ_{ij}^* and G^* depend on the stress mode, the theory used, and the linearization method.

In the case of simple deformation (deformation of an element of the body along straight or nearly straight paths), in linearizing Eqs. (2.81) by the method of elastic solutions, we assume that $G^* = G_0$ and $K = K_0$ are, respectively, the shear and

bulk moduli of the material at normal temperature T_0 and some initial stress mode angle. The additional stresses σ_{ij}^* are defined by (2.56).

When the equations of thermoplasticity are linearized by the method of variable elastic parameters, G^* in Eqs. (2.81) is the secant modulus that depends on the inelastic strain, temperature, and stress mode and is defined by (2.58), and the additional stresses are defined by (2.64) rather than (2.56).

If the equations of thermoplasticity describing the deformation of elements of a body along paths of small curvature are linearized by the method of additional stresses, G^* is the shear modulus G at current temperature and stress mode angle, and the additional stresses σ_{ij}^* are defined by (2.66).

As in the case of independence of the material properties of the stress mode, the nonlinear constitutive equations are linearized by the method of successive approximations using the instantaneous stress–strain curves (2.80) and the creep curves corresponding to the temperature at the current step and the stress mode angle calculated in the previous approximation:

$$\sigma_0 = \Phi^*(\bar{\varepsilon}_0^*, T_m, \vartheta_{k-1}), \qquad S = F^*(\Gamma^*, T_m, \vartheta_{k-1}), \tag{2.82}$$

where m is the step number; k is the approximation number.

The stress–strain curves are used to calculate the plastic function ω and the secant modulus G^* in solving a boundary-value problem for simple deformation processes by the method of successive approximations. In solving a problem of deformation along paths of small curvature, relations (2.82) are used to calculate the increments of the inelastic shear-strain intensity $\Delta_k \Gamma^n$. Then these values are used to calculate the additional stresses σ_{ij}^* appearing in Eqs. (2.81).

This approach was successfully used in [55, 129, etc.] in analyzing the thermal stress–strain state of structural members in the form of solids of revolution with material properties depending on the stress mode,

2.3. State of Orthotropic and Isotropic Bodies Subject to Deformation and Damage. Elaborating upon the studies [20, 28, 37, 85, 98, 115, 116], a method for analyzing the stress–strain state of compound solids of revolution made of isotropic and orthotropic materials subject to damage was developed.

At each step of loading, the effect of creep damage of an isotropic material on the deformation of the body is modeled using a damage parameter ω^p to characterize the decrease in the effective volume in which the corresponding stresses act, and true stresses rather than engineering stresses are used [53]:

$$\tilde{\sigma}_{ij} = \frac{\sigma_{ij}}{1-\omega^p}, \tag{2.83}$$

where σ_{ij} are engineering stresses, i.e., loads per undamaged area elements of the body.

This damage parameter characterizes the change in the initial structure of the material, the nucleation, growth, and coalesce of microdefects during deformation, which decrease the effective areas over which the stresses are distributed. The relationship between stresses σ_{ij} and strains ε_{ij} (1.1) linearized by the method of additional stresses taking into account (2.65) remains in the form

$$\sigma_{zz} = (2G_0 + \lambda_0)\varepsilon_{zz} + \lambda_0(\varepsilon_{rr} + \varepsilon_{\varphi\varphi}) - \sigma_{zz}^*, \qquad \sigma_{zr} = 2G_0\varepsilon_{zr} - \sigma_{zr}^*, \quad (z, r, \varphi), \tag{2.84}$$

where the additional terms σ_{ij}^* are represented as

$$\sigma_{zz}^* = (1-\omega^p)\left[(2G\varepsilon_{zz}^n + 2G_0\omega\varepsilon_{zz} + K\varepsilon_T + 3\lambda_0\omega_1\varepsilon_0\right] + \omega^p\left[(2G_0 + \lambda_0)\varepsilon_{zz} + \lambda_0(\varepsilon_{rr} + \varepsilon_{\varphi\varphi})\right];$$

$$\cdots\cdots\cdots\cdots\cdots\cdots\cdots\cdots \tag{2.85}$$

$$\sigma_{r\varphi}^* = (1-\omega^p)\left[2G_0\omega\varepsilon_{r\varphi} + 2G\varepsilon_{r\varphi}^n\right] + 2G_0\omega^p\varepsilon_{r\varphi}.$$

At the end of the *m*th step of loading, the nonlinear strains ε_{ij}^{n} (sum of plastic (ε_{ij}^{p}) and creep (ε_{ij}^{c}) strains) are defined by formulas (2.70) and (2.71) for $\varepsilon_{0}^{n}=0$ and are calculated from the instantaneous thermomechanical surface $S=F^{*}(\Gamma^{*},T)$ and creep curves $\varepsilon^{c}=\varepsilon^{c}(\sigma,T,t)$ until the fracture of the specimen. The scalar damage parameter ω^{p} is determined from a kinematic equation where the rate of variation in damage is related to some equivalent stress, using stress rupture curves, also obtained in uniaxial-tension tests. The equivalent stress is determined from a failure criterion. It is assumed that the damage parameter is a functional of the loading process. A method for determining it is detailed in [51, 111, 117, etc.]. Another, simpler approach is to use the ratio of current creep strain to maximum creep strain as a damage parameter. The onset of fracture of a body at a given point of its element can be estimated by either using a damage parameter or comparing the equivalent stresses to the ultimate strength.

The process of successive approximations in solving boundary-value problems of thermoviscoplasticity is detailed in [36, 80, 95, 141, etc.].

For orthotropic materials, at each step of loading, the effect of damage on the deformation of the body is described using six damage parameters that characterize the reduction in the effective areas on which corresponding stresses act and using true stresses rather than engineering stresses [62, 63]:

$$\widetilde{\sigma}_{ij}=\frac{\sigma_{ij}}{1-\omega_{ij}^{P}}, \tag{2.86}$$

where σ_{ij} are engineering stresses, i.e., loads per undamaged area elements of the body; ω_{ij}^{P} are damage parameters. This damage parameter characterizes the change in the initial structure of the material, the nucleation, growth, and coalesce of pores and formation of microdefects during deformation, which decrease the effective areas over which the stresses are distributed. These damage parameters help to explain the nonlinearity of tensile, torsion, or shear stress–strain curves.

For such materials subject to damage, the stress–strain relationship can be represented in the form (2.12) where the additional terms σ_{ij}^{*} are

$$\begin{aligned}\sigma_{zz}^{*}&=A_{zzzz}\varepsilon_{zz}^{T}+A_{zzrr}\varepsilon_{rr}^{T}+A_{zz\varphi\varphi}\varepsilon_{\varphi\varphi}^{T}+A_{zzzz}^{0}\omega_{zzzz}\varepsilon_{zz}+A_{zzrr}^{0}\omega_{zzrr}\varepsilon_{rr}+A_{zz\varphi\varphi}^{0}\omega_{zz\varphi\varphi}\varepsilon_{\varphi\varphi}\\&+\omega_{zz}^{P}[A_{zzzz}(\varepsilon_{zz}-\varepsilon_{zz}^{T})+A_{zzrr}(\varepsilon_{rr}-\varepsilon_{rr}^{T})+A_{zz\varphi\varphi}(\varepsilon_{\varphi\varphi}-\varepsilon_{\varphi\varphi})],\\\sigma_{r\varphi}^{*}&=(A_{r\varphi r\varphi}^{0}\omega_{r\varphi r\varphi}+A_{r\varphi r\varphi}\omega_{r\varphi}^{P})\varepsilon_{r\varphi}\end{aligned} \tag{2.87}$$

for cylindrically orthotropic material and

$$\begin{aligned}\sigma_{zz}^{*}&=(1-\omega_{zz}^{p})[A_{zztz}^{0}\omega_{zzzz}\varepsilon_{zz}+A_{zzrr}^{0}\omega_{zzrr}\varepsilon_{rr}+A_{zz\varphi\varphi}^{0}\omega_{zz\varphi\varphi}\varepsilon_{\varphi\varphi}\\&-2A_{zzr\varphi}(\varepsilon_{r\varphi}-\varepsilon_{r\varphi}^{T})+A_{zzzz}\varepsilon_{zz}^{T}+A_{zzrr}\varepsilon_{rr}^{T}+A_{zz\varphi\varphi}\varepsilon_{\varphi\varphi}^{T}]+\omega_{zz}^{p}(A_{zzzz}^{0}\varepsilon_{zz}+A_{zzrr}^{0}\varepsilon_{rr}+A_{zz\varphi\varphi}^{0}\varepsilon_{\varphi\varphi}),\\\sigma_{r\varphi}^{*}&=(1-\omega_{r\varphi}^{p})[A_{r\varphi r\varphi}^{0}\omega_{r\varphi r\varphi}\varepsilon_{r\varphi}+A_{r\varphi r\varphi}\varepsilon_{r\varphi}^{T}-A_{zzr\varphi}(\varepsilon_{zz}-\varepsilon_{zz}^{T})\\&-A_{rrr\varphi}(\varepsilon_{rr}-\varepsilon_{rr}^{T})-A_{\varphi\varphi r\varphi}(\varepsilon_{\varphi\varphi}-\varepsilon_{\varphi\varphi}^{T})]-A_{r\varphi}^{0}\omega_{r\varphi}^{p}\varepsilon_{r\varphi}\end{aligned} \tag{2.88}$$

for rectilinearly orthotropic material.

Both relations (2.84) with (2.85) for isotropic materials and relations (2.12) with (2.87), (2.88) for orthotropic materials are nonlinear. This nonlinearity is due to the fact that the plastic strains ε_{ij}^{n} and the damage parameters ω^{p}, ω_{ij}^{P} on which the stresses depend, in turn, depend on the stress state of elements of the body. These relations are linearized using the method of successive approximations, calculating the inelastic strain ε_{ij}^{n} and the damage parameters ω^{p}, ω_{ij}^{P} from the previous approximation. The instantaneous thermomechanical surfaces $S=F^{*}(\Gamma^{*},T)$ for different fixed temperatures are used for

isotropic materials and six instantaneous thermomechanical surfaces $\sigma_{ij} = F_{ij}(\varepsilon_{ij}^*, T)$ obtained from tension–compression or torsion–shear tests for orthotropic materials.

A method for calculating the damage parameters for an orthotropic material is as follows. These parameters are set equal to zero in the first approximation of the first step of loading and heating. At the subsequent steps, they are set equal to their values obtained in the last approximation of the previous step. In each approximation, the values of the damage parameters cannot be less than their values in the last approximation of the previous step, i.e., it is assumed that damages do not heal. By solving the elastic boundary-value problem with additional stresses in the first approximation of the *k*th step of loading, we obtain the distribution of the stresses σ_{ij} and ε_{ij} in each element of the body, and we can also calculate the strains $\varepsilon_{ij}^* = \sigma_{ij} / [E_{ij}(1-\omega_{ij}^{\mathrm{P}(k-1)})]$ corresponding to the stresses σ_{ij} under uniaxial loading. Here $E_{ij} = E_i$ for $i = j$ and $E_{ij} = 2G_{ij}$ for $i \neq j$, and $\omega_{ij}^{\mathrm{P}(K-1)}$ are the values of the damage parameters at the previous step of loading or at the end of the previous approximation. Then we use the curves $\sigma_{ij} = F_{ij}(\varepsilon_{ij})$ for the temperature T_K of the *m*th step of loading of an element of the body plotted by linear interpolation with respect to the temperature of the instantaneous thermomechanical surfaces $\sigma_{ij} = F_{ij}(\varepsilon_{ij}, T)$ to find the values of σ_{ij}^{D} and $\varepsilon_{ij}^{\mathrm{D}}$ such that $(\sigma_{ij}^{\mathrm{D}} \cdot \varepsilon_{ij}^{\mathrm{D}}) = (\sigma_{ij} \cdot \varepsilon_{ij}^*)_K$ for each σ_{ij}-vs.-ε_{ij} curve. These values of σ_{ij}^{D} and $\varepsilon_{ij}^{\mathrm{D}}$ are used to determine the damage parameters ω_{ij}^{P} by the formulas $(\omega_{ij}^{\mathrm{P}})_K = 1 - \sigma_{ij}^{\mathrm{D}} / (E_{ij}\varepsilon_{ij}^{\mathrm{D}})$. Knowing the values of the damage parameters, we can again solve the boundary-value problem to determine the stresses and strains and then calculate the new values of the parameters ω_{ij}^{P}. The process of successive approximations is terminated once the values of the strain energy $U = \sigma_{ij}(\varepsilon_{ij} - \varepsilon_{ij}^T)/2$ in each element of the body found in two subsequent approximations differ by less than a predefined amount.

The results of analyzing the thermostressed state of solids of revolution taking into account the damage of the material during loading are reported in [62, 66, 111, 117, 133, 135, 141, 148, etc.].

3. Variational Equations of Nonstationary Heat Conduction and Thermoviscoplasticity for Isotropic and Orthotropic Materials. In solid mechanics, there are very many variational equations and variational principles equivalent to various relations in Sec. 2. Many of them are detailed in the literature. We will consider the variational heat-conduction equation and the Lagrange equation that replace the differential heat-conduction equation and heat-transfer boundary conditions, equilibrium equations, and static boundary conditions and exist irrespective of the state (elastic, plastic, or viscoplastic) of the material.

3.1. Variational Heat-Conduction Equation. To determine the temperature of anisotropic structural members, we will use the following differential heat-conduction equation [95, 132]:

$$c\rho \frac{\partial T}{\partial t} = -\mathrm{div}\ \vec{p}, \tag{3.1}$$

where $\vec{p} = -\lambda \nabla T$ is the heat flow vector in the body; c is the specific heat per unit mass of the body; t is time; ρ is the density of the material; $\lambda(\lambda_{ij})$ is the thermal-conductivity tensor; T is temperature.

Equation (3.1) is based on the assumption that there are no heat sources in the body and that no heat is generated during deformation. The differential equation (3.1) should be subject to initial conditions ($T = T_0$ at $t = t_0$) and boundary conditions $\vec{n} \cdot \vec{p} = \alpha(T - \theta) + \vec{n}\vec{p}^*$ (Newton's law of cooling of the surface Σ of the compound body). Here t_0 and T_0 are the initial time and temperature; $\vec{n}$ is the outward normal to the surface of the compound body; α is the thermal transmittance; θ is the ambient temperature; $\vec{p}^*$ is the given external heat flow.

Multiplying the heat-conduction equation and boundary conditions by the temperature variation δT, integrating the first equation over the volume V of the body and the second equation over the surface Σ that bounds this volume, summing them, and performing simple transformations, we obtain the variational heat-conduction equation

$$\int_V \left[c\rho \frac{\partial T}{\partial t} \partial T - \vec{p} \cdot \delta \nabla T \right] dV + \int_\Sigma [\alpha(T - \theta) + \vec{n} \cdot \vec{p}^*] \delta T d\Sigma. \tag{3.2}$$

The heat-conduction problem is solved in orthogonal curvilinear coordinate axes q_i $(i = 1, 2, 3)$ that are not aligned with the principal axes q_i' of anisotropy of the orthotropic material. Then we can use the transformation formulas to express the components of the thermal-conductivity tensor λ_{ij} in the coordinate system q_i in terms of their principal values λ_n' as follows:

$$\lambda_{ij} = \lambda_n' l_{ni} l_{nj} \quad (n = 1, 2, 3). \tag{3.3}$$

In this coordinate system, the variational heat-conduction equation (3.2) has the form

$$\int_V \left[c\rho \frac{\partial T}{\partial t} \delta T + \frac{\lambda_{ij}}{H_i} \frac{\partial T}{\partial q_i} \delta \left(\frac{1}{H_i} \frac{\partial T}{\partial q_i} \right) \right] dV + \int_\Sigma [(\alpha(T - \theta) + p_n^*)] \delta T d\Sigma = 0 \quad (i, j = 1, 2, 3), \tag{3.4}$$

where α is the convective heat-transfer factor from the body to the ambient medium of temperature θ; t is the current time of heating; p_n^* is the projection of the external heat flow vector onto the normal to the surface of the body; H_i is the Lame parameter in the coordinate system q_i.

As already mentioned earlier, we will consider solids of revolution. The solution will be sought in a cylindrical coordinate system for isotropic materials, cylindrically orthotropic materials, and rectilinearly orthotropic materials. The variational heat-conduction equation (3.4) takes the form

$$\int_V \left[c\rho \frac{\partial T}{\partial t} \delta T - q_z \delta \left(\frac{\partial T}{\partial z} \right) - q_r \left(\frac{\partial T}{\partial r} \right) - q_\varphi \left(\frac{\partial T}{r \partial \varphi} \right) \right] dV + \int_\Sigma [(\alpha(T - \theta) + Q_n)] \delta T d\Sigma = 0, \tag{3.5}$$

where q_z, q_r, q_φ are the heat flows in the corresponding directions,

$$q_z = -\left(\lambda_{zz} \frac{\partial T}{\partial z} + \lambda_{zr} \frac{\partial T}{\partial r} + \lambda_{z\varphi} \frac{1}{r} \frac{\partial T}{\partial \varphi} \right),$$

$$q_r = -\left(\lambda_{zr} \frac{\partial T}{\partial z} + \lambda_{rr} \frac{\partial T}{\partial r} + \lambda_{r\varphi} \frac{1}{r} \frac{\partial T}{\partial \varphi} \right),$$

$$q_\varphi = -\left(\lambda_{z\varphi} \frac{\partial T}{\partial z} + \lambda_{r\varphi} \frac{\partial T}{\partial r} + \lambda_{\varphi\varphi} \frac{1}{r} \frac{\partial T}{\partial \varphi} \right), \tag{3.6}$$

Q_n is the projection of the given heat flow vector onto the normal to the surface of the body; λ_{ij} are the components of the thermal-conductivity tensor ($\lambda_{ij} = \lambda \cdot \delta_{ij}$ for an isotropic material and are expressed in terms of the principal values $\lambda_{zz}, \lambda_{xx}, \lambda_{yy}$ by the transformation formulas (between the coordinate systems z, x, y and z, r, φ) for a rectilinearly orthotropic material).

3.2. Variational Lagrange Equation. Let us write the variational Lagrange equation describing the stress–strain state of a solid instead of the differential equilibrium equation

$$\text{div } T_\sigma + \vec{K} = 0 \tag{3.7}$$

and the static boundary conditions $\vec{t}_n = T_\sigma \cdot \vec{n}$ or $t_{\alpha n} = \sigma_{\alpha\beta} l_{\beta n}$. Here l_β (l_1, l_2, l_3) are the direction cosines of the outward normal $\vec{n}$ to the surface Σ_t of the body; $t_{\alpha n}$ (t_{1n}, t_{2n}, t_{3n}) are the projections of the surface forces onto the orthogonal coordinate axes q_α; the dot denotes scalar product of a tensor and a vector; the second equality relates the stresses $t_{\alpha n}$ acting on the area with the outward normal $\vec{n}$ and the stresses $\sigma_{\alpha\beta}$ acting on three mutually perpendicular areas that coincide with the coordinate surfaces and adjoin the area with the normal $\vec{n}$.

Let surface forces $\vec{t}_n$ (t_{in}) be specified on a portion Σ_t of the outside surface and displacements $\vec{u}(u_i)$ on a portion Σ_u. Then the variational equation becomes

$$\int_V (\sigma_{ij} \delta \varepsilon_{ij} - \vec{K} \cdot \delta \vec{u}) dV - \int_{\Sigma_t} \vec{t}_n \cdot \delta \vec{u} d\Sigma = 0 \quad (i, j = 1, 2, 3). \tag{3.8}$$

Here the surface integral is evaluated over that part of the surface of the body on which only surface forces are specified because the displacement variations Σ_u on the surface are equal to zero.

Substituting (1.1) into the variational equation (3.8) and assuming that the additional stress σ_{ij}^* and parameters A_{ijmn} do not vary because they are known functions or constants in each approximation, we obtain the following variational equation to determine the stress–strain state:

$$\delta\Im = \delta\int_V \left(\frac{1}{2}A_{ijmn}\varepsilon_{ij}\varepsilon_{mn} - \sigma_{ij}^*\varepsilon_{ij} - K_i u_i\right)dV - \delta\int_{\Sigma_t} t_{in}u_i\,d\Sigma = 0 \quad (i, j, m, n = 1, 2, 3). \tag{3.9}$$

If the constitutive equations have the form (2.12), we have the following variational equation for determining the stress–strain state in the cylindrical coordinate system:

$$\begin{aligned}\delta\Im = \delta\Bigg\{\int_V [0{,}5(A^0_{zzzz}\varepsilon^2_{zz} + A^0_{rrrr}\varepsilon^2_{rr} + A^0_{\varphi\varphi\varphi\varphi}\varepsilon^2_{\varphi\varphi}) + 2(A^0_{zrzr}\varepsilon^2_{zr} + A^0_{z\varphi z\varphi}\varepsilon^2_{z\varphi}\\ + A^0_{r\varphi r\varphi}\varepsilon^2_{r\varphi}) + A^0_{zzrr}\varepsilon_{zz}\varepsilon_{rr} + A^0_{zz\varphi\varphi}\varepsilon_{zz}\varepsilon_{\varphi\varphi} + A^0_{rr\varphi\varphi}\varepsilon_{rr}\varepsilon_{\varphi\varphi}\\ - \sigma^*_{zz}\varepsilon_{zz} - \sigma^*_{rr}\varepsilon_{rr} - \sigma^*_{\varphi\varphi}\varepsilon_{\varphi\varphi} - 2\sigma^*_{zr}\varepsilon_{zr} - 2\sigma^*_{z\varphi}\varepsilon_{z\phi} - 2\sigma^*_{r\varphi}\varepsilon_{r\varphi} - K_z u_z\\ - K_r u_r - K_\varphi u_\varphi]rdzdrd\varphi - \int_{\Sigma_t}(t_{nz}u_z + t_{nr}u_r + t_{n\varphi}u_\varphi)rdsd\varphi\Bigg\} = 0.\end{aligned} \tag{3.10}$$

If the coefficients A_{ijkl} are defined by (2.6), (2.7), and the additional stresses σ_{ij}^* by (2.13), then Eq. (3.10) is a variational equation describing the stress–strain state of a cylindrically orthotropic material. For a rectilinearly orthotropic material, the coefficients A_{ijkl} in (3.10) are defined by (2.9), (2.10), and the additional stresses by (2.14). The form of the variational equation is the same for isotropic and orthotropic materials. This allows us to use well-known algorithms to solve three-dimensional problems of thermoviscoplasticity for layered solids of revolution made of inelastic isotropic materials and elastic orthotropic materials and subject to nonaxisymmetric thermomechanical loading [95, 142].

For a structural member made of an isotropic material described by constitutive equations in the form (2.75), the variational equation of thermoviscoplasticity is as follows [100]:

$$\delta\Im = \delta\int_V \left(G'\varepsilon_{ij}\varepsilon_{ij} + \frac{1}{2}\lambda'\theta^2 - \sigma_{ij}^*\varepsilon_{ij} - K_i u_i\right)rdzd\varphi - \delta\int_{\Sigma_t} t_{in}u_i\,d\Sigma = 0 \quad (i, j, m, n = 1, 2, 3). \tag{3.11}$$

Attaching the kinematic equations and kinematic boundary conditions on the surface Σ_u to the variational equations (3.9)–(3.11), we obtain a closed system of equations that allows a step-wise analysis of an extensive class of processes of loading and heating of various structural members made of isotropic and orthotropic materials.

4. Numerical Solution of the Problem of Heat Conduction and Thermoviscoplasticity for Compound Bodies. As indicated earlier, the analysis of the three-dimensional thermostressed state of compound bodies is reduced to the sequential solution of the nonstationary heat-conduction problem (determination of the temperature fields in the body) and the thermoplastic problem (determination of the stress–strain state of the body). Selecting the temperature T and displacements as the basic unknowns, we will use the variational heat-conduction equations (3.4) and the variational Lagrange equation (3.8) and discretize them by the finite-element method.

We will review studies in which no constraints are imposed on the shape of the body and the three-dimensional thermoviscoplastic problem is solved in a Cartesian or cylindrical coordinate system. Which of the coordinate systems is chosen is determined by the convenience of describing the shape of the body.

4.1. Solution of the Thermoviscoplastic Problem in a Cartesian Coordinate System. An approach to solving the three-dimensional thermoviscoplastic problem for prismatic isotropic bodies in a Cartesian coordinate system is given in

[38–40, 36, 88, 95, 121]. As in the previous case, we solve the problem using the variational equation (3.11), where $i, j = z, x, y$, and the finite-element method. To this end, the volume V occupied by the body is partitioned into M finite elements in the form of triangular pyramids. Then the surface Σ bounding this volume appears partitioned into triangles, which are the pyramid sides lying on the surface of the body. The body is partitioned into finite elements as follows: first, the body is divided into elements in the form of octagonal hexahedral elements with rectilinear edges belonging to one material; then each of them is divided into five tetrahedrons with no additional nodes. As a result, each pyramid is made of only one material. The basic independent variables are taken to be $u_{i\alpha}$ ($i = 1, 2, 3$, $\alpha = 1, 2, \ldots, N$) at the nodes with coordinates $(x_1, x_2, x_3)_\alpha$. Their variation within an individual finite element with nodes α, β, k, q is approximately described by linear functions:

$$u_i = a_0^i + a_1^i x_1 + a_2^i x_2 + a_3^i x_3 \quad (i = 1, 2, 3), \tag{4.1}$$

where $a_0^i, a_1^i, a_2^i, a_3^i$ are constant coefficients. They are expressed in terms of the displacements at the nodes of the element and the coordinates of these nodes. Substituting the displacement and the coordinates of the nodes of the element into (4.1), we obtain three systems of algebraic equations of the fourth order for the unknown coefficients $a_0^i, a_1^i, a_2^i, a_3^i$, solving which yields

$$a_j^{i(m0)} = \frac{1}{A^{(m)}} a_{jc}^{(m)} u_{jc}^{(m)} u_{ic}^{(m)} \quad (c = \alpha, \beta, k, q), \quad \langle i = 1, 2, 3; j = 0, 1, 2, 3; m = 1, 2, \ldots, M \rangle, \tag{4.2}$$

where $A^{(m)}$ is the determinant of such system of equations; $a_{jc}^{(m)}$ is the algebraic complement of the jth column of the determinant; m is the finite-element number.

Replacing the integration over volume and surface of the body by the sums of integrals over volumes and finite-element sides lying on the surface of the body, we obtain an expression for the functional $\Im$ that is a function of unknown discrete displacements at nodes of finite elements. Next, we derive a system of $3N$ algebraic equations for the unknown discrete displacements at nodes from the extremality condition for the functional $\Im$:

$$\sum_{m=1}^{M} [B_{1c}^{l\alpha(m)} u_{ic} + B_{2c}^{l\alpha(m)} u_{2c} + B_{3c}^{l\alpha(m)} u_{3c}] = D_{l\alpha} \quad \langle l = 1, 2, 3 \rangle \quad (c = \alpha, \beta, k, q), \tag{4.3}$$

$$\left\{ B_{jc}^{i\alpha(m)} = \frac{1}{6|A^{(m)}|} [\langle G' \rangle_m (a_{pc}^{(m)} a_{p\alpha}^{(m)} \delta_{ij} + a_{ic}^{(m)} a_{j\alpha}^{(m)}) + \langle \lambda' \rangle_m a_{i\alpha}^{(m)} a_{jc}^{(m)}] \quad (p = 1, 2, 3), \right. \tag{4.4}$$

$$D_{i\alpha} = \sum_{m=1}^{M} (\langle \sigma_{ij} \rangle_m a_{j\alpha}^{*(m)} + \frac{|A^{(m)}|}{24} \langle K_i \rangle_m) + \frac{1}{3} \sum_{l=1}^{L} \langle t_{ni} \rangle_l \Sigma_l \quad (j = 1, 2, 3), \tag{4.5}$$

$$\left. a_{j\alpha}^{*(m)} = \frac{|A^{(m)}|}{6A^{(m)}} a_{j\alpha}^{(m)} \right\}. \tag{4.6}$$

In (4.4) and (4.5), the angular brackets denote averaging. The first summation in (4.5) is over all finite elements; the second summation is over all triangular sides of the finite element that lie on the surface of the body and have nodes one of which is α.

The nodal displacements obtained by solving this system of equations are used to calculate the strains and stresses for each finite element using (4.1) and (4.2). Due to the adopted law of variation in displacements within each element, the strains and stresses are constant and are determined by the nodal displacements within elements and the coordinates of their nodes. Therefore, it is usually assumed that they correspond to the center of gravity of a finite element. The strains and stresses at the internal nodes are calculated as averages over the elements joining at the point of interest.

This approach was used to analyze the thermoelastoplastic stress–strain state of cubical bodies under mechanical and thermal loading [38 – 40, 88, 95] and the stress state of a quadrangular shell with a conical hole at the center of the bottom heated from inside [40, 121], etc.

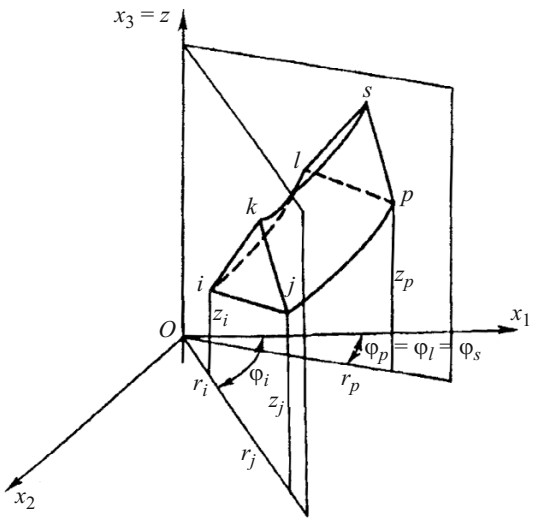

Fig. 3

4.2. Solution of the Thermoviscoplastic Problem in a Cylindrical Coordinate System. A Cartesian coordinate system is convenient for prismatic bodies, while the cylindrical coordinate system is convenient for analyzing the stress–strain state of parts of solids of revolution resulting from the intersection between the coordinate surfaces and the body.

As with thermoviscoplastic problems in a Cartesian coordinate system, the solution in a cylindrical coordinate system is found using the variational equation (3.11) and the finite-element method. To this end, the volume V occupied by the body is divided by N nodal circles and associated H meridional sections into M ring elements in the form of curvilinear triangular prisms. The total number of nodes $N^* = N \cdot H$. The surface Σ bounding this volume is divided into L areas that are the sides of a finite element that lie on the surface of the body. A small number of finite elements in the form of a circumferentially curvilinear triangular prism are sufficient for good approximation of a solid of revolution of arbitrary meridional cross-section or its part cut by two meridional sections (a nonclosed solid of revolution).

Denote the coordinates by z_i, r_i, φ_i and the displacements of the node i ($\beta = z, r, \varphi$; $i = 1, 2, \ldots, N^*$ is the node number) by $u_{\beta i}$ ($i = 1, 2, \ldots$). Let the nodal displacements be the basic unknowns.

Their variation in the ith finite element (Fig. 3) with node numbers i, j, k, l, p, s can be described by a bilinear function:

$$u_\beta = b_1^\beta + b_2^\beta z + b_3^\beta r + \varphi\ (b_4^\beta + b_5^\beta z + b_6^\beta r)$$

$$\langle \beta = z, r, \varphi \rangle, \tag{4.7}$$

where b_n^β are constant coefficients for the finite element. They can be expressed in terms of the displacements $u_{\beta i}, u_{\beta j}, u_{\beta k}, u_{\beta l}$, $u_{\beta p}, u_{\beta s}$ at the nodes of the finite element. Substituting these displacements and associated node coordinates into (4.7), we obtain a system of algebraic equations of the sixth order, solving which gives

$$b_n^{\beta(m)} = a_{nc}^{(m)} u_{\beta c} \quad \langle \beta = z, r, \varphi;\ n = 1, 2, \ldots, 6 \rangle \quad (c = i, j, k, l, p, s), \tag{4.8}$$

where $a_{nc}^{(m)}$ are the elements of the matrix inverse of the matrix of the system from which the coefficients b_n^β are determined.

We replace the integration over volume V and the surface Σ of the body by sums of the integrals over the volumes and surfaces of finite elements, considering that either triangular side i, j, k or l, p, s or quadrangular side $i, j, p, 1$, $i, k, s, 1$ or j, p, s can lie on the surface of the body. Using bilinear function (4.7), the kinematic equations, and expressions (4.8), we represent the functional $\Im$ in Eq. (3.12) as a function of unknown discrete displacements at nodes of finite elements. To find them, we derive the following system of $3N^*$ linear algebraic equations from the extremality condition for this expression:

$$\sum_{m=1}^{M}[B_{zc}^{\beta i(m)}u_{zc}+B_{rc}^{\beta i(m)}u_{rc}+B_{\varphi c}^{\beta i(m)}u_{\varphi c}]=D_{\beta i},$$

$$\langle\beta=z,r,\varphi,\quad(c=i,j,k,l,p,s),\quad\langle i=1,2,\ldots,N^{*}\rangle, \tag{4.9}$$

where

$$B_{zc}^{zi(m)}=\int_{V_m}[(2G'+\lambda')c_{zz}^{zi}c_{zz}^{zc}+4G'(c_{zr}^{zi}c_{zr}^{zc}+c_{z\varphi}^{zi}c_{z\varphi}^{zc})]rdzdrd\varphi,$$

$$B_{rc}^{zi(m)}=\int_{V_m}[4G'c_{zr}^{zi}c_{zr}^{rc}+\lambda'c_{zz}^{zi}(c_{rr}^{rc}+c_{\varphi\varphi}^{rc}]rdzdrd\varphi,$$

$$B_{\varphi c}^{zi(m)}=\int_{V_m}[4G'c_{z\varphi}^{zi}c_{z\varphi}^{\varphi c}+\lambda'c_{zz}^{zi}c_{\varphi\varphi}^{\varphi c}]rdzdrd\varphi,$$

$$\ldots\ldots\ldots\ldots\ldots\ldots\ldots\ldots\ldots\ldots\ldots\ldots\ldots\ldots \tag{4.10}$$

$$D_{zi}=\sum_{m=1}^{M}\left[\langle\sigma_{\rho q}\rangle_m C_{\rho q}^{zi(m)}+\frac{1}{6}\langle K_z\rangle_m V_m\right]+\sum_{l=1}^{L}\left[\langle t_{nz}\rangle_l\left(\frac{\Sigma_l^0}{4}+\frac{\Sigma_l^{\Delta}}{3}\right)\right]\quad(z,r,\varphi),\quad(\rho,q=z,r,\varphi)$$

$$c_{zz}^{zc}=a_{2c}+a_{5c}\varphi,\quad c_{zr}^{zc}=\frac{1}{2}(a_{3c}+a_{6c}\varphi),\quad c_{z\varphi}^{zc}=\frac{1}{2r}(a_{4c}+a_{5c}z+a_{6c}r),$$

$$\ldots\ldots\ldots\ldots\ldots\ldots\ldots\ldots\ldots\ldots\ldots\ldots\ldots\ldots$$

$$C_{zz}^{zc(m)}=\int_{V_m}c_{zz}^{zc}rdzdrd\varphi,\quad C_{zr}^{zc(m)}=\int_{V_m}c_{zr}^{zc}rdzdrd\varphi, \tag{4.11}$$

$$\ldots\ldots\ldots\ldots\ldots\ldots\ldots\ldots\ldots\ldots\ldots\ldots\ldots\ldots$$

The first summation in (4.10) is over all finite elements; the second summation is over all sides of the finite element that lie on the surface of the body and have nodes one of which is i. If one of the sides lying on the surface of the body is quadrangular, then $\Sigma_i^{\Delta}=0$ in (4.10). If it is triangular, then $\Sigma_i^0=0$, where Σ^{Δ}, Σ^0 are the areas of the corresponding sides of the finite element.

This approach was used to analyze the thermoelastoplastic stress state of circumferentially nonclosed solids of revolution such as a nonuniformly heated cylindrical sector under no external mechanical loading [72–75, 88] and a nonuniformly heated conical sector with mixed boundary conditions [75, 95, 152, etc.].

4.3. Solving the Thermoviscoplastic Problem in a Cylindrical Coordinate System by the Semianalytic Finite-Element Method. Applying three-dimensional finite elements to analyze the stress–strain state of closed solids of revolution is labor-consuming and costly. The approach proposed below allows reducing the three-dimensional problems of heat conduction and thermoviscoplasticity for compound solids of revolution made of isotropic and orthotropic materials to a number of two-dimensional problems in the meridional cross-section of the body. This approach involves the representation of the unknown functions in one direction in terms of continuous smooth basis functions and the finite-element discretization of a plane perpendicular to this direction. The original three-dimensional problem can be reduced to a number of two-dimensional problems. The capability of this approach is restricted by how well the load and unknown functions are approximated by several terms of the series. This efficiency of the approach is maximum when solving thermoviscoplastic problems for axisymmetric objects. In this case, using the temperature and displacements u_z, u_r, u_{φ} as the basic unknowns for both heat-conduction problem (determination of the temperature distribution in a body) and boundary-value problem (determination of the stress–strain state of a compound solid of revolution), we employ the semianalytic finite-element method [36, 61, 91, 95, 131, 137, etc.] representing the candidate solution by a trigonometric series:

$$T(z,r,\varphi,t)=\sum_{m=0}^{\infty}\overline{T}_m(z,r,t)\cos m\varphi+\sum_{m=1}^{\infty}\overline{\overline{T}}_m(z,r,t)\sin m\varphi, \tag{4.12}$$

$$u_z(z,r,\varphi,t)=\sum_{m=0}^{\infty}\overline{u}_z^{(m)}(z,r,t)\cos m\varphi+\sum_{m=1}^{\infty}\overline{\overline{u}}_z^{(m)}(z,r,t)\sin m\varphi \quad (z,r),$$

$$u_\varphi(z,r,\varphi,t)=\sum_{m=1}^{\infty}\overline{u}_\varphi^{(m)}(z,r,t)\sin m\varphi+\sum_{m=0}^{\infty}\overline{\overline{u}}_\varphi^{(m)}(z,r,t)\cos m\varphi. \tag{4.13}$$

The coefficients of these series are determined using the finite-element method in the meridional cross-section of the body, the variational heat-conduction equation (3.5), and the variational Lagrange equation (3.8).

To find the stationary values of functionals (3.5) and (3.8), the meridional cross-section F of the body is partitioned into M triangular finite elements with N nodes. Then the boundary of this section appears divided into N_1 segments that are sides of triangles. The partition is made so that each element corresponds to only one material. The temperature and displacements at nodes are used as the basic unknowns.

It is assumed that the temperature and displacements within a finite element with nodes i, j, k can be accurately approximated by linear functions:

$$T=b_1^T+b_2^T z+b_3^T r, \tag{4.14}$$

$$u_\alpha=a_1^\alpha+a_2^\alpha z+a_3^\alpha r \quad (\alpha=z,r), \tag{4.15}$$

where $b_1^T, b_2^T, b_3^T, a_1^\alpha, a_2^\alpha, a_3^\alpha$ are constant coefficients. They are expressed in terms of the temperatures T_i, T_j, T_k and displacements $u_{\alpha i}, u_{\alpha j}, u_{\alpha k}$ at the nodes of an element as follows:

$$b_p^T=\frac{a_{pc}^{(m)}T_c}{2F_m^*} \tag{4.16}$$

$$[a_p^\alpha=\frac{a_{pc}^{(m)}u_{\alpha c}}{2F_m^*} \quad (c=i,j,k); \quad \langle p=1,2,3,\ \alpha=z,r; \quad m=1,2,\ldots,M\rangle], \tag{4.17}$$

where $a_{pc}^{(m)}$ and F_m^* are constants expressed in terms of the coordinates of the nodes as

$$a_{1i}^{(m)}=z_j r_k-z_k r_j, \quad a_{2i}^{(m)}=r_j-r_k, \quad a_{3i}^{(m)}=z_k-r_j \quad (i,j,k),$$

$$2F_m^*=z_i(r_j-r_k)+z_j(r_k-r_i)+z_k(r_i-r_j). \tag{4.18}$$

Let us replace the integration over the area F and boundary L by the sum of the integrals over the area F_m of elements and the sides L_i lying on the boundary L_t. Substituting temperature (4.14) or displacements (4.15) and the strains obtained from the kinematic equations into the corresponding variational equations and assuming that the quantities characterizing the surface load vary linearly between nodes, we represent the functionals by a function of discrete temperatures or displacements at nodes of finite elements.

The thermal conductivities λ_{ij} appearing in the variational equation (3.5) depend on temperature and vary in the circumferential direction and in the meridional cross-section. Expressing the thermal conductivity λ_{ij} as $\lambda_{ij}=\lambda_{ij}^0(1-\omega_{ij}^T)$ and assuming that the heat-transfer factor α, ambient temperature θ, and the product $c\rho$ at some fixed instant are known functions of the coordinates and do not vary, we represent the variational equation (3.5) as

$$\delta\left\{\int_V\left[\int_{T_0}^{T} c\rho\frac{\partial T}{\partial t}dT+\frac{\lambda_{zz}^0}{2}\left(\frac{\partial T}{\partial z}\right)^2+\frac{\lambda_{rr}^0}{2}\left(\frac{\partial T}{\partial r}\right)^2+\frac{\lambda_{\varphi\varphi}^0}{2}\left(\frac{1}{r}\frac{\partial T}{\partial\varphi}\right)^2\right.\right.$$

$$\left.\left.-q_z^*\frac{\partial T}{\partial z}-q_r^*\frac{\partial T}{\partial r}-q_\varphi^*\frac{1}{r}\frac{\partial T}{\partial\varphi}\right]rdzdrd\varphi+\int_\Sigma\frac{\alpha T}{2}(T-2\theta)rdsd\varphi\right\}=0, \tag{4.19}$$

where

$$q_z^*=\lambda_{zz}^0\omega_{zz}^T\frac{\partial T}{\partial z},\qquad q_r^*=\lambda_{rr}^0\omega_{rr}^T\frac{\partial T}{\partial r}+\lambda_{r\varphi}\frac{1}{r}\frac{\partial T}{\partial\varphi},$$

$$q_\varphi^*=\lambda_{r\varphi}\frac{\partial T}{\partial r}+\lambda_{\varphi\varphi}^0\omega_{\varphi\varphi}^T\frac{1}{r}\frac{\partial T}{\partial\varphi}, \tag{4.20}$$

which are assumed to be known functions of the coordinates.

Expanding the ambient temperature θ and additional terms (4.20) into Fourier series, we reduce the three-dimensional heat-conduction problem (4.19) to a number of two-dimensional variational problems for the unknown coefficients in series (4.12), which can then be determined by the finite-element method. We will partition the meridional cross-section of the body into triangular finite elements with a linear law of variation in $\overline{T}_m$ and $\overline{\overline{T}}_m$ within them. To determine the coefficients $\overline{T}_m$ at the nodes (i,j,k) of finite elements with the side *ij* lying on the surface of the body, we will use the following explicit difference scheme, which allows calculating the coefficients $\overline{T}_m$ at $t+\Delta t$ from their values at *t*:

$$\overline{T}_{mi}(t+\Delta t)=\overline{T}_{mi}(t)+\frac{\Delta t}{\sum_{q=1}^{M}\langle c\rho\rangle_q H_i^{(q)}}\sum_{q=1}^{M}\Big[A_{ij}\overline{\theta}_{mi}(t+\Delta t)+B_{ij}\overline{\theta}_{mj}(t+\Delta t)$$

$$-(D_{ii}+m^2N_{ii}+A_{ij})\overline{T}_{mi}(t)-(D_{ij}+m^2N_{ij}+B_{ij})\overline{T}_{mj}(t)-(D_{ik}+m^2N_{ik})\overline{T}_{mk}(t)$$

$$+L_i(\overline{q}_z^{*(m)}(t)-\overline{\overline{q}}_{z\varphi}^{*(m)}(t))_i+P_i(\overline{q}_r^{*(m)}(t)-\overline{\overline{q}}_{r\varphi}^{*(m)}(t))_i-mR_i\overline{q}_{\varphi\,i}^{*(m)}(t)\Big]_q, \tag{4.21}$$

or the following implicit difference scheme:

$$\sum_{q=1}^{M}[(D_{ii}+m^2N_{ii}+\frac{1}{\Delta t}\langle c\rho\rangle H_i+A_{ij})\overline{T}_{mi}(t+\Delta t)+(D_{ij}+m^2N_{ij}+B_{ij})\overline{T}_{mj}(t+\Delta t)$$

$$+(D_{ik}+m^2N_{ik})\overline{T}_{mk}(t+\Delta t)]_q=\sum_{q=1}^{M}\Big[\frac{1}{\Delta t}\langle c\rho\rangle H_i\overline{T}_{mi}(t)+A_{ij}\overline{\theta}_{mi}(t+\Delta t)+B_{ij}\overline{\theta}_{mj}(t+\Delta t)$$

$$+L_i(\overline{q}_z^{*(m)}(t)-\overline{\overline{q}}_{z\varphi}^{*(m)}(t))+P_i(\overline{q}_r^{*(m)}(t)-\overline{\overline{q}}_{r\varphi}^{*(m)}(t))-mR_i\overline{q}_\varphi^{*(m)}(t)\Big]_q \qquad (i=1,2,\ldots,N), \tag{4.22}$$

where *m* is harmonic number; *N* is the number of nodes; *M* is the number of triangular finite elements in the meridional section of the body; *q* is the number of a triangular element; $\overline{\theta}_{mi}$ and $\overline{\overline{\theta}}_{mi}$ are the coefficients of the expansion of ambient temperature into trigonometric series similar to (4.12):

$$H_i=b_{1i}\int_\Delta rdzdr+b_{2i}\int_\Delta zrdzdr+b_{3i}\int_\Delta r^2dzdr,$$

$$D_{ij} = \lambda^0_{zz} b_{2i} b_{2j} \int_\Delta r dz dr + \lambda^0_{rr} b_{3i} b_{3j} \int_\Delta r dz dr,$$

$$N_{ij} = \lambda^0_{\varphi\varphi} [b_{1i} (b_{1j} \int_\Delta \frac{1}{r} dz dr + b_{2j} \int_\Delta \frac{z}{r} dz dr + b_{3j} \int_\Delta dz dr)$$

$$+ b_{2i} (b_{1j} \int_\Delta \frac{z}{r} dz dr + b_{2j} \int_\Delta \frac{z^2}{r} dz dr + b_{3j} \int_\Delta z dz dr) + b_{3i} (b_{1j} \int_\Delta dz dr + b_{2j} \int_\Delta z dz dr + b_{3j} \int_\Delta r dz dr), \quad (4.23)$$

$$A_{ij} = \operatorname{sign} F_\Delta \frac{l_{ij}}{10} \left[\alpha_i \left(2r_i + \frac{r_j}{2} \right) + \alpha_j \left(\frac{r_i}{2} + \frac{r_j}{3} \right) \right],$$

$$B_{ij} = \operatorname{sign} F_\Delta \frac{l_{ij}}{10} \left[\alpha_i \left(\frac{r_i}{2} + \frac{r_j}{3} \right) + \alpha_j \left(\frac{r_i}{3} + \frac{r_j}{2} \right) \right],$$

$$L_i = b_{2i} \int_\Delta r dz dr, \quad P_i = b_{3j} \int_\Delta r dz dr, \quad R_i = b_{1i} \int_\Delta dz dr + b_{2i} \int_\Delta z dz dr + b_{3i} \int_\Delta r dz dr,$$

$$b_{1j} = \frac{z_k r_i - z_i r_k}{2F_\Delta}, \quad b_{2j} = \frac{r_k - r_i}{2F_\Delta}, \quad b_{3j} = \frac{z_i - z_k}{2F_\Delta},$$

$$F_\Delta = \frac{1}{2} [z_i (r_j - r_k) + z_j (r_k - r_i) + z_k (r_i - r_j)], \quad l_{ij} = \sqrt{(z_i - z_j)^2 + (r_i - r_j)^2}. \quad (4.24)$$

In deriving the variational equations for the calculation of the temperature amplitude and discretizing them using the finite-element method, use is made of the method of successive approximations assuming that the additional terms $q^*_z, q^*_r, q^*_\varphi$ are known from the previous time step or the previous approximation. However, since the step Δt of integration over time of the heat-conduction equation is rather small, the temperature amplitudes appearing on the right-hand side and the additional terms averaged over each finite element are determined from the previous time step.

The coefficients $\overline{\overline{T}}_m$ are defined by (4.21) and (4.22) where m should be replaced by $-m$, and overbars and double overbars should be exchanged.

Knowing $\overline{T}_m$ and $\overline{\overline{T}}_m$ at all points of the finite-element partition of the meridional cross-section of the body, we can find the temperature in the body by calculating the trigonometric series (4.12).

To solve the thermoviscoplastic problem for compound solids of revolution made of isotropic and orthotropic materials with the semianalytic finite-element method, we expand the projections of the surface (t_{ni}) and bulk (K_i) forces and the function σ^*_{ij} into series similar to (4.13). Substituting these series, expression (4.13), and the expressions for the strains derived from (4.13) using the kinematic equations into the variational equation (3.10), we obtain the following system of equations for determining the displacement amplitudes $\overline{u}^{(m)}_i$ and $\overline{\overline{u}}^{(m)}$:

$$(1 + \delta_{0m}) \pi \delta \overline{\Im}_m = 0, \quad (1 + \delta_{0m}) \pi \delta \overline{\overline{\Im}}_m = 0, \quad (4.25)$$

$$\overline{\Im}_m = \int_F \left[\frac{1}{2} (A^0_{zzzz} \overline{\varepsilon}^{(m)2}_{zz} + A^0_{rrrr} \overline{\varepsilon}^{(m)2}_{rr} + A^0_{\varphi\varphi\varphi\varphi} \overline{\varepsilon}^{(m)2}_{\varphi\varphi}) + 2 (A^0_{zrzr} \overline{\varepsilon}^{(m)2}_{zr} + A^0_{z\varphi z\varphi} \overline{\varepsilon}^{(m)2}_{z\varphi} \right.$$

$$\left. + A^0_{r\varphi r\varphi} \overline{\varepsilon}^{(m)2}_{r\varphi}) + A^0_{zzrr} \overline{\varepsilon}^{(m)}_{zz} \overline{\varepsilon}^{(m)}_{rr} + A^0_{zz\varphi\varphi} \overline{\varepsilon}^{(m)}_{zz} \overline{\varepsilon}^{(m)}_{\varphi\varphi} + A^0_{rr\varphi\varphi} \overline{\varepsilon}^{(m)}_{rr} \overline{\varepsilon}^{(m)}_{\varphi\varphi} - \overline{\sigma}^*_{zz} \overline{\varepsilon}^{(m)}_{zz} \right.$$

$$\left. - \overline{\sigma}^*_{rr} \overline{\varepsilon}^{(m)}_{rr} - \overline{\sigma}^*_{\varphi\varphi} \overline{\varepsilon}^{(m)}_{\varphi\varphi} - 2\overline{\sigma}^*_{zr} \overline{\varepsilon}^{(m)}_{zr} - 2\overline{\sigma}^*_{z\varphi} \overline{\varepsilon}^{(m)}_{z\varphi} - 2\overline{\sigma}^*_{r\varphi} \overline{\varepsilon}^{(m)}_{r\varphi} - \overline{K}^{(m)}_z \overline{u}^{(m)}_z \right.$$

$$-\bar{K}_r^{(m)}\bar{u}_r^{(m)} - \bar{K}_\varphi^{(m)}\bar{u}_\varphi^{(m)}\Big]rdzdr - \int_S (\bar{t}_{nz}^{(m)}\bar{u}_z^{(m)} + \bar{t}_{nr}^{(m)}\bar{u}_r^{(m)} + \bar{t}_{n\varphi}^{(m)}\bar{u}_\varphi^{(m)})\,rds \quad (m = 0,1,\dots), \tag{4.26}$$

where $\bar{K}_i^{(m)}, \bar{t}_{ni}^{(m)}, \bar{\sigma}_i^{*(m)}$ are the coefficients of a trigonometric series in the circumferential coordinate; F is the half-area of the meridional cross-section of the body; S is its boundary. The expressions for $\bar{\bar{\Im}}_m$ are similar. The variational equation for $\bar{\Im}_0$ describes the axisymmetric stress state of a body subject to no torsion, while the equation for $\bar{\bar{\Im}}_0$ describes the stress state of a body subject to torsion.

To determine the stationary values of functionals (4.26), we use the finite-element method. As with the heat-conduction problem, we partition the meridional cross-section of the body into triangular finite elements with linear approximation of the coefficients of series (4.13). Determining the coefficients $\bar{u}_\alpha^{(m)}$ and $\bar{\bar{u}}_\alpha^{(m)}$ $(\alpha = z, r, \varphi)$ at the nodes (i, j, k) of triangular finite elements q in each approximation, we obtain a system of $3N$ linear algebraic equations for each harmonic:

$$\sum_{q=1}^{M} (B_{zp}^{\beta i(q)} u_{zp} + B_{rp}^{\beta i(q)} u_{rp} + B_{\varphi p}^{\beta i(q)} u_{\varphi p}) = D_{zi} \quad \langle \beta = z, r, \varphi \rangle,$$

$$(p = i, j, k), \quad \langle i = 1, 2, \dots, N \rangle. \tag{4.27}$$

Such systems are as many as there remain terms in solution (4.13).

The elements of the matrix of system (4.27) are calculated from the coefficients of Eqs. (2.12) and the coordinates of the nodes of finite elements in the meridional plane, and the right-hand side of the system is calculated from the amplitudes of the additional stresses σ_{ij}^* and the body and surface loads at the corresponding points of the meridional cross-section.

For an individual triangular element with nodes i, j, k, they are the following:

$$B_{zj}^{zi} = \int_{F_\Delta} (A_{11}^0 b_{2i} b_{2j} + A_{44}^0 b_{3i} b_{3j} + m^2 A_{55}^0 \Delta_{1i} \Delta_{1j}) rdzdr,$$

$$B_{rj}^{zi} = \int_{F_\Delta} (A_{44}^0 b_{3i} b_{2j} + A_{12}^0 b_{2i} b_{3j} + A_{13}^0 b_{2i} \Delta_{1j}) rdzdr,$$

$$B_{\varphi j}^{zi} = m \int_{F_\Delta} (-A_{55}^0 b_{2j} \Delta_{1i} + A_{13}^0 b_{2i} \Delta_{1j}) rdzdr,$$

$$\dots\dots\dots\dots\dots\dots\dots\dots\dots\dots\dots\dots\dots\dots\dots\dots\dots\dots\dots\dots\dots\dots\dots\dots$$

$$B_{\varphi j}^{\varphi i} = \int_{F_\Delta} (A_{55}^0 b_{2i} b_{2j} + A_{66}^0 \Delta_{2i} \Delta_{2j} + m^2 A_{33}^0 \Delta_{1i} \Delta_{1j}) rdzdr, \tag{4.28}$$

$$D_{zi} = \sum_{q=1}^{M} \int_{F_\Delta} [\sigma_{zz}^* b_{2i} + \sigma_{zr}^* b_{3i} - (m\sigma_{z\varphi}^* - K_z \cdot z)\Delta_{1i}] rdzdr$$

$$+ \sum_{l=1}^{L} \frac{l_{ij}}{12} \operatorname{sign} F_\Delta [t_{nz_i} (3r_i + r_j) + t_{nz_j} (r_i + r_j)], \tag{4.29}$$

$$\dots\dots\dots\dots\dots\dots\dots\dots\dots\dots\dots\dots\dots\dots\dots\dots\dots\dots\dots\dots\dots\dots\dots\dots$$

$$\Delta_{1j} = b_{3j} + b_{2j} \frac{z}{r} + b_{1j} \frac{1}{r}, \quad \Delta_{2j} = b_{2j} \frac{z}{r} + b_{1j} \frac{1}{r}. \tag{4.30}$$

The first summation in (4.29) is over all finite elements; the second summation is over all sides of the finite element that lie on the boundary of the meridional cross-section and have nodes one of which is *i.* The missing coefficients in (4.27) can be obtained from (4.28) by replacing the index j with i or k.

Determining the displacement amplitudes from the solutions of systems (4.27), we use formulas (2.23), (4.23), and (4.27) to calculate displacements, strains, and stresses in each approximation at the instant of interest. The process of successive approximations is terminated once the difference between the stress–strain states found in two sequential approximations has been less than a predefined error.

5. Axisymmetric Nonstationary Heat-Conduction Problems and Thermoviscoplastic Problems for Compound Solids of Revolution. Let us address the studies [35, 54, 89, 90, 91, etc.] carried out to solve axisymmetric problems of thermoviscoplasticity for isotropic bodies whose stress–strain state is determined by displacements u_z, u_r, stresses σ_{zz}, σ_{rr}, $\sigma_{\varphi\varphi}$, σ_{zr}, and associated strains. Two problem-solving methods were used, depending on the shape of the solid of revolution. For canonical solids of revolution such as hollow and solid cylinders, the solution can be found analytically. In analyzing the stress–strain state of solids of revolution of arbitrary meridional cross-section, the thermoviscoplastic problem is solved using the finite-element method.

5.1. Analytical Solution of the Thermoplastic Problem for Cylinders of Finite Length. An approach employing an analytic solution of a thermoelastic problem in each approximation and the solution of the class of boundary-value problems of thermoviscoplasticity for cylinders of finite length can be found in [5, 6, 10–14, 77–79, 91, 106]. In these papers, the axisymmetric problem of thermoviscoplasticity for a cylinder ($0 \le z \le l, r_0 \le r \le R$) is solved for displacements in a cylindrical coordinate system. The temperature field of the cylinder is supposed known at an arbitrary time. The cylinder is rotating with angular velocity $\Omega(t)$ subject to a balanced system of surface loads that are known functions of the coordinates z and r.

The thermoviscoplastic problem for a short circular cylinder at an arbitrary time is reduced in each approximation to a system of two partial differential equations for the displacement u_z and u_r with some additional body and surface forces determined by the stress–strain state of the cylinder in the previous approximation. In each approximation, the general solution of this system is analytically represented as the sum of the general solution of a homogeneous system of equations and the partial solutions corresponding to external loading and additional body forces. The general solution of the homogeneous system of equations is expanded into infinite series of zero- and first-order Bessel functions of the first kind J_0 and J_1 and zero- and first-order Bessel functions of the second kind Y_0 and Y_1 multiplied by a sine or a cosine of the corresponding angles. The partial solutions are found by expanding the additional body forces into double series of full orthogonal systems of zero- and first-order Bessel functions of the first and second kind and trigonometric functions. The sum of these two solutions exactly satisfies the boundary conditions on the cylindrical surfaces and integrally satisfies the condition at the cylinder ends. For more accurate satisfaction of the end conditions, Lurie–Prokopov homogeneous solutions are used [51]. Then the analytic solution of the thermoplastic problem for a hollow cylinder that does not change from approximation to approximation and from step to step of loading is represented as follows [13, 92]:

$$u_z(z,r) = D_0 z - \sum_{i=1}^{\infty} \left\{ \alpha_i r I_1(k_i r) + \left(\alpha_i + 4\frac{1-\nu}{k_i}\gamma_i \right) I_0(k_i r) + \beta_i r K_1(k_i r) \right.$$

$$\left. + \left(\beta_i + 4\frac{1-\nu}{k_i}\delta_i \right) K_0(k_i r) \right\} \sin k_i z + \sum_{i=1}^{\infty} \left\{ B_{i0} + \sum_{j=1}^{\infty} B_{ij} \Phi_0(\lambda_j r) \right\} \sin k_i z$$

$$+ \sum_{s=1}^{N_1} \{ \mathrm{Im}[N_s^* w_1(r)] \cos k_s (l-z) - \mathrm{Re}[N_s^* w_1(r)] \sin k_s (l-z) \}$$

$$+ \sum_{s=1}^{N_2} \{ \mathrm{Im}[N_s w_1(r)] \cos k_s z - \mathrm{Re}[N_s w_1(r)] \sin k_s z \}, \qquad (5.1)$$

$$u_r(z,r) = \frac{A_0}{r} + B_0 r + \frac{\gamma}{g} \frac{r^3 \Omega^2}{16 G_0} \frac{1-2\nu}{1-\nu}$$

$$+\sum_{i=1}^{\infty}\{\alpha_i r I_0(k_i r)+\gamma_i I_1(k_i r)+\beta_i r K_0(k_i r)+\delta_i K_0(k_i r)\}\cos k_i z+\sum_{i=0}^{\infty}\sum_{j=1}^{\infty}A_{ij}\Phi_1(\lambda_j r)\cos k_i z$$

$$+\sum_{s=1}^{N_1}\{\mathrm{Re}[N_s^* u_1(r)]\cos k_s(l-z)-\mathrm{Im}[N_s^* u_1(r)]\sin k_s(l-z)\}$$

$$+\sum_{s=1}^{N_2}\{\mathrm{Re}[N_s u_1(r)]\cos k_s z-\mathrm{Im}[N_s u_1(r)]\sin k_s z\},$$

where $\Phi_0(\lambda_j r)$ and $\Phi_1(\lambda_j r)$ denote the functions

$$\Phi_i(\lambda_j r)=J_1(\lambda_j)Y_i(\lambda_j r)-Y_1(\lambda_j)J_1(\lambda_j r)\qquad (i=0,1), \tag{5.2}$$

where λ_j are the roots of the equation $\Phi_1(\lambda r_0)=0$.

The functions $w_1(r)$ and $u_1(r)$ appearing in the homogeneous solutions are expressed in terms of the modified zero- and first-order Bessel functions of the first (I_0, I_1) and second (K_0, K_1) kinds:

$$w_1(r)=r\left[\mu_2 I_1(k_s r)-\mu_4 K_1(k_s r)\right]+\left(4\frac{1-\nu}{k_s}\mu_2-\mu_1\right)I_0(k_s r)+\left(4\frac{1-\nu}{k_s}\mu_4+\mu_3\right)K_0(k_s r),$$

$$u_1(r)=\mu_1 I_1(k_s r)+\mu_3 K_1(k_s r)-r\left[\mu_2 I_0(k_s r)+\mu_4 K_0(k_s r)\right]. \tag{5.3}$$

Having the expressions for displacements (5.1), we can derive the expressions for the strains from the kinematic equations and the expressions for the stresses from relations (1.60).

The arbitrary constants appearing in (5.1) can be determined from boundary conditions: the constants A_0, B_0, D_0, α_i, β_i, γ_i, δ_i are found from the boundary conditions on the cylindrical surfaces by expanding them into Fourier series in z and considering that the axial stress resultant is equal to the force; the complex constants N_s^* and N_s are determined from the end conditions, i.e., the condition that the stresses σ_{zz} and σ_{zr} are equal to the values specified on the boundary at a finite number of points N_1 at the right end and N_2 at the left end of the cylinder or the condition that the standard deviation of the stresses σ_{zz} and σ_{zr} from the boundary conditions specified at these points is minimum.

The solution of the thermoviscoplastic problem for a solid cylinder can be found from (5.1) by replacing the functions $\Phi_0(\lambda_j r)$ and $\Phi_1(\lambda_j r)$ with $J_0(\lambda_j r)$ and $J_1(\lambda_j r)$, respectively, for $A_0=\beta_i=\delta_i=0$. Functions (5.3) appearing in the homogeneous solutions become simpler:

$$w_1(r)=\gamma_s I_0(k_s r)+g_s\left(r+4\frac{1-\nu}{k_s}\right)I_1(k_s r),$$

$$u_1(r)=g_s r I_0(k_s r)+\gamma_s I_1(k_s r), \tag{5.4}$$

where g_s and γ_s are complex constants related to the modified Bessel functions $I_0(Rk_s)$ and $I_1(Rk_s)$.

Thus, the thermoviscoplastic problem for hollow and solid cylinders is solved at each step of loading by calculating the additional surface and body loads, expanding them into series, and calculating the constants of integration in (5.1). The resulting solutions exactly satisfy the boundary conditions on the cylindrical surfaces and approximately (with the error specified above) satisfy the end conditions. They were used to analyze the stress–strain state of solid cylinders undergoing either simple deformation [6, 10–14, 79, 91, 106] or deformation along paths of small curvature [6, 91, 106] under various types of loading and heating.

5.2. Numerical Solution of Thermoviscoplastic Problems for Compound Solids of Revolution with Arbitrary Meridional Cross-Section. Let us address the studies [7, 18, 25–27, 35, 42–47, 54, 64, 67–71, 88, 94, 95, 114, 127, 144, 146] where the finite-element method was used to solve axisymmetric problems of thermoviscoplasticity for layered (compound) solids of revolution with arbitrary meridional cross-section. In these papers, it was assumed that the interface conditions between the components of a compound body made of dissimilar materials are perfect thermomechanical contact and no slipping and

separation. To find the solution in a cylindrical coordinate system z, r, φ, we use the constitutive equations (2.75) and the Lagrange equation (3.11) in which it is necessary to equate to zero the components K_φ and $t_{n\varphi}$ of the body and surface loads and u_φ, $\varepsilon_{z\varphi}$, $\varepsilon_{r\varphi}$ if the thermoviscoplastic problem is axisymmetric. Supplementing this variational equation with the kinematic equations and kinematic boundary conditions, we obtain a closed-form system of equations that allows describing, step by step, the deformation of the body and to determine the displacements, strains, and stresses at an arbitrary point of the body.

To find the stationary values of functional (3.11), the domain F of the meridional cross-section of the body is partitioned into M triangular finite elements with N nodes. Then the boundary of this section appears divided into N_1 segments that are sides of triangles. The partition is made so that each element corresponds to only one material. The nodal displacements are used as the basic unknowns.

It is assumed that the displacements within a finite element with nodes i, j, k can be accurately approximated by linear functions:

$$u_\alpha = a_1^\alpha + a_2^\alpha z + a_3^\alpha r \qquad (\alpha = z, r), \tag{5.5}$$

where $a_1^\alpha, a_2^\alpha, a_3^\alpha$ are constant coefficients. They are expressed in terms of the nodal displacements $u_{\alpha i}, u_{\alpha j}, u_{\alpha k}$ as follows:

$$a_p^\alpha = \frac{a_{pc}^{(m)} u_{\alpha c}}{2F_m^*} \qquad (c = i, j, k); \quad \langle p = 1, 2, 3; \quad \alpha = z, r; \quad m = 1, 2, \ldots, M\rangle, \tag{5.6}$$

where $a_{pc}^{(m)}$ and F_m^* are constants expressed in terms of the coordinates of the nodes as

$$a_{1i}^{(m)} = z_j r_k - z_k r_j, \qquad a_{2i}^{(m)} = r_j - r_k, \qquad a_{3i}^{(m)} = z_k - r_j \qquad (i, j, k),$$

$$2F_m^* = z_i (r_j - r_k) + z_j (r_k - r_i) + z_k (r_i - r_j). \tag{5.7}$$

Replacing the integration over the area F and boundary L by the sum of the integrals over the area F_m of finite elements and the sides L_i lying on the boundary L_t, substituting displacements (4.15) and the strains obtained from the kinematic equations into (3.11), and assuming that the components of the surface load vary linearly between nodes, we represent the functional $\Im$ as a function of discrete displacements at nodes of finite elements. To find them, we derive the following system of $2N$ linear algebraic equations from the extremality condition for this expression:

$$\sum_{m=1}^{M} (B_{zp}^{zi(m)} u_{zp} + B_{rp}^{zi(m)} u_{rp}) = D_{zi},$$

$$\sum_{m=1}^{M} (B_{zp}^{ri(m)} u_{zp} + B_{rp}^{ri(m)} u_{rp}) = D_{ri} \qquad (p = i, j, k), \quad \langle i = 1, 2, \ldots, N\rangle, \tag{5.8}$$

where the following notation is used for the mth triangular element with nodes i, j, k:

$$B_{zj}^{zi(m)} = \frac{1}{4F_m^2} \int_{F_m} ((2G' + \lambda') a_{2i} a_{2j} + G' a_{3i} a_{3j}) r dz dr,$$

$$\ldots\ldots\ldots\ldots\ldots\ldots\ldots\ldots\ldots\ldots\ldots\ldots\ldots\ldots\ldots\ldots \tag{5.9}$$

$$B_{rj}^{ri(m)} = \frac{1}{4F_m^2} \int_{F_m} \left[((2G' + \lambda') a_{3i} a_{3j} + \Delta_{1i} \Delta_{ij}) + G' a_{2i} a_{2j} + \lambda' (a_{31} \Delta_{1j} + a_{1i} a_{3j}) \right] r dz dr,$$

$$D_{zi} = \sum_{m=1}^{M} \frac{1}{2F_m^*} \int_{F_m} [\sigma_{zz}^* a_{2i} + \sigma_{zr}^* a_{3i} + K_z z \Delta_{1i}] r dz dr + \sum_{l=1}^{N_1} \frac{l_{ij}}{12} \operatorname{sign} F_m^* [t_{nz_i} (3r_i + r_j) + t_{nz_j} (r_i + r_j)], \tag{5.10}$$

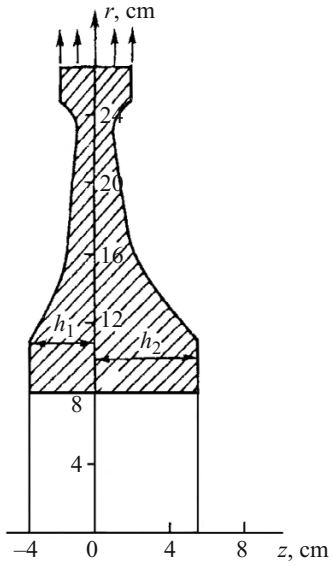

Fig. 4

.....

$$F_m = |F_m^*|, \qquad \Delta_{1j} = a_{3j} + a_{2j}\frac{z}{r} + a_{1j}\frac{1}{r}, \qquad l_{ij} = \sqrt{(z_i - z_j)^2 + (r_i - r_j)^2}. \tag{5.11}$$

The missing coefficients can be obtained from (5.10) by replacing the index j with i or k. Finding the nodal displacements and, hence, the displacement distribution (5.5) in each finite element by solving system (5.8), we can determine the strains from the kinematic equations and the stresses from formulas (2.75) for each finite element.

Following this approach, we can use the method of successive approximations to calculate the displacements, strains, and stresses in a solid of revolution subject to external forces and nonuniform heating. The process of successive approximations in elements of the body at a step of loading is arranged in the same way as in Sec. 2 for various deformation paths. The constitutive equations of thermoviscoplasticity are linearized by either the method of elastic solutions, or the method of variable elastic parameters, or the method of additional stresses.

This approach was used to solve specific problems of thermoviscoplasticity for various components of engineering structures. For example, the stress–strain state of the following components was analyzed: short hollow and solid cylinders under a ring load or nonuniform heating [45, 94, 114], the rotor of the fifth low-pressure stage of a K-300-240 turbine [45, 90], the solid rotor of a gas turbine during start-up [42, 94], and a piston of an internal combustion engine [64]. The interference-fit stresses for a thick disk on a shaft were determined in [46] and their relaxation during operation was analyzed in [26, 44]. The stresses in the seat of the injection valve in a rocket engine as a two-layer solid of revolution subject to nonuniform heating due to convective heat exchange with the ambient medium were determined in [69]. The stress state of the gate of the injection valve in a rocket engine under stepwise-varying loading and heating conditions was analyzed in [32, 67, 144, 146]. The thermostressed state of the disk of the gas turbine of a transport aircraft and the disk of the turbine of a fighter's jet engine was analyzed in [66, 91] considering the variability of the thermomechanical load during the entire period from takeoff to landing.

An analysis of the results of the stress–strain analysis of the valve gate and turbine disks reveals that the loading history has a considerable effect on the magnitude and behavior of the stresses near the heating surfaces (the results obtained with and without regard to the loading history differ not only in magnitude, but also in sign). For example, allowing for the loading history leads to an almost 50% decrease in the hoop stresses in the disk rim at the 300th second of heating and allowing for the unloading occurring on the outside surface of the injection valve gate leads to the occurrence of tensile stresses equal to or even higher than the compressive stresses obtained regardless of the loading history.

In solving specific problems, the applicability of the constitutive equations to the description of nonisothermal loading was analyzed by plotting and analyzing the deformation paths in the Il'yushin's five-dimensional space [21]. The developed

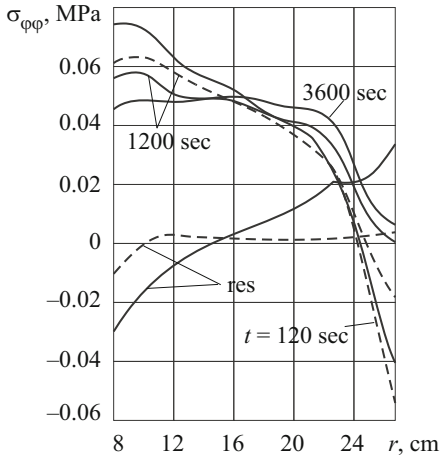

Fig. 5

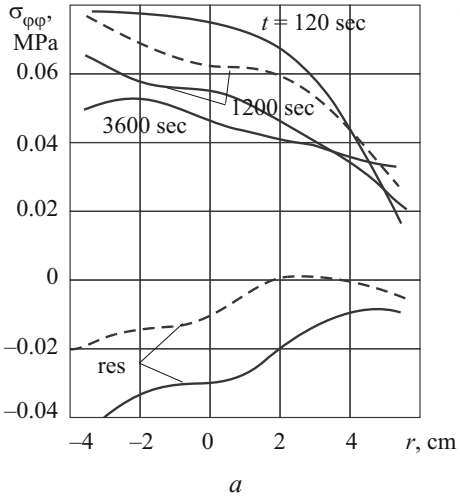

a

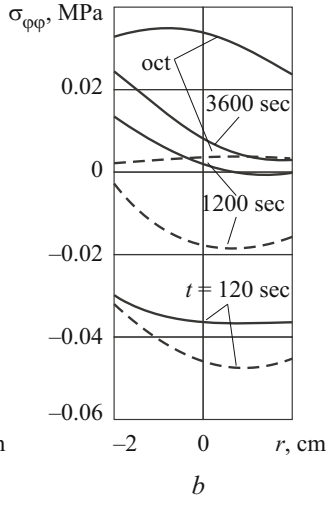

b

Fig. 6

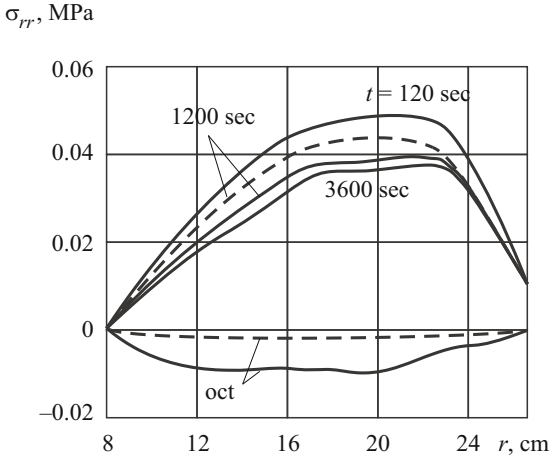

Fig. 7

methods and algorithms for solving axisymmetric problems of thermoplasticity were implemented in applied software packages [18, 35, 54, 74, 94], which differ in the constitutive equations used and the level of automation of computations.

Let us discuss, as an example, results on the axisymmetric thermoviscoplastic state of the disk of the gas-turbine of a transport aircraft [67, 95]. Half of its meridional cross-section is shown in Fig. 4. The results were obtained using the theory of thermoviscoplasticity describing deformation along paths of small curvature with and without regard to creep strains.

The disk, which is initially in natural stress-free state at temperature $T_0 = 20$ °C, is subjected to the body and surface forces caused by its rotation and nonuniform heating by gas flow. The gas temperature is 750 °C on the side of the blades and 350 °C and 550 °C on the lateral surface of the disk at $z = -h_1(r)$ and $z = h_2(r)$, respectively. The heat-transfer factor is 0.02 W/(cm^2·K) on the lateral surfaces and 0.1 W/(cm^2·K) on the rim of the disk. The speed of the disk varied linearly until the 60th second and then remained constant and equal to 1150 sec^{-1}. The action of the repelled blades on the disk rim was modeled by a distributed load varying uniformly with time and reaching a maximum of 120 MPa at the 60th second. The disk of the turbine is made of EI437 steel whose mechanical characteristics can be found in [96]. The meridional cross-section of the disk was covered by a nonuniform finite-element mesh refined near the disk rim and in areas of sharp change in geometry. The temperature distribution at different times was determined by solving the nonstationary heat-conduction problem [35, 54, 91, 95].

An analysis of the temperature fields in the disk shows that the temperature varies nonlinearly throughout the thickness at the early stages of heating, gradually equalizing with time. The temperature distribution becomes stationary at the 1200th

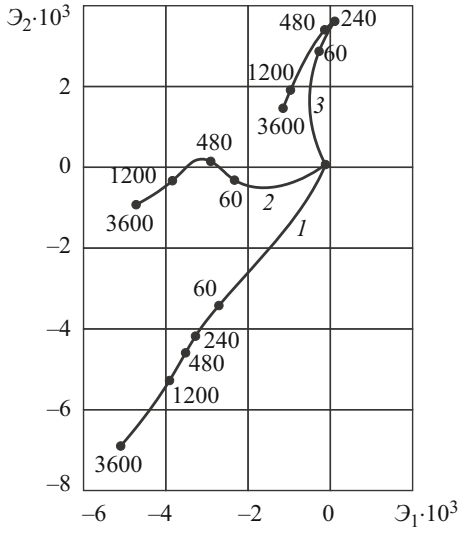

Fig. 8

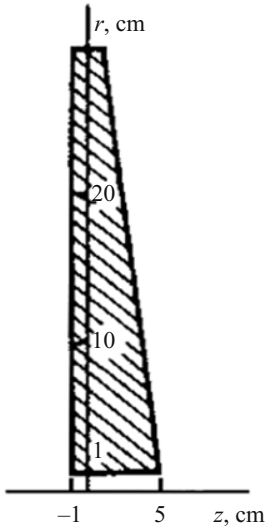

Fig. 9

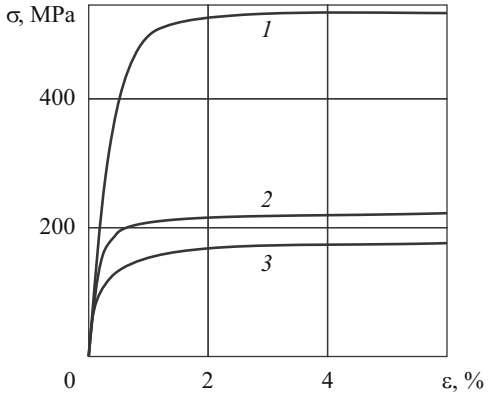

Fig. 10

second, the maximum temperature drop being 285 °C across the radius and 450 °C across the thickness. To calculate the stresses, the process is divided into steps of different duration.

The distribution of stresses over the meridional cross-section of the disk is shown in Figs. 5–7 in the form of diagrams of circumferential $\sigma_{\varphi\varphi}$ (Figs. 5 and 6) and radial σ_{rr} (Fig. 7) stresses in the disk calculated with (solid lines) and without (dashed lines) regard to the creep strains at different times. The dashed lines for $t = 1200$ sec and 3600 sec coincide. The figures also show diagrams of residual stresses in the disk after stopping and slow cooling.

Figures 5 and 7 shows the variation in the stresses $\sigma_{\varphi\varphi}$ and σ_{rr} in the disk at $z = 0$, and Fig. 6 shows the variation in the hoop stresses $\sigma_{\varphi\varphi}$ throughout the thickness of the disk near the inside cylindrical surface ($r = 8.5$ cm) and the disk rim ($r = 26.5$ cm).

The calculations suggest that the creep strains increase the hoop stresses near the disk rim by a factor of 3.5 during the stationary stage of loading. The creep strains also increase the diameter of the disk by 0.54 mm.

Figure 8 shows the projections of the deformation path onto the plane $Э_1 0 Э_2$ of Il'yushin's five-dimensional space [21, 93] for the following three points of the meridional cross-section of the disk: the point with coordinates $z = 0$, $r = 8$ cm on the inside surface of the disk (curve *1*), the point $z = 17.06$ cm in the middle of the disk, and the point $z = 26.75$ cm on the rim of the disk. Since $Э_3$ is small, the projections onto the other planes are not shown.

An analysis of the plotted paths reveals that the deformation process on the inside surface of the disk (curve *1*) is close to simple. Near the disk rim (curve *3*), the deformation path is of small curvature until the 240th second, after which unloading occurs. During the period of loading from $t = 240$ sec to 600 sec, the radius of curvature of the deformation path in the middle of

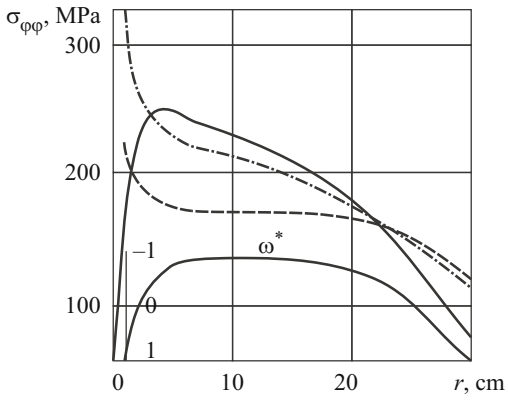

Fig. 11

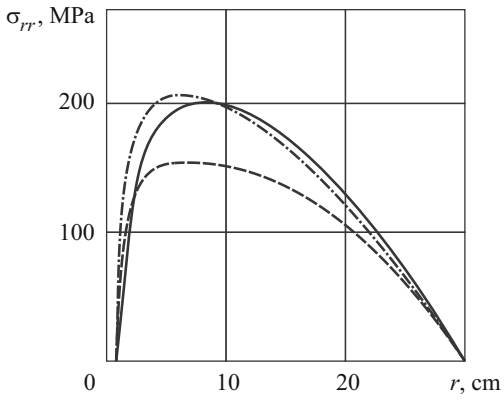

Fig. 12

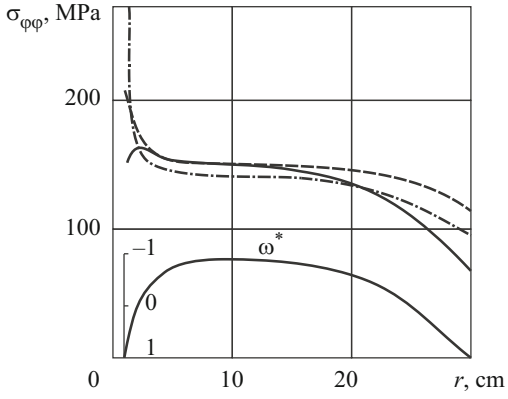

Fig. 13

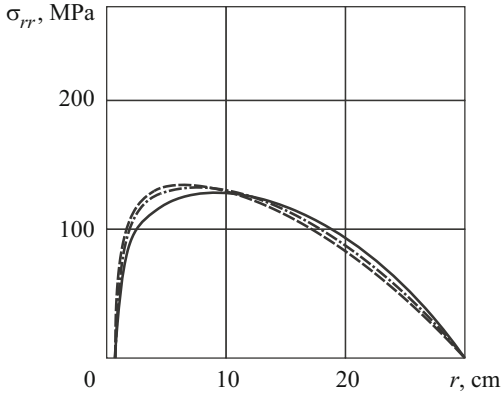

Fig. 14

the disk (curve *2*) is much smaller than the lag path of the vector properties of the material. This suggests that the results corresponding to this period of loading are approximate and it is necessary to take into account the lag of the vector properties of the material of which the disk is made. For the other periods of time, the theory of thermoviscoplasticity describes the loading process with adequate accuracy.

To assess the effect of the stress mode on the solution of the plastic problem, the stress–strain state of a conical disk (its half meridional cross-section is shown in Fig. 9) under centrifugal forces was analyzed. The disk is made of metal with mechanical characteristics similar to those of SCh 12-28 case iron with density $\gamma / g = 0.785$ Pa·sec^2/cm^2. Its elastic characteristics for different stress mode angles are the following [1, 41]: tension: $E = 9.326 \cdot 10^4$ MPa, $\nu = 0.25$; torsion: $E = 10.878 \cdot 10^4$ MPa, $\nu = 0.25$; compression: $E = 10.878 \cdot 10^4$ MPa, $\nu = 0.25$. Compression, torsion, and tension $\sigma - \varepsilon$ curves for cylindrical specimens made of this material are presented in Fig. 10 (curves *1*, *2*, *3*, respectively).

The disk, which is in a stress-free state at a temperature of 20 °C, is subjected to body forces caused by its rotation with a speed of 836.76 sec^{-1}. While the disk spins up to reach the required speed, it undergoes active deformation along straight paths. This assumption allows solving the plastic problem in one stage.

The stresses are so distributed in the disk that the stress mode angle changes considerably along radius.

Some results of calculations performed using various tension, torsion, and compression diagrams for cylindrical specimens are presented in Figs. 11–16.

In these figures, the solid curves correspond to the case of accounting for the stress mode, the dashed curves to the case of using only tension stress–strain curves, and the dash-and-dot curves to the case of using only compression stress–strain curves. How the circumferential and radial stresses near the surface $z = -1$ cm and in the middle of the disk vary along its radius is shown in Figs. 11, 12 and Figs. 13, 14, respectively. The radial variation of $\omega^* = 3\sqrt{3}\, I_3 / 2S^3$ is shown in Figs. 11 and 13. The variation of the stresses throughout the thickness of a disk with $r = 2.5$ cm is shown in Fig. 15.

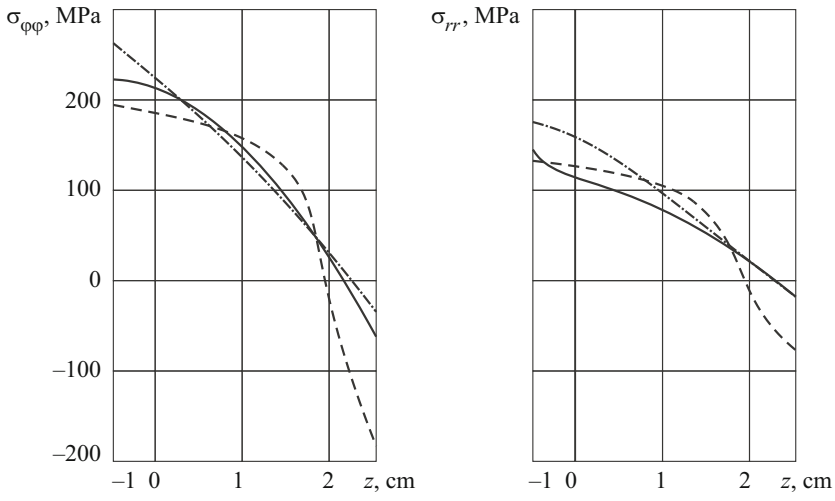

a *b*

Fig. 15

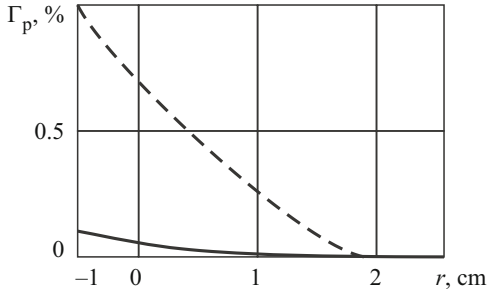

Fig. 16

It can be seen that using stress–strain curves for different stress modes leads to substantially different results. For example, the stresses $\sigma_{\varphi\varphi}$ can differ by almost 50% (Fig. 11), whereas the plastic strains by an order of magnitude (Fig. 16). Figure 16 shows the variation of the plastic-strain intensity throughout the thickness for $r = 2.5$ cm calculated taking into account the stress mode and using tension stress–strain curves.

Also, the rate of convergence of successive approximations was estimated in solving a boundary-value problem by the proposed and conventional approaches. For example, in analyzing the stress state of the disk using only tension stress–strain curves, the process converged after the 41st approximation in the former case and after the 79th approximation in the latter case.

Thus, allowing for the third invariant of the deviatoric stress tensor in analyzing the stress–strain state of compound solids of revolution improves substantially the solution of the corresponding boundary-value problem of plasticity.

To test the approach proposed in Sec. 2 to describe the damages of a material, the stress–strain state and strength of the turbine disk of a fighter's jet engine were analyzed considering the system of forces [66] that act on the disk during the period from takeoff to landing (see Fig. 17 for a design model).

The disk, which is initially at a temperature of 20 °C, is subjected to the body forces caused by the rotation of the disk and to surface forces uniformly distributed over the disk rim and generated by the repelled blades. The surface forces depend on the speed as follows: $t_{nr} = 174\,(n / n_{\max})^2$ MPa, where n and $n_{\max}$ are, respectively, the current speed and the maximum speed (13,300 rpm).

How the speed varies during one cycle from takeoff to landing is shown in Fig. 18. The temperature field for the same time interval and for several values of the radius was measured with thermocouples. The temperature for the other values of the radius was found by linear interpolation. It was assumed that the temperature is constant throughout the thickness of the disk.

The boundary conditions specified on the surface AB (Fig. 17) prohibited displacements of the disk along the axis of rotation (the axial displacements u_z and the shear stresses t_{zr} were set at zero).

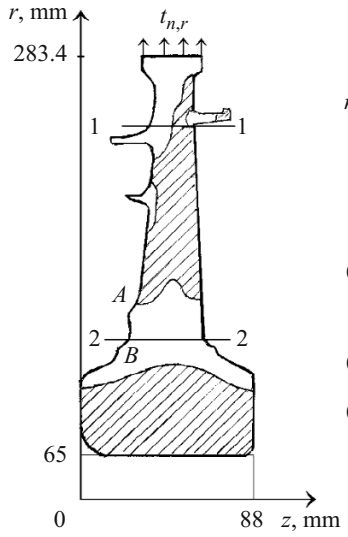

Fig. 17

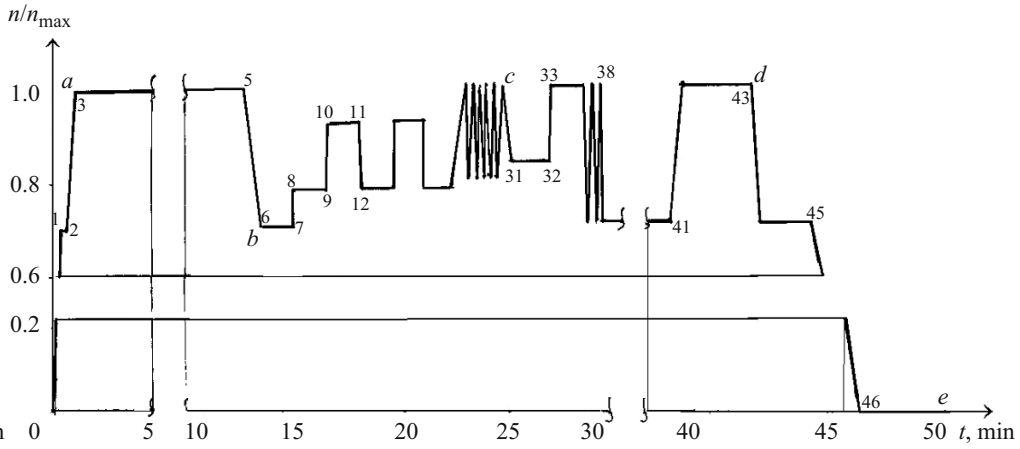

Fig. 18

TABLE 1

Stage number	1st cycle				2nd cycle				3rd cycle			
	$\varepsilon_{\varphi\varphi}$	Γ	$\sigma_{\varphi\varphi}$	S	$\varepsilon_{\varphi\varphi}$	Γ	$\sigma_{\varphi\varphi}$	S	$\varepsilon_{\varphi\varphi}$	Γ	$\sigma_{\varphi\varphi}$	S
41	0.5364	0.1410	331	207	0.5946	0.2034	121	79	0.5990	0.2076	117	77
42	0.8491	0.3876	683	423	0.8755	0.4145	623	388	0.8795	0.4184	618	385
43	0.9752	0.4600	736	452	0.9784	0.4682	737	455	0.9800	0.4698	736	456
44	0.6831	0.2840	318	196	0.7469	0.2882	314	194	0.7469	0.2890	313	193

The period from takeoff to landing is divided into 48 stages, according to the disk speed change program. At the last stage, the speed dropped to zero, the temperature of the disk being quite high. The residual stresses and displacements were determined after cooling of the engine at $n = 0$ and $T = 20$ °C. The stages are numbered in Fig. 18.

The calculations show that plastic strains in the disk occur at the instant denoted by "*a*" in Fig. 18 in section *1–1* (Fig. 17) near the right lateral surface of the disk. The plastic zone grows into the disk with time. In Fig. 17, the portion of the disk's cross-section that undergoes plastic deformation throughout the entire cycle, i.e., to the 48th stage, is hatched. The shape of the plastic area suggests that the rotation and surface load cause bending of the disk. The temperature of the disk and the time of operation of the engine during one cycle are such that creep strains hardly develop. As indicated in [53], the creep strains should be taken into account when they exceed the instantaneous strains by more than 10%.

Some of the calculated results are presented in Figs. 19 and 20. Figure 19 shows the radial and hoop stresses in sections *1–1* (*a*) and *2–2* (*b*) at the instants denoted by *b*, *d*, *e* in Fig. 18. The dashed lines represent the residual stresses after full cooling of the disk in the first cycle.

The distribution of the residual radial (*u*) and axial (*w*) displacements on the surface of the disk rim (*a*) and on the surface of the central hole (*b*) is shown in Fig. 20. In these figures, h_1, h_2, h_3, h_4 denote the thickness of the disk in sections *1–1* and *2–2*, on the disk rim, and hole, respectively.

To estimate the change in the stress–strain state with increase in the number of cycles, the behavior of the disk loaded in a simpler way was analyzed. The loading program was simplified by excluding the intervals at whose ends the speeds are equal and the temperature differ by less than 5–7 °C at stages 18–30 and 34–39. Such intervals were replaced by one point with average

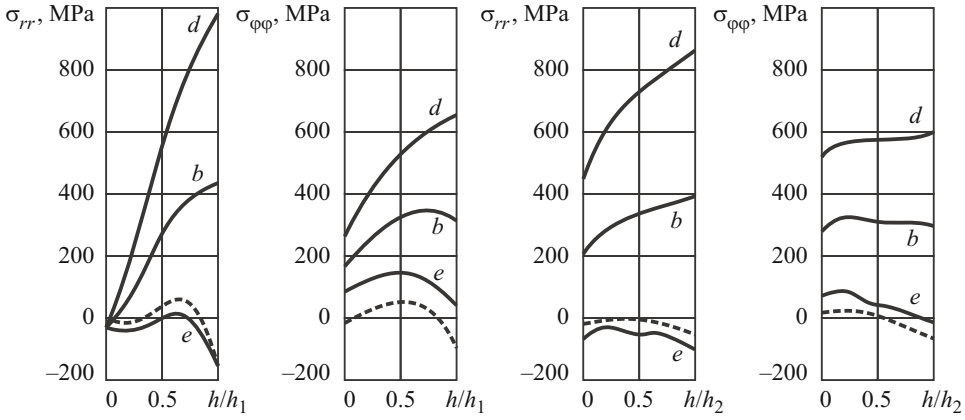

Fig. 19

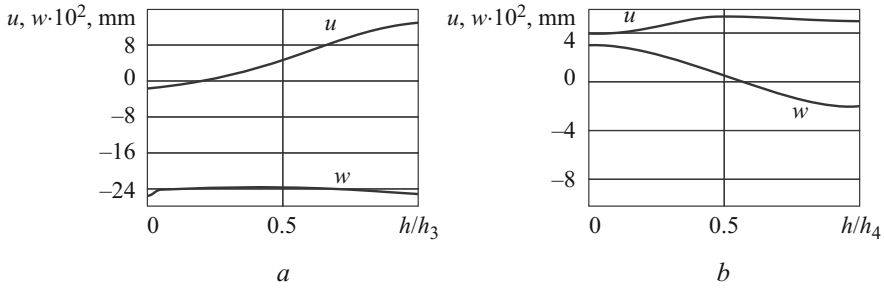

Fig. 20

temperature. The calculated strain $\varepsilon_{\varphi\varphi}$ and shear-strain intensity Γ (both in %) and the stress $\sigma_{\varphi\varphi}$ and shear-stress intensity S (both in MPa) in the middle of the meridional cross-section of the disk on the inner hole for three cycles are summarized in Table 1.

It can be seen that the cyclic nature of loading is manifested only in the second and third cycles. In the fourth cycle, the accumulated plastic strains have no effect.

The calculated results suggest that the stress–strain state near the rim and hub of the disk displays strongly pronounced spatial behavior. Therefore, using plate theory or shell theory to analyze the state of the disk would lead to significant errors. Failure to account for the changes in the disk speed during flight would results in an even larger error. However, if the disk is subject to repeated loading, i.e., if the engine operates following the same program, the stress–strain state will stabilize after the third cycle. The strength of the disk subject to such a loading program was assessed as the ratio of the maximum to allowed value of the shear-stress intensity that does not exceed 0.6–0.7. This is indicative of an adequate safety factor for the disk.

6. Nonaxisymmetric Problems of Nonstationary Heat Conduction and Thermoviscoplasticity for Compound Structural Members Made of Isotropic and Anisotropic Materials. Let us address studies where three-dimensional thermoviscoplastic problems were solved using the semianalytic finite-element method. This approach to the solution of a nonaxisymmetric thermoviscoplastic problem for isotropic solids of revolution with a complex meridional cross-section was used in [15–17, 61, 64, 91, 95, 108, 126, 137, etc.]. These papers report results of analyzing the stress–strain state of short hollow cylinders under circumferentially varying ring loads or nonuniform heating [16, 95, 108], the nonaxisymmetrically heated gate of the injection valve of a rocket engine [16], a rocket engine's injection valve seat as a two-layer [15, 16] or a three-layer solid of revolution [137] subject to nonaxisymmetric heating, a circumferentially compound solid of revolution [126], etc.

We will discuss, as an example, the results of a stress–strain analysis of the seat of the injection valve of a rocket engine modeled by a three-layer isotropic solid of revolution convectively heated from an initial temperature of 20 °C by the ambient medium of temperature $\theta = 3000(1 + 0.1\cos\varphi)$ °C. Half the meridional cross-section is shown in Fig. 21. The mechanical and thermal characteristics of the layers can be found in [137]. The surface of the body is heat-insulated on the section *ADC*. The heat-transfer factor between the ambient medium and the body varies linearly from 0 at the point *A* to 0.35 W/cm^2 at the point *B*

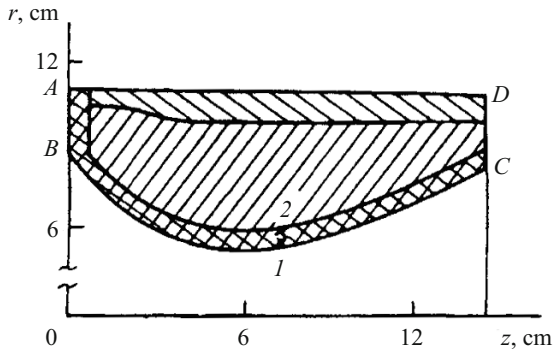

Fig. 21

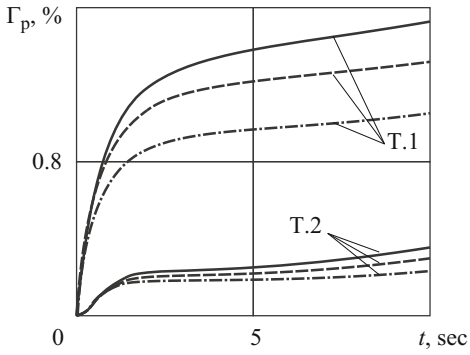

Fig. 22

on the section *AB* and is constant and equal to 0.35 W/cm^2 on the section *BC*. The temperature field of the heated body was determined by solving a nonstationary heat-conduction problem by the method proposed in [67, 91, 93]. The meridional cross-section of the body was partitioned into 1508 triangular finite elements. Five terms were kept in the trigonometric series (4.13), i.e., in each approximation of an arbitrary step of loading, the problem was reduced to five linear systems of algebraic equations of the 2391st order solved by Gaussian elimination. The thermoviscoplastic equations describing deformation along paths of small curvature were used as constitutive equations. They were linearized using both the proposed and conventional methods of successive approximations.

The stress–strain state of the body was analyzed using 30 stages of loading and the following steps of heating: 0.05 sec at the first to fourth stages, 0.1 sec at the fifth to seventh stages, 0.25 sec at the eighth to 16th stages, 0.5 sec at the 18th to 30th stages. The very small step at the beginning of the process was chosen because high temperature gradients occur in the body near the inside surface due to the contact with the ambient medium of very high temperature. An analysis of the calculated results (Fig. 22) shows that high plastic strains occur in the coating on the inside surface of the body: the intensity of accumulated plastic shear strains near point *1* of the meridional cross-section reaches 1.5% at the end of the process and increases in a similar way to temperature. The intensity of accumulated plastic strains near point 2 is lower (0.4%). Their variation during heating at points *1* and *2* is shown in Fig. 22. Figure 23 shows the variation in the shear-stress intensity at the 10th second of heating in the cross-section coming through points *1* and *2* and being perpendicular to the axis of revolution. The solid curves correspond to $\varphi = 0$, the dashed curves to $\varphi = \pi / 2$, and the dash-and-dot curves to $\varphi = \pi$. The absence of dashed or dash-and-dot lines in Fig. 23 means that they coincide with the solid curves.

Figure 24 shows the total number Σn of successive approximations needed to solve the problem by the two methods with a prescribed error of 1%, depending on the stage *l*. The solid curve corresponds to the modified method, and the dash-and-dot curve to the conventional method. Thus, changing the method of calculating the increments of the plastic-strain intensity, we can reduce the total number of approximations over 30 stages of loading from 235 to 170, i.e., by more than 25%.

Comparing the results obtained using the two methods of linearizing the constitutive equations, we conclude that modified method of additional stresses can effectively be used to solve nonaxisymmetric three-dimensional problems of thermoplasticity that require much computer resourses.

The use of composites in multilayer elements of firings of reentry vehicles, rocket nozzles, parabolic antennas of communication satellites, etc. necessitated development of effective algorithms and numerical methods for analyzing the thermostressed state of multilayer (compound) isotropic and anisotropic solids of revolution subject to nonaxisymmetric mechanical loading and heating. To this end, as with isotropic materials, nonaxisymmetric problems were solved using the semianalytic finite-element method [36, 61, 91, 95, 131, etc.].

To validate the proposed method of stress–strain analysis of solids of revolution made of orthotropic materials, test problems that have analytic solutions were solved [141].

The plane stress state of a rotating solid thin rectilinearly orthotropic disk is known [32, 129] to be axisymmetric and is described in cylindrical coordinates by the formulas

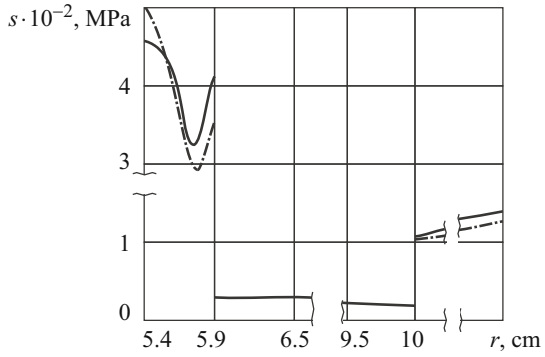

Fig. 23

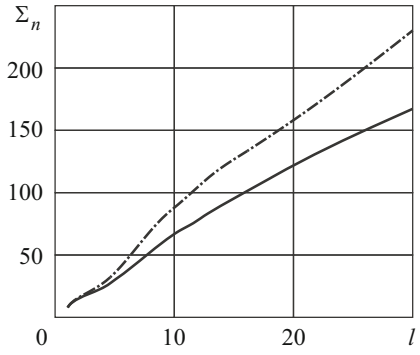

Fig. 24

$$\sigma_{rr} = \frac{\omega^2 \rho R^2}{2}(1-\beta)\left(1-\frac{r^2}{R^2}\right), \qquad \sigma_{\varphi\varphi} = \sigma_{rr} + \omega^2 \rho \beta r^2,$$

where ω is the angular velocity of the disk; R is its outer radius.

The anisotropy of the material of the disk is characterized by the dimensionless parameter

$$\beta = \left(\frac{1}{E_x} + \frac{1}{E_y} - \frac{2\nu_{xy}}{E_x}\right) \Big/ \left(\frac{3}{E_x} + \frac{3}{E_y} - \frac{2\nu_{xy}}{E_x} + \frac{1}{G_{xy}}\right).$$

The stress state of a thin rectilinearly orthotropic circular plate subject to nonuniform axisymmetric heating was also analyzed. The plane stress state of the plate with temperature varying quadratically and $E_x = E_y, \alpha^T_{xx} = \alpha^T_{yy}$ is axisymmetric and described by the following formulas in cylindrical coordinates [120]:

$$\sigma_{rr} = \beta \frac{E_x \alpha^T_{xx} T_1}{(1-\nu_{xy})}\left(1-\frac{r^2}{R^2}\right), \qquad \sigma_{\varphi\varphi} = \beta \frac{E_x \alpha^T_{xx} T_1}{1-\nu_{xy}}\left(1-\frac{3r^2}{R^2}\right),$$

$$\left[\beta = (1-\nu_{xy}) \Big/ \left(3-\nu_{xy} + \frac{E_x}{2G_{xy}}\right)\right].$$

The calculated stresses are in good agreement with the exact solution, which allows the developed approach to be applied to the analysis of the thermostressed state of specific structural members in the form of orthotropic solids of revolution.

The thermostressed state of solids of revolution was determined in [93, 125, 131, 132, 136, 137, 139, 149, 150, 151, etc.], where curvilinearly orthotropic materials of two types were considered: (i) anisotropic materials with one of the principal axes of anisotropy coinciding with the axis φ of the cylindrical coordinate system and the other two axes located in the plane $z0r$ and rotated through some angle around the coordinate axis φ and (ii) cylindrically orthotropic materials with principal axes of anisotropy coinciding with the axes of the cylindrical coordinate system and rectilinearly orthotropic materials with one of the principal axes of anisotropy coinciding with the axis of revolution of the body.

The stress–strain state at the interface between isotropic and curvilinearly orthotropic materials of a compound cylindrical structural member subject to internal pressure and axial acceleration was analyzed in [93, 150]. An analysis was also made of the thermostressed state of a nonaxisymmetrically heated two-layer solid cylinder with the inside layer made of an isotropic material and the outside layer made of a cylindrically orthotropic material [131], the thermoelastoplastic state of a nonaxisymmetrically heated three-layer structural member of compound meridional cross-section with the outside layer made of a cylindrically orthotropic material and the other two layers made of isotropic materials [138], the nonaxisymmetric thermostressed state of the axisymmetricaly or nonaxisymmetrically heated seat of a rocket engine's injection valve as a three-layer solid of revolution with the inside layer made of an isotropic material, the middle layer made of a rectilinearly orthotropic carbon–carbon composite, and the outside layer made of a cylindrically orthotropic material [125, 139], etc.

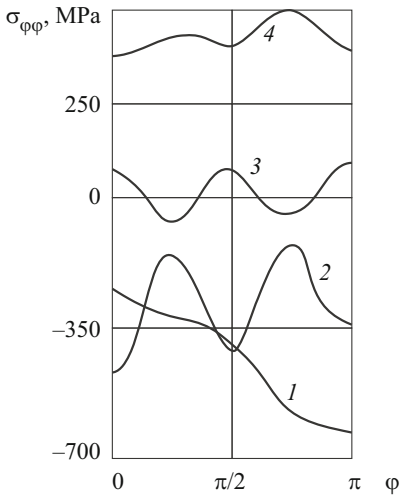

Fig. 25

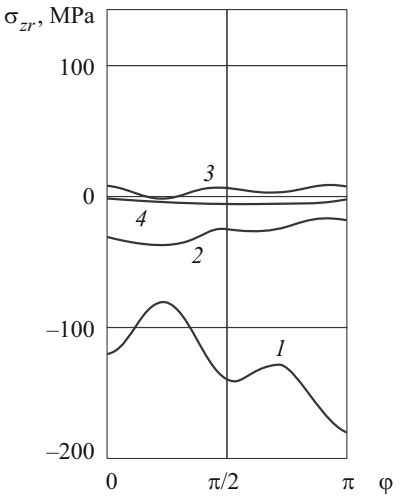

Fig. 26

In [125], it was shown that the distribution of temperature, stresses, and strains in an axisymmetrically heated rectilinearly orthotropic material is substantially nonaxisymmetric because of the circumferential variability of its mechanical characteristics. The shear stresses σ_{zr} and $\sigma_{r\varphi}$ reach 10% of the maximum normal stresses σ_{zz} and $\sigma_{\varphi\varphi}$ at the 2nd second of heating not only in the carbon–carbon composite, but also in the adjacent isotropic material.

While the above-cited studies address the stress–strain state of compound solids of revolution made of inelastic isotropic materials and elastic anisotropic, the paper [149] deals with the axisymmetric stress–strain state of a solid of revolution consisting two of joined (by a thin-walled tube) isotropic and cylindrically orthotropic cylinders with nonlinear shear characteristic subject to axial mechanical load and three modes of uniform heating.

Let us discuss, as an example, the results [139] of analyzing the thermostressed state of the seat of a rocket engine's injection valve as a three-layer solid of revolution (Fig. 21) in which the inside layer remains isotropic and the other materials are replaced by composites: graphite is replaced by a carbon–carbon composite made by weaving a spatial (in a Cartesian coordinate system) matrix of mutually orthogonal carbon fibers and filling the space between them with carbon, the outside cylindrical shell is replaced by a cylindrically orthotropic material. The loading and heating conditions remain the same as in the previous example. The carbon–carbon composite is assumed to be homogeneous and rectilinearly orthotropic with the principal axes aligned with the Cartesian coordinate axes. The mechanical and thermal characteristics of the layers can be found in [139]. The temperature field after 30 sec of heating was determined by solving the corresponding heat-conduction problem by the method from [132]. The process of loading was divided into 24 stages with a variable time step (a small step up to the 10th second and then, when the gradients in the inside layer decrease considerably, a step of 5 sec). At each stage, the deformation of the isotropic material was described using the constitutive equations of the theory of deformation along paths of small curvature linearized by the method of additional stresses. Elleven terms were kept in the trigonometric series (4.13). Calculations revealed that all the six stress components in the structural element are commensurable. With such heating conditions and material properties of the layers, however, the hoop stresses $\sigma_{\varphi\varphi}$ and the shear stresses $\sigma_{z\varphi}$, $\sigma_{r\varphi}$ caused by the rectilinear orthotropy of one of the materials are maximum. The results of analysis of the stress state of a solid of revolution at $z = 12.875$ cm (Fig. 21) after the 30th second of heating are presented in Figs. 25–28. Curves *1–4* shows the variation in the normal ($\sigma_{\varphi\varphi}$) and shear (σ_{zr}, $\sigma_{z\varphi}$, $\sigma_{r\varphi}$) stresses in the circumferential direction at four points: point *1* corresponds to radius $r = 7.875$ cm and is located in the middle of the inside layer, points *2* and *3* are located in the second material and correspond to radii $r = 8.27$ cm and $r = 9.35$, respectively, and point *4* is located in the outside layer and corresponds to $r = 10.25$ cm (Figs. 27 and 28).

An analysis of the calculated results shows that the variation of the mechanical characteristics of the carbon–carbon composite in the circumferential direction makes the stress state of the body strongly nonaxisymmetric. The nonaxisymmetry of heating has a weaker effect than the orthotropy of the carbon–carbon composite. The shear stresses $\sigma_{z\varphi}$ and $\sigma_{r\varphi}$ in the cross-section of interest are commensurable with σ_{rr} and σ_{zr}. An analysis of the stress–strain state of the structural member at

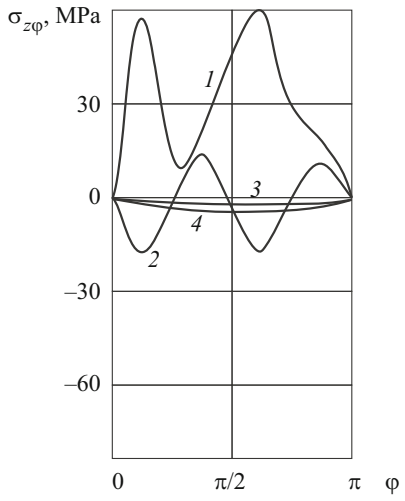

Fig. 27

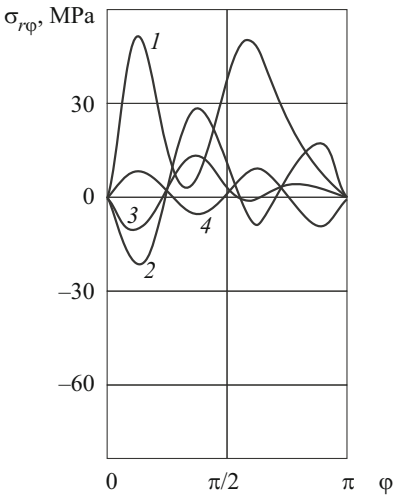

Fig. 28

the 30th second of heating at one stage shows that allowing for the loading history decreases the stresses in the inside isotropic layer by 30–40%. In the other two layers, the stresses insignificantly (by 10%) increase.

Conclusions. Our review of the studies cited above indicates that there are effective numerical methods for solving three-dimensional thermoviscoplastic problems for various isotropic and orthotropic structural members undergoing complex nonisothermal deformation along straight paths and paths of small curvature. The methods allow for the loading history and creep strains.

In solving specific problems, the constitutive equations used were validated by analyzing deformation paths in Il'yushin's five-dimensional space [21, 95].

The analysis of the effect of the loading history, creep strains, stress mode, and constitutive equations of thermoviscoplasticity on the stress–strain state showed that allowing for the loading history leads to a qualitatively different stress and strain distribution in the body, while allowing for the other factors leads to quantitative changes in the stresses and strains.

The analysis of the stress state of compound solids of revolution made of isotropic and orthotropic materials suggests that the rectilinear orthotropy of one of the materials has a strong effect on the stress state in all parts of the body. For example, when a layered solid of revolution with one of the layers is rectilinearly orthotropic is axisymmetrically heated, the shear stresses $\sigma_{z\varphi}$ and $\sigma_{r\varphi}$ are proportional to the other stresses.

The developed methods were applied to real structural members, thus providing a scientific prerequisite for the impovement of the configuration of the objects of interest, reduction of materials consumption, determinatin of the critical nonisothermal loading parameters, etc.

There are tasks that appear to be of importance and interest for future thermoviscoplasticity research:

– development of methods for solving thermoviscoplastic problems using constitutive equations that allow for the geometry of the deformation paths of elements of the body;

– development of methods for solving thermoviscoplastic problems for high strains and technological contact-interaction problems;

– study of dynamic processes in thermoviscoplastic problems;

– development of methods for solving thermoviscoplastic problems for layered anisotropic materials with damage in separate layers;

– development of methods for solving thermoviscoplastic problems for cyclic loading, thermomechanical coupling, etc.

REFERENCES

1. S. A. Ambartsumyan, *A Multimodulus Elasticity Theory* [in Russian], Nauka, Moscow (1982).
2. A. V. Amel'yanchik, V. T. Laptev, Z. L. Mel'nikova, and E. L. Strunina, "Computation of stress and displacement fields in welded joints of pipelines subject to elastoplastic deformation and creep on a Ural-2 mainframe computer," *Tepl. Napyazh. Elem. Konstr.*, **8**, 171–176 (1969).
3. A. V. Amel'yanchik, V. T. Laptev, and E. L. Strunina, "Strength analysis of solid-forged multidisk rotors of thermal turbines on a Ural-2 mainframe computer," *Dinam. Prochn. Mashin*, **5**, 80–85 (1967).
4. A. V. Amel'yanchik, V. T. Laptev, and E. L. Strunina, "Solution of two-dimensional axisymmetric problems of elasticity, elastoplasticity, and creep on a Ural-2 mainframe computer," *Tepl. Napryazh. Elem. Konstr.*, **7**, 18–23 (1967).
5. M. E. Babeshko, "Stress state of a short solid cylinder under nonisothermal loading," *Tepl. Napryazh. Elem. Konstr.*, **11**, 121–127 (1971).
6. M. E. Babeshko, *Thermoplastic Stress State of Short Cylinders with Loading History* [in Russian], Author's Abstract of PhD Thesis, Inst. Mekh. S. P. Timoshenko NANU, Kyiv (1975).
7. M. E. Babeshko, V. V. Piskun, V. G. Savchenko, and Yu. L. Shevchenko, "Analysis of the elastoplastic state of elements of engineering structures subject to complex nonisothermal loading," in: *General Problems for and Methods of Studying the Plasticity and Viscoelasticity of Materials and Structures* [in Russian], UNTs AN SSSR, Sverdlovsk (1986), pp. 3–9.
8. M. O. Babeshko and V. G. Savchenko, "Mathematical modeling of operating and limiting states of structural elements in the form of solids of revolution under repeated thermomechanical loading," in: *Trans. Dniprodzerzhinsk National Technical University* [in Ukrainian], Issue 1(26), DDTU, Dniprodzerzhinsk (2015), pp. 3–9.
9. M. E. Babeshko and V. G. Savchenko, "Modification of methods of successive approximations in boundary-value problems of thermoplasticity," *Vestn. Nats. Tekhn. Univ. KhPI*, **9**, 39–42 (2002).
10. M. E. Babeshko and V. K. Stryuk, "Analysis of the elastoplastic stress state of short solid cylinders subject to nonuniform heating," *Tepl. Napyazh. Elem. Konstr.*, **13**, 28–32 (1973).
11. M. E. Babeshko and V. K. Stryuk, "Revisiting the analysis of the elastoplastic stress state of a short solid cylinder subject to nonuniform heating," *Tepl. Napyazh. Elem. Konstr.*, **14**, 28–33 (1974).
12. M. E. Babeshko and V. K. Stryuk, "Thermoplastic stress state of a cylinder asymmetrically loaded along the length," *Tepl. Napyazh. Elem. Konstr.*, **15**, 49–53 (1975).
13. M. E. Babeshko and V. K. Stryuk, "Thermoplasticity of cylinders of finite length," *Vych. Prikl. Mat.*, **48**, 119–127 (1982).
14. M. E. Babeshko and V. K. Stryuk, "Thermoelastoplastic stress state of compound cylinders," *Tepl. Napyazh. Elem. Konstr.*, **18**, 40–43 (1978).
15. V. I. Bobyr', "Stress state of an engine valve under nonaxisymmetric heating," in: *Proc. 11th Sci. Conf. of Young Scientists of the Institute of Mechanics of the Academy of Sciences of the Ukrainian SSR* [in Russian], Part 3, Deposit No. 5507-V86, VINITI, July 28 (1986), pp. 439–443.
16. V. I. Bobyr', *Thermoelastoplastic State of Solids of Revolution Subject to Nonaxisymmetric Loading along Paths of Small Curvature* [in Russian], Author's Abstract of PhD Thesis, Inst. Mekh. S. P. Timoshenko NANU, Kyiv (1988).
17. V. I. Bobyr' and D. A. Ishchenko, "Nonaxisymmetric deformation of bodies of revolution under simple loading," in: *Proc. Sem. of Young Scientists of the Institute of Mechanics of the Academy of Sciences of the UkrSSR on Nonclassical and Mixed Problems in Solid Mechanics* [in Russian], Deposit No. 5531-85DEP, VINITI, July 29 (1985), pp. 6–8.
18. V. I. Bobyr', D. A. Ishchenko, V. G. Savchenko, and I. K. Sakhatskaya, *Program of Research of the Axisymmetric Elastoplastic Stress–Strain State of Structural Members under Variable Mechanical Loading and Heating Taking into Account the Secondary Plastic Strains* [in Russian], Kyiv (1986).
19. V. S. Bondar', *Inelasticity: Versions of the Theory* [in Russian], Fizmatlit, Moscow (2004).
20. A. A. Il'yushin, "A theory of long-term strength," *Izv. AN SSSR*, *MTT*, No. 3, 21–35 (1967).
21. A. A. Il'yushin, *Plasticity: Fundamentals of the General Mathematical Theory* [in Russian], Izd. AN SSSR, Moscow (1963).
22. V. N. Ionov, "Calculation of stresses in cylindrical bodies of arbitrary cross-section," *Izv. Vuzov*, *Mashinostr.*, No. 11, 55–63 (1959).
23. V. N. Ionov, "A method to solve three-dimensional problems," *Izv. Vuzov*, *Mashinostr.*, No. 1, 3–9 (1960).

24. V. N. Ionov and P. M. Ogibalov, *Strength of Three-dimensional Structural Members* [in Russian], Vyssh. Shk., Moscow (1972).
25. D. A. Ishchenko, "Solving an axisymmetric problem of thermoplasticity for cyclic loading," *Prikl. Mekh.*, **20**, No. 7, 108–111 (1984).
26. D. A. Ishchenko, *Elastoplastic State of Solids of Revolution Subject to Cyclic Axisymmetric Thermal and Mechanical Loading* [in Russian], Author's Abstract of PhD Thesis, Inst. Mekh. S. P. Timoshenko NANU, Kyiv (1984).
27. D. A. Ishchenko and V. G. Savchenko, "Kinetics of viscoplastic contact interaction of disk and shaft in turbine rotor," *Strength of Materials*, **20**, No. 4, 440–443 (1988).
28. L. M. Kachanov, *Fundamentals of Fracture Mechanics* [in Russian], Nauka, Moscow (1974).
29. L. M. Kachanov, *Fundamentals of the Theory of Plasticity*, Dover, New York (2004).
30. B. I. Koval'chuk, "Theory of plastic deformation of anisotropic materials," *Strength of Materials*, **7**, No. 9, 1050–1055 (1975).
31. A. A. Lebedev (ed.), B. I. Koval'chuk, F. F. Giginyak, and V. P. Lamashuvskii, *Mechanical Properties of Structural Materials in Complex Stress State* [in Russian], In Yure, Kyiv (2003).
32. S. G. Lekhnitskii, *Anisotropic Plates*, Gordon and Breach, New York (1968).
33. S. G. Lekhnitskii, *Theory of Elasticity of an Anisotropic Body*, Mir, Moscow (1981).
34. N. N. Malinin, *Applied Theory of Plasticity and Creep* [in Russian], Mashinostroenie, Moscow (1975).
35. Yu. N. Shevchenko, V. G. Savchenko, and D. A. Ishchenko, *Method and Software for Analysis of the Nonstationary Heat Conduction in and the Elastoplastic Stress–Strain State of Structural Members such as Solids of Revolution under Axisymmetric Mechanical and Thermal Loads* [in Russian], Guidelines, Inst. Mekh. AN USSR, Kyiv (1988).
36. Ya. M. Grigorenko, Yu. N. Shevchenko, A. T. Vasilenko, et al., *Numerical Methods*, Vol. 11 of the 12-volume series *Mechanics of Composite Materials* [in Russian], A.S.K., Kyiv (2002).
37. I. V. Namestnikov and S. A. Shesterikov, "Vector representation of the damage parameter," in: *Deformation and Fracture of Solids* [in Russian], Izd. MGU, Moscow (1985), pp. 43–52.
38. V. M. Pavlychko, "Solution of three-dimensional problems of thermoplasticity with simple loading processes," *Strength of Materials*, **18**, No. 1, 81–86 (1986).
39. V. M. Pavlychko, "Solving three-dimensional problems of thermoplasticity with allowance for the loading history," in: *Proc. 10th Sci. Conf. of Young Scientists of the Institute of Mechanics of the Academy of Science of the USSR* [in Russian], Dep. VINITI 7/30/84, No. 5535-84 Dep, Kyiv (1984), pp. 113–117.
40. V. M. Pavlychko, *Three-Dimensional Thermoelastoplastic Stress–Strain State of Complex Bodies under Simple Loading* [in Russian], Authors's Abstract of PhD Thesis, Inst. Mekh. S. P. Timoshenko NANU, Kyiv (1988).
41. G. S. Pisarenko, A. P. Yakovlev, and V. V. Matveev, *Strength of Materials* [in Russian], Naukova Dumka, Kyiv (1988).
42. V. V. Piskun and V. G. Savchenko, "Change in the strains in a rotor of complex configuration during elastoplastic deformation," *Tepl. Napryazh. Elem. Konstr.*, **16**, 85–89 (1976).
43. V. V. Piskun and V. G. Savchenko, "Applying the finite-element method to the analysis of the thermoplastic state of bodies of revolution," *Tepl. Napryazh. Elem. Konstr.*, **13**, 23–28 (1973).
44. V. V. Piskun and V. G. Savchenko, "Relaxation of interference-fit stresses in a compound rotor," *Tepl. Napryazh. Elem. Konstr.*, **18**, 34–36 (1978).
45. V. V. Piskun, V. G. Savchenko, and Yu. N. Shevchenko, "Solution of a three-dimensional axisymmetrical problem of thermoplasticity in relation to thick turbine disks," *Strength of Materials*, **6**, No. 5, 530–536 (1974).
46. V. V. Piskun, V. G. Savchenko, and Yu. N. Shevchenko, "Stressed state of compound rotor taking into account interference stresses," *Strength of Materials*, **9**, No. 6, 744–747 (1977).
47. V. V. Piskun, V. G. Savchenko, and Yu. N. Shevchenko, "Applying the finite-element method to the analysis of the thermal stresses in disks," *Tepl. Napryazh. Elem. Konstr.*, **15**, 54–57 (1975).
48. A. N. Podgornyi, "Differential equilibrium equations for a thick-walled cylinder of finite length subject to creep," *Prikl. Mekh.*, **9**, No. 1, 77–85 (1963).
49. A. N. Podgornyi, "Creep of a thick-walled cylinder of finite length," *Tepl. Napryazh. Elem. Konstr.*, **5**, 260–269 (1965).
50. A. N. Podgornyi, "Steady-state and transient creep of a thick-walled cylinder of finite length," *Tepl. Napryazh. Elem. Konstr.*, **8**, 236–243 (1969).

51. V. K. Prokopov, “Homogeneous solutions in the theory of elasticity and their application to the theory of thin plates,” in: *Proc. 2nd All-Union Congr. on Theoretical and Applied Mechanics* [in Russian], Nauka, Moscow (1966), pp. 253–259.
52. Yu. N. Rabotnov, *Solid Mechanics* [in Russian], Nauka, Moscow (1979).
53. Y. N. Rabotnov and S. T. Mileiko, *Transient Creep* [in Russian], Nauka, Moscoe (1970).
54. Yu. N. Shevchenko, V. G. Savchenko, D. A. Ishchenko, and V. M. Pavlychko, *Method and Applied Software for Analysis of the Nonstationary Heat Conduction in and the Elastoplastic Stress–Strain State of Structural Members such as Solids of Revolution under Axisymmetric Mechanical and Thermal Loads* [in Russian], Recommendations R 54-284-90, VNIINMASh, Moscow (1990).
55. V. G. Savchenko, “Analysis of the axisymmetric inelastic deformation of solids of revolution taking into account the stress mode,” in: *Trans. Dniprodzerzhinsk State Technical University* [in Russian], Issue 2(19) (Mathematical Problems of Engineering Mechanics), DDTU, Dniprodzerzhinsk (2012), pp. 13–17.
56. V. G. Savchenko, “Nonaxisymmetric thermostressed state of orthotropic compound solids of revolution with different tensile and compressive moduli of elasticity,” in: *Proc. 3rd All-Ukrainian Sci. Conf. on Mathematical Problems of Technical Mechanics* [in Ukrainian], Dniprodzerzhinsk, April 22–24 (2003), p. 38.
57. V. G. Savchenko, “Nonaxisymmetric thermostressed state of compound solids of revolution made of elastic orthotropic materials with different tensile and compressive moduli of elasticity,” in: *Systems Technologies* [in Ukrainian], Issue 4 (33), Dnepropetrovsk (2004), pp. 39–44.
58. V. G. Savchenko, “Nonaxisymmetric thermostressed state of compound solids of revolution made of rectilinearly orthotropic materials with different tensile and compressive moduli of elasticity,” in: *Systems Technologies* [in Ukrainian], Issue 4 (57), Dnepropetrovsk (2008), pp. 9–14.
59. V. G. Savchenko, “Deformation of compound solids of revolution made of rectilinearly orthotropic materials with different tensile and compressive moduli of elasticity,” in: *Proc. Int. Sci. Conf. on Mathematical Problems of Technical Mechanics* [in Ukrainian], Dnipropetrovsk–Dniprodzerzhinsk, April 21–24 (2008), p. 15.
60. V. G. Savchenko, “Some approaches to the solution of nonaxisymmetric problems of elasticity for solids of revolution made of orthotropic materials with different tensile and compressive moduli of elasticity,” in: *Proc. Int. Sci. Conf. on Mathematical Problems of Technical Mechanics* [in Ukrainian], Dnipropetrovsk–Dniprodzerzhinsk, April 20–23 (2009), p. 16.
61. V. G. Savchenko, “A method of solving a three-dimensional nonaxisymmetric problem of thermoplasticity,” *Tepl. Napryazh. Elem. Konstr.*, **18**, 24–29 (1978).
62. V. G. Savchenko, “A method of describing damage in analyzing the nonaxisymmetric thermostressed state of orthotropic solids of revolution,” in: *Systems Technologies* [in Ukrainian], Issue 2 (25), Dnepropetrovsk (2003), pp. 134–138.
63. V. G. Savchenko, “A method of describing the damage of an orthotropic material in problems of thermomechanics for compound solids of revolution,” in: *Proc. Int. Conf. on Dynamical System Modelling and Stability Investigation* [in Russian], Kyiv, May 27–30 (2003), p. 352.
64. V. G. Savchenko, “Determination of the temperature fields in and the elastoplastic stress state of a piston in an internal combustion engine,” *Dinam. Prochn. Mashin*, **35**, 55–58 (1982).
65. V. G. Savchenko, “Ways of constructing the compliance matrix for materials with different tensile and compressive moduli,” in: *Trans. Dniprodzerzhinsk State Technical University* [in Russian], Issue 2(19) (Mathematical Problems of Engineering Mechanics), DDTU, Dniprodzerzhinsk (2012), pp. 17–23.
66. V. G. Savchenko, “Thermoviscoelastic state of bodies of revolution subject to creep damage under nonaxisymmetric thermomechanical loading,” in: *Trans. Dniprodzerzhinsk State Technical University* [in Russian], Issue 1(24), DDTU, Dniprodzerzhinsk (2014), pp. 170–174.
67. V. G. Savchenko, *Elastoplastic Deformation of Solids of Revolution Subject to Complex Nonaxisymmetric Loading* [in Russian], Author’s Abstract of DSci Thesis, Inst. Mekh. S. P. Timoshenko NANU, Kyiv (1983).
68. V. G. Savchenko, “Numerical analysis of the nonaxisymmetric deformation of solids of revolution taking into account the stress mode,” in: *Systems Technologies* [in Ukrainian], Issue 4 (51), Dnipropetrovsk (2007), pp. 59–64.
69. V. G. Savchenko, V. V. Piskun, M. B. Babeshko, and I. V. Prokhorenko, “A numerical method for solving axisymmetric problems of heat conduction and thermoplasticity for solids of revolution,” *Tepl. Napryazh. Elem. Konstr.*, **19**, 38–43 (1979).

70. V. G. Savchenko and Yu. N. Shevchenko, *Three-Dimensional Problems of Thermoviscoplasticity*, Vol. 1 of the six-volume series *Advances in Mechanics* [in Russian], ASK, Kyiv (2006), pp. 625–660.
71. V. G. Savchenko and Yu. N. Shevchenko, "Elastoplastic state of thick circular plates with stepwise varying geometry under nonisothermal loading," in: *Proc. 12th All-Union Conf. on the Theory of Plates and Shells* [in Russian], Vol. 3, Izd. Yerevan. Univ. (1980), pp. 192–198.
72. I. K. Sakhatskaya, "Analysis of the thermoelastoplastic stress state of a cylindrical sector," in: *Proc. 10th Sci. Conf. of Young Scientists of the Institute of Mechanics of the Academy of Sciences of the Ukrainian SSR* [in Russian], Part 1, Deposit No. 5535-V84Dep, VINITI, July 30 (1984), pp. 141–145.
73. I. K. Sakhatskaya, "Solution of the problem of thermoplasticity for circumferentially nonclosed solids of revolution," *Prikl. Mekch.*, **19**, No. 9, 113–117 (1983).
74. I. K. Sakhatskaya, "Thermoelastoplastic stress–strain state of a cylindrical sector with loading history," in: *Proc. 11th Sci. Conf. of Young Scientists of the Institute of Mechanics of the Academy of Sciences of the Ukrainian SSR* [in Russian], Deposit No. 5507-V86Dep, VINITI, July 27 (1986), pp. 582–587.
75. I. K. Sakhatskaya, *Elastoplastic Stress State of Solids of Revolution Subject to Nonaxisymmetric Nonisothermal Loading* [in Russian], Author's Abstract of PhD Thesis, Inst. Mekh. S. P. Timoshenko NANU, Kyiv (1984).
76. V. V. Sokolovskii, "Expressions for the stress components in the theory of plasticity," *Dokl. AN SSSR*, **61**, No. 2, 86–94 (1948).
77. V. K. Stryuk, "Thermoelastoplastic stress state of a thick-walled cylinder of finite length," *Tepl. Napryazh. Elem. Konstr.*, **10**, 57–67 (1970).
78. V. K. Stryuk, "Elastoplastic stress state of a short cylinder," *Tepl. Napryazh. Elem. Konstr.*, **9**, 183–191 (1970).
79. V. K. Stryuk, *Elastoplastic Stress State of Short Cylinders under Nonaxisymmetric Loading* [in Russian], Author's Abstract of PhD Thesis, Inst. Mekh. S. P. Timoshenko NANU, Kyiv (1973).
80. V. G. Savchenko and Yu. N. Shevchenko, *Three-Dimensional Problems of Thermoviscoplasticity*, Vol. 1 of the six-volume series *Advances in Mechanics* [in Russian], ASK, Kyiv (2006), pp. 625–660.
81. Yu. N. Shevchenko and R. G. Terekhov, *Studying the Thermoviscoplastic Deformation of a Solid under Complex Nonisothermal Loading*. Part 1, Vol. 2 of the six-volume series *Advances in Mechanics* [in Russian], ASK, Kyiv (2006), pp. 218–248.
82. Yu. N. Shevchenko and R. G. Terekhov, *Studying the Thermoviscoplastic Deformation of a Solid under Complex Nonisothermal Loading*. Part 2, Vol. 2 of the six-volume series *Advances in Mechanics* [in Russian], ASK, Kyiv (2006), pp. 415–446.
83. Yu. N. Shevchenko and M. E. Babeshko, *Thermoviscoelastoplastic State of Shells of Revolution Undergoing Axisymmetric Deformation along Various Plane Paths*, Vol. 2 of the six-volume series *Advances in Mechanics* [in Russian], ASK, Kyiv (2006), pp. 539–573.
84. V. L. Fomin, "Elastoplastic equilibrium of a hollow cylinder with an axisymmetric temperature field," *Izv. AN SSSR*, *Otd. Tekhn. Nauk*, *Mekh. Mashinostr.*, No. 5, 127–128 (1961).
85. G. M. Khazhinskii, "Theory of creep and stress rupture of metals," *MTT*, No. 6, 29–36 (1971).
86. Yu. N. Shevchenko, "Deformation theory of thermoviscoelastoplastic deformation of orthotropic bodies taking into account the loading history," *Strength of Materials*, **32**, No. 5, 454–461 (2000).
87. Yu. N. Shevchenko, *Thermoplasticity under Variable Loading* [in Russian], Naukova Dumka, Kyiv (1970).
88. Yu. N. Shevchenko, *Numerical Methods for Solving Applied Problems*, Vol. 2 of the six-volume series *Three-Dimensional Problems in Elasticity and Plasticity* [in Russian], Naukova Dumka, Kyiv (1986).
89. Yu. N. Shevchenko, M. E. Babeshko, V. V. Piskun, et al., *Solving an Axisymmetric Problem of Thermoplasticity for Thin-Walled and Thick-Walled Solids of Revolution on a Unified-System Computer* [in Russian], Naukova Dumka, Kyiv (1980).
90. Yu. N. Shevchenko, M. E. Babeshko, V. V. Piskun, et al., "Solving axisymmetric problems of thermoplasticity on a mainframe computer," *Prikl. Probl. Prochn. Plast.*, **1**, 67–76 (1975).
91. Yu. N. Shevchenko, M. E. Babeshko, V. V. Piskun, and V. G. Savchenko, *Three-Dimensional Problems of Thermoplasticity* [in Russian], Naukova Dumka, Kyiv (1980).
92. Yu. N. Shevchenko, M. E. Babeshko, and R. G. Terekhov, *Thermoviscoelastoplastic Processes of Combined Deformation of Structural Members* [in Russian], Naukova Dumka, Kyiv (1992).

93. Yu. N. Shevchenko, V. V. Piskun, and V. A. Kovalenko, *Software for Solving Problems of the Thermoelastic Axisymmetric Stress–Strain State of Curvilinearly Orthotropic Multilayer Solids of Revolution* [in Russian], No. 50850001048, GFAP, Kyiv (1985).
94. Yu. N. Shevchenko, V. V. Piskun, and V. G. Savchenko, *Solving Axisymmetric Three-Dimensional Problem of Thermoplasticity on an M-220 Mainframe Computer* [in Russian], Naukova Dumka, Kyiv (1975).
95. Yu. N. Shevchenko and V. G. Savchenko, *Thermoviscoplasticity*, Vol. 2 of the five-volume series *Mechanics of Coupled Fields in Structural Members* [in Russian], Naukova Dumka, Kyiv (1987).
96. Yu. N. Shevchenko and R. G. Terekhov, *Constitutive Equations of Thermoviscoplasticity* [in Russian], Naukova Dumka, Kyiv (1982).
97. Yu. N. Shevchenko and N. N. Tormakhov, "Constitutive equations of thermoplasticity describing processes of proportional loading and incorporating the stress mode," in: *Mathematical Problems of Engineering Mechanics* [in Russian], Issue 2 (19), Dniprodzerzhinsk, DDTU (2012), pp. 69–73.
98. H. Altenbach, "Creep theory: Present-day problems and applications," *Int. Appl. Mech.*, **39**, No. 6, 631–655 (2003).
99. M. E. Babeshko and V. G. Savchenko, "Method of successive approximation in boundary-value problems of thermoplasticily," *Int. Appl. Mech.*, **34**, No. 3, 232–238 (1998).
100. M. E. Babeshko and V. G. Savchenko, "Improving the convergence of the additional-strain method in thermoplasticity boundary problems with deformation along small-curvature trajectories," *Int. Appl. Mech.*, **34**, No. 8, 771–776 (1998).
101. M. E. Babeshko and Yu. N. Shevchenko, "Describing the thermoelastoplastic deformation of compound shells under axisymmetric loading with allowance for the third invariant of stress deviator," *Int. Appl. Mech.*, **46**, No. 12, 1362–1371 (2010).
102. M. E. Babeshko and Yu. N. Shevchenko, "Elastoplastic stress–strain state of flexible layered shells made of isotropic and transversely isotropic materials with different moduli and subjected to axisymmetric loading," *Int. Appl. Mech.*, **43**, No. 11, 1208–1217 (2007).
103. M. E. Babeshko and Yu. N. Shevchenko, "Method of successive approximations for solving boundary-value problems of plasticity with allowance for the stress mode," *Int. Appl. Mech.*, **46**, No. 7, 744–752 (2010).
104. M. E. Babeshko, Yu. N. Shevchenko, and N. N. Tormakhov, "Constitutive equations of elastoplastic isotropic materials that allow for the stress mode," *Int. Appl. Mech.*, **45**, No. 11, 1189–1195 (2009).
105. M. E. Babeshko, Yu. N. Shevchenko, and N. N. Tormakhov, "Approximate description of the inelastic deformation of an isotropic material with allowance for the stress mode," *Int. Appl. Mech.*, **46**, No. 2, 139–148 (2010).
106. M. E. Babeshko and V. K. Stryuk, "Calculating the stress state of a solid cylinlder on the basis of the theory of flow with isotropic hardening," *Sov. Appl. Mech.*, **10**, No. 6, 587–591 (1974).
107. A. Baltov, "Materials sensitive to the type of the process," *Int. Appl. Mech.*, **40**, No. 4, 361–369 (2004).
108. V. I. Bobyr, "Thervoelasticity problem for solids of revolution with a nonaxisymmttric load over a small-curvature deformation trajectory," *Sov. Appl. Mech.*, **22**, No. 7, 636–639 (1986).
109. R. M. Jones, "Stress–strain relations for materials with different moduli in tension and compression," *AIAA J.*, **15**, No. 1, 16–23 (1977).
110. R. M. Jones, "Modeling nonlinear deformation of carbon–carbon composite materials," *AIAA J.*, **18**, No. 8, 995–1001 (1980).
111. A. Z. Galishin, "Determining the thermoviscoplastic state of shells of revolution subject to creep damage," *Int. Appl. Mech.*, **40**, No. 5, 537–545 (2004).
112. H. Hencky, "Zur Theorie plastischer Deformationen und der hierdurch im Material hervorgerufenen Nachspannungen," *ZAMM*, **4**, No. 4, 323–334 (1924).
113. R. Hill, *Mathematical Theory of Plasticity*, University Press, Oxford (1950).
114. D. A. Ishchenko and V. G. Savchenko, "Influence of taking account of secondary plastic deformations on the solution of the axisymmetric thermoplasticity problem," *Sov. Appl. Mech.*, **24**, No. 3, 229–233 (1988).
115. L. P. Khoroshun and E. N. Shikula, "A note on the theory of short-term microdamageability of granular composites under thermal actions," *Int. Appl. Mech.*, **38**, No. 1, 60–67 (2002).
116. L. P. Khoroshun and E. N. Shikula, "Short-term microdamageability of laminated materials under thermal actions," *Int. Appl. Mech.*, **38**, No. 4, 432–439 (2002).

117. Yu. I. Lelyuckh, “Analyzing methods to allow for the damage of material in thermoviscoelastoplastic deformation,” *Int. Appl. Mech.*, **43**, No. 12, 1396–1405 (2007).
118. Yu. I. Lelyukh and Yu. N. Shevchenko, “On finite-element solution of spatial thermoviscoelastoplastic problems,” *Int. Appl. Mech.*, **42**, No. 5, 507–515 (2006).
119. W. Lode, “Versuche uber den Einfluss der mittleren Hauptspannung auf das Fliessen der Metals – Eisen, Kupfer und Nickel,“ *Z. Physik*, **36**, 913–939 (1926).
120. G. C. Pardoen, “Improved structural analysis technique for orthogonal weave carbon-carbon materials,” *AIAA J.*, **13**, No. 6, 756–761 (1995).
121. V. M. Pavlychko, “Numerical solution of three-dimensional thermoplasticity problems for bodies of complex shape,” *Sov. Appl. Mech.*, **24**, No. 8, 748–752 (1988).
122. A. N. Podgornyi, “Thermal creep of a cylinder of finite length,” *Sov. Appl. Mech.*, **6**, No. 12, 1314–1317 (1970).
123. L. Prandtl, “Anwendungsbeispile zu einem Henckyschen Satz uber das plastische Gleichgewicht,“ *ZAMM*, **3**, No. 6, 401–406 (1923).
124. A. Reuss, “Berucksichtigung der elastischen Formanderung in der Plastizitatstheorie,“ *ZAMM*, **10**, No. 3, 266–274 (1930).
125. V. G. Savchenko, “Calculation of nonaxisymmetric thermally stressed state of discrete homogeneous bodies of revolution with orthotropic layers,” *Int. Appl. Mech.*, **32**, No. 2, 122–127 (1996).
126. V. G. Savchenko, “Calculating the stress–strain state of solids of revolution that are sectional in the circumferential direction,” *Int. Appl. Mech.*, **32**, No. 7, 518–523 (1996).
127. V. G. Savchenko, “Elastic-plastic state of bodies of revolution under variable nonisothermal loading, taking account of creep,” *Sov. Appl. Mech.*, **18**, No. 12, 1053–1058 (1982).
128. V. G. Savchenko, “Influence of the direction of principal anisotropy in a rectilinearly orthotropic material on the stress state of a compound solid of revolution subject to nonaxisymmetric heating,” *Int. Appl. Mech.*, **39**, No. 6, 713–720 (2003).
129. V. G. Savchenko, “A method to study the nonaxisymmetric plastic deformation of solids of revolution with allowance for the stress mode,” *Int. Appl. Mech.*, **44**, No. 9, 975–981 (2008).
130. V. G. Savchenko, “Nonaxisymmttric deformation of solids of revolution made of elastic orthotropic materials with different tensile and compressive moduli,” *Int. Appl. Mech.*, **41**, No. 7, 748–756 (2005).
131. V. G. Savchenko, “Nonaxisymmetric temperature and thermostress in isotropic and curved orthotropic layered solids of revolution,” *Int. Appl. Mech.*, **29**, No. 8, 602–609 (1993).
132. V. G. Savchenko, “Nonaxisymmetric thermal and stressed state of layered bodies of revolution with rectilinearly orthotropic layers,” *Int. Appl. Mech.*, **30**, No. 9, 650–656 (1994).
133. V. G. Savchenko, “Numerical nonaxisymmetric thermostress analysis of compound solids of revolution with damage,” *Int. Appl. Mech.*, **40**, No. 3, 275–282 (2004).
134. V. G. Savchenko, “Influence of the direction of principal anisotropy in a rectilinearly orthotropic material on the stress state of a compound solid of revolution subject to nonaxisymmetric heating,” *Int. Appl. Mech.*, **39**, No. 6, 713–720 (2003).
135. V. G. Savchenko, “Stress state of compound solids of revolution made of damaged orthotropic materials with different tensile and compressive moduli,” *Int. Appl. Mech.*, **42**, No. 11, 1246–1255 (2006).
136. V. G. Savchenko, “Thermal stress state of laminated solids of revolution of isotropic and linearly orthotropic materials,” *Int. Appl. Mech.*, **31**, No. 4, 249–254 (1995).
137. V. G. Savchenko and M. E. Babeshko, “Solution of nonaxisymmetric three-dimensional thermoplasticity problem by the secondary-stress method,” *Int. Appl. Mech.*, **35**, No. 12, 1207–1213 (1999).
138. V. G. Savchenko and M. E. Babeshko, “The nonaxisymmetric elastoplastic state of isotropic and cylindrically orthotropic solids of revolution under nonisothermal loading,” *Int. Appl. Mech.*, **36**, No. 2, 216–224 (2000).
139. V. G. Savchenko and M. E. Babeshko, “The nonaxisymmetric thermostressed state of laminated isotropic and rectilinearly orthotropic solids of revolution,” *Int. Appl. Mech.*, **36**, No. 4, 501–508 (2000).
140. V. G. Savchenko and Yu. N. Shevchenko, “Methods for investigating thermoviscoplastic deformation of three-dimensional structural members (review),” *Int. Appl. Mech.*, **29**, No. 9, 677–691 (1993).

141. V. G. Savchenko and Yu. N. Shevchenko, “Nonaxisymmetrical thermal stressed state of laminated bodies of revolution of orthotropic materials under nonisothermic loading,” *Mech. Comp. Mater.*, **40**, No. 6, 731–751 (2004).
142. V. G. Savchenko and Yu. N. Shevchenko, “Spatial thermoviscoplastic problems,” *Int. Appl. Mech.*, **36**, No. 11, 1399–1433 (2000).
143. Yu. N. Shevchenko, “Determining equations of thermoviscoplasticity describing the strain processes experienced by an element of an orthotropic body along low-curvature trajectories,” *Int. Appl. Mech.*, **34**, No. 10, 1042–1048 (1998).
144. Yu. N. Shevchenko, “Study of thermoviscoelastoplastic processes in the deformation of structural elements,” *Int. Appl. Mech.*, **35**, No. 9, 861–870 (1999).
145. Yu. N. Shevchenko, “Thermoviscoplasticity boundary problems with complex nonisothermal loading processes,” *Sov. Appl. Mech.*, **21**, No. 4, 413–420 (1985).
146. Yu. N. Shevchenko, “Transformation of thermoviscoelastoplastic stress-deformed state of some constructions elements depending on heating regime,” in: *Proc. 3rd Int. Congr. on Thermal Stresses*, Thermal Stresses’99, Cracow, Poland, June 13–17, (1999), pp. 223–226.
147. Yu. N. Shevchenko and M. I. Goikhman, “Study of laws governing the elastoplastic deformation of transversely isotropic bodies,” *Sov. Appl. Mech.*, **26**, No. 9, 643–845 (1990).
148. Yu. N. Shevchenko and V. N. Mazur, “Solution of plane and axisymmetric boundary-value problems of thermoviscoplasticity with allowance for creep damage to the material,” *Sov. Appl. Mech.*, **22**, No. 8, 695–704 (1986).
149. Yu. N. Shevchenko and V. V. Piskun, “Thermoelastoplastic state of discretely inhomogeneous orthotropic bodies of revolution with a nonlinear shear characteristic,” *Int. Appl. Mech.*, **31**, No. 6, 441–447 (1995).
150. Yu. N. Shevchenko, V. V. Piskun, and V. A. Kovalenko, “Elastoplastic states of axisymmetrically loaded laminated bodies on revolution made of isotropic and ortotropic materials,” *Int. Appl. Mech.*, **28**, No. 1, 25–32 (1992).
151. Yu. N. Shevchenko, V. V. Piskun, and V. A. Kovalenco, “Thermostress state of curvilinear orthotropic inhomogeneous bodies of revolution,” *Sov. Appl. Mech.*, **19**, No. 7, 567–573 (1983).
152. Yu. N. Shevchenko and I. K. Sakhatskaya, “Mixed thermoplasticity problem for open solids of revolution,” *Sov. Appl. Mech.*, **24**, No. 6, 535–539 (1988).
153. Yu. N. Shevchenko and V. G. Savchenko, “Numerical modeling of process of heat treatment of details with the use of equations of thermoviscoplasticity,” in: *Abstracts European Mech. Collog. 263. The Effect of Phase Transformations in Solids on Constitutive Laws*, Vienna (1990), p. 16.
154. Yu. N. Shevchenko and R. G. Terekhov, “Studying the laws of the thermoviascoplastic deformation of a solid under nonisothermal complex loading. Part 2,” *Int. Appl. Mech.*, **37**, No. 6, 701–727 (2001).
155. Yu. N. Shevchenro, R. G. Terekhov, and N. N. Tormakhov, “Linear relationship between the first invariants of the stress and strain tensors in theories of plasticity with strain hardening,” *Int. Appl. Mech.*, **43**, No. 3, 291–302 (2007).
156. Yu. N. Shevchenko, R. G. Terekhov, and N. N. Tormakhov, “Elastoplastic deformation of elements of an isotropic solid along paths of small curvature: Constitutive equations incorporating the stress mode,” *Int. Appl. Mech.*, **43**, No. 6, 621–630 (2007).
157. Yu. N. Shevchenko, R. G. Terekhov, and N. N. Tormakhov, “Constitutive equations for describing the elastoplastic deformation of elements of a body along small-curvature paths in view of the stress mode,” *Int. Appl. Mech.*, **42**, No. 4, 421–430 (2006).
158. Yu. N. Shevchenko and N. N. Tormakhov, “Constitutive equations of thermoplasticy including the third invariant,” *Int. Appl. Mech.*, **46**, No. 6, 613–624 (2010).
159. Yu. N. Shevchenko and N. N. Tormakhov, “Thermoviscoplastic deformation along paths of small curvature: Constitutive equations including the third deviatoric stress invariant,” *Int. Appl. Mech.*, **48**, No. 6, 688–699 (2012).
160. J. H. Weiner and J. V. Huddleston, “Transient and residual stresses in heat-treated cylinders,” *Paper. Amer. Soc. Mech. Engns.*, No. A-21, 9 (1958).
161. M. Zyczkowski, *Combined Loadings in the Theory of Plasticity*, PWN–Polish Scientific Publishers (1981).